

https://dspace.org/

# Functional analysis of the cydDC encoded ABC-type transporter in mycobacterium smegmatis

**Moeketsi, Moseki Raymond**

**2017**
http://hdl.handle.net/10539/23320

Downloaded from a DSpace repository. https://dspace.org/

`

# Functional analysis of the *cydDC* encoded ABC-type transporter in *Mycobacterium smegmatis*

**Moseki Raymond Moeketsi**

**Degree of Master of Science in Medicine**

Dissertation Submitted to the Faculty of Health Sciences, University of the Witwatersrand, Johannesburg, in the fulfilment of the requirement for the degree of Master of Science in Medicine by Research.

Johannesburg, 2017

`

**Declaration**

I Moseki Raymond Moeketsi declare that, this is my own work. It is being submitted for the degree of Masters of Science in Medicine (by Research) at the University of the Witwatersrand, Johannesburg. It has not been submitted before for any degree or examination at this or any other University

Moseki Raymond Moeketsi

31 March 2017

BSc, BSc (Hons)

`

**Dedication**

I dedicate this work to the one who inspired me to continue studying, to live life without ceilings. The one who brought the realization that, humans are progressive beings, and that achieving is their natural state. To my mother, Menyane Grace Sedibe, this is all for you.

`

**Presentations from this study**

1. Moeketsi Raymond Moseki and Bavesh Kana. Functional analysis of *cydDC* encoded type ABC transporter in *Mycobacterium smegmatis.* 3 December 2015, Molecular Biosciences Research Thrust (MBRT) Symposium, Wits University, Johannesburg, South Africa**.**

2. Moeketsi Raymond Moseki and Bavesh Kana. Functional analysis of *cydDC* encoded type ABC transporter in *Mycobacterium smegmatis.* 1 September 2016, Faculty of Health Sciences Biennial Research Day and Postgraduate Expo, Wits University, Johannesburg, South Africa**.**

3. Moeketsi Raymond Moseki and Bavesh Kana. Functional analysis of *cydDC* encoded type ABC transporter in *Mycobacterium smegmatis.* 8 December 2016, Molecular Biosciences Research Thrust (MBRT) Symposium, Wits University, Johannesburg, South Africa**.**

`

**Abstract**

Electron transport and respiration in *Mycobacterium tuberculosis* (Mtb), the causative agent of tuberculosis (TB) occurs through the use of the $aa_3$ type cytochrome *c* oxidase (C*c*O) under normoxic conditions or cytochrome *bd* oxidase (C*bd*O) under microaerophillia. Using these oxidases, Mtb couples substrate level oxidation to generation of metabolic energy in the form of adenosine triphosphate (ATP) under aerobic conditions. The presence of the C*bd*O is expected to allow for growth and survival of Mtb in the oxygen restricted environment of the human TB granuloma, thus rendering it an important enzyme for further study. C*bd*O is comprised of two structural subunits, CydA (subunit I) and CydB (subunit II), which are encoded by the *cydAB* operon. Both subunits span the cytoplasmic membrane to form part of the mycobacterial electron transport chain. Notably, two other genes that are transcribed separately from the *cydAB* operon, the *cydDC* operon, have been proposed to be required for the synthesis of a functional C*bd*O. Based on amino acid sequence and structural predictions, the *cydDC* encode heterodimeric members of the ATP Binding Cassette ABC-type transporters. In other organisms, the *cydDC* functions to transport reducing agents to the periplasm, thus contributing to periplasmic redox homeostasis. In this study we aimed to analyze the function of the *cydDC* genes in *Mycobacterium smegmatis.* Through bioinformatics analyses, it was demonstrated that the CydDC subunits retain conserved residues associated with the ABC domain and adopt a three-dimensional fold that is similar to their counterparts in *Escherichia coli*. However, the published sequence of *M. smegmatis* suggests that *cydC* is a pseudogene, which was inconsistent with the demonstrated evidence of a functional C*bd*O in this organism. In this study, using standard DNA sequencing, it was demonstrated that the CBTBR laboratory strain of *M. smegmatis* does not harbor a *cydC* pseudogene but rather has a functional *cydC* gene. Next, we interrogated the function of the *M. smegmatis and* Mtb *cydDC* genes by heterologous expression in an *E. coli cydD* mutant. Heterologous expression of the Mtb *cydDC* genes restored C*bd*O biogenesis in the *E. coli* mutant. Using various microbiological approaches, we demonstrated that the mycobacterial *cydDC* was able to revert the stationary phase exit defect, high temperature sensitivity and increased oxidative stress susceptibility defects of the *E. coli cydD* mutant.

`

Collectively, these data provided strong evidence that the mycobacterial *cydDC* genes encode a functional transporter that contributes to periplasmic redox homeostasis. Following this, we generated a double deletion mutant of the *cydDC* operon in *M smegmatis*. We confirmed the genetic integrity of the Δ*cydDC* strain by Southern Blot analysis and proved by absorption difference spectroscopy that this strain is defective in the ability to synthesize a functional C*bd*O, as measured by the lack of a heme *d* peak in membrane preparations from the mutant. In addition, the Δ*cydDC* mutant displayed increased sensitivity to oxidative stress and a reduced ability to exit stationary phase, phenotypic defects that were consistent with the lack of C*bd*O. In summary, this study provides the first evidence that loss of the *M. smegmatis cydDC* genes affects C*bd*O biogenesis. These data also confirm that the CydDC ABC-type transporter most likely transports reducing equivalents that allow for maturation of C*bd*O in the periplasm. Collectively, our observations advance the understanding of the mycobacterial electron transport chain and provide new evidence to assist in the development of C*bd*O as a TB drug target.

`

**Acknowledgements**

First, I would like to acknowledge my first love-my heavenly father the creator of all universes- my God. Thank you for bringing me this far. I have now past the stage of believing, I live with the knowing that, there is an omnipotent God who rewards man according to his deeds- good or bad. Your holy spirit that resides in me, is my navigation system when I am lost, it is my comfort when I am distraught and a source of my joy in the daily rigours of life. Your Holy Bible has been a mother, a father and a friend to me. My gratitude to you God, lives through double infinities, Thank you for the gift of life.

To my kind, loving mother, my family: “Mosetsanyana”, all I know is that I am blessed! I am not sure who packs lunch for a twenty something year old but somehow I feel like you are the only one. Thank you for the giant lunch box you packed every day, most of the time at one O’ clock in the morning coming from work. In my journey as a masters student, you have shown me support in every way possible. I look at you and I think, heaven must be missing an angel. Thank you mama.

It is my pleasure also, to recognize and acknowledge all the funding bodies who took interest in my career development, without whose continued financial support might have stunted my growth as a scientist. The National Research Foundation through the Wits node of the Department of Science and Technology in the Center of Excellence for Biomedical Tuberculosis Research (DST/ NRF-CBTBR), and the Belgian Technical Cooporation (BTC), I say to you: if you plant a seed on good soil and nurse it, you never have to worry about the harvest.

I would also like to acknowledge the National Health Laboratory Services (NHLS) for the premises where the research for this wonderful study was conducted. To my team at the CBTBR, the last two years has provided me with a profound learning experience. I had a chance to learn from a scientifically sound and inquisitive bunch, who are always trying to push boundaries as far as the science is concerned. From the closed doors in the seminar room discussing articles for journal club, to the open spaces in the lab, the mind filling conversation that stretched my thinking in new directions will always be cherished.

`

To my supervisor Professor Bavesh Kana, thank you for affording me the opportunity of being a member of the CBTBR. Your lab is the soil that I have been planted in for growth. You planted me, nursed me, and throughout the growing process I have experienced your guidance and support, personally, academically and financially. The environment you and management have created, truly epitomizes the spirit of excellence. I say to you and management, that same spirit permeates my being and I can feel it growing and trickling down to my personal life. Thank you for everything that you have been to me.

To the post docs in the lab: Chris, Julian and Melissa, the conversations, the jokes and the moral support provided stamina for the long learning experience I had to endure, thank you! To Melissa, your ability to recognize and stimulate human potential is impeccable. It is rare to find a person whose spirit of Ubuntu exceeds their need for recognition in their profession. You are an invaluable resource to the lab, somehow, I idolize you.

Without order, to the PhD students, Andrea, Ditshego, Nicole, Sibusiso, Zaahida, Gadisi and Amanda, I extend my gratitude to you. I have deep respect for you all when it comes to the science. I can unequivocally say, you are some of the most scientifically interrogative minds I have met to date. Without a doubt, the future of research is in the right hands. To Ditshego, Sibusiso and Nicole, thank you for the small talk and the many laughs (directly translate: ditshego). You helped me maintain perspective and sanity when things were not working for a long time. Also, thank you for the advice pertaining to this project and the empathy during trying times.

To the Honors and MSc students, Lethabo, Nelia, Tebogo, Moagi, Masethabela, Poppy and Nombeko, thank you guys for the memorable journey. In you I learned the spirit of caring. Thank you for the love and the many hysterical laughs we shared. You are an amazing bunch and I am glad to have had this kind of encounter with you. You are all recognized without any hierarchy and thank you for all that you've been to me.

Fiona, Tshepiso, Ruth, Waheeda and the NRF guy, the administrative officers at the CBTBR and the senate house. Thank you for the service. Always smiling and

`

processing order documents every week. Your kindness is testament that the world is not at all a rotten place. I literally could have not functioned as efficient on my own. Thank you all.

Last but not least, to Promise and the retired Mom Leeyah, I mean the working place is always in a spotless hygienic condition. To Promise, to do what you do 8 hours a day, 5 days a week with the heart that you do it with, shows that you are in synchrony with the spirit of excellence that stems from the science carried out at the CBTBR. Your efforts do not go unrecognized, thank you.

Every journey has its conclusion, and this is mine for this MSc journey.

`

**List of Figures**

Figure 1.1…… 1

Figure 1.2…… 4

Figure 1.3…… 11

Figure 1.4…….. 12

Figure 1.5…….. 14

Figure 1.6…….. 17

Figure 1.7…….. 20

Figure 1.8…….. 23

Figure 1.9…….. 26

Figure1.10…… 30

Figure 2.1…… 52

Figure 2.2…… 54

Figure 2.3…… 56

Figure 2.4…… 57

Figure .2.5…… 57

Figure 3…… 69

Figure 3.1…… 70

Figure 3.1.1…… 71

Figure 3.2…… 73

Figure 3.3…… 74

`

Figure 3.4…… 76

Figure 3.5…… 78

Figure 3.6…… 79

Figure 3.7…… 82

Figure 3.8…… 84

Figure 3.9…… 85

Figure 3.10…….. 87

Figure 3.11…….. 89

Figure 3.11.1…….. 90

Figure 3.12…….. 93

Figure 3.13…….. 94

Figure 3.14…….. 96

Figure 3.15…….. 97

Figure 3.16…….. 98

Figure 3.17…….. 99

Figure 4…… 101

Appendix A 10…… 116

Appendix A 10.1…… 117

Appendix B 1…….. 118

`

List of Tables

Table 2…… 34

Table 2.1…… 38

Table 2.2…… 44

Table 2.3…… 45

Table 2.4…… 45

Table 2.5…… 46

Table 2.6…… 58

Table 2.7…… 59

Table 2.8…… 59

Table A1…… 112

Table A2…… 112

Table A3…… 113

Table A4…… 113

Table A5…… 113

Table A6…… 114

Table A7…… 114

Table A8…… 114

Table A9…… 115

`

## Contents

Declaration ..... II

Dedication ..... III

Presentations from this study ..... IV

Abstract ..... V

Acknowledgements ..... VII

List of Figures ..... X

List of Tables ..... XII

Abbreviations ..... XIX

1 Introduction ..... 1

1.1 Tuberculosis diagnosis and challenges ..... 1

1.2 TB Transmission and Pathogenesis ..... 3

1.3 Treatment and drug resistance ..... 6

1.4 New drugs for TB ..... 8

1.4.1 Benzothiazinone ..... 8

1.4.2 Q203 ..... 9

1.4.3 Bedaquiline ..... 9

1.5 The Electron transport chain ..... 9

1.5.1 The aerobic branch of the mycobacterial ETC ..... 10

1.5.2 The composition of the mycobacterial aerobic electron transport chain ..... 11

1.6 NADH dehydrogenase ..... 13

1.6.1 NDH-1 ..... 13

1.6.2 NDH-2 ..... 15

1.7 Succinate dehydrogenase (SDH) ..... 16

1.8 Menaquinone ..... 18

`

1.9 Cytochrome $bc_1/aa_3$ super complex ..... 19
1.10 Cytochrome *bd* Oxidase (C*bd*O) ..... 21
1.10.1 Distribution and evolution ..... 21
1.10.2 Genetics and physiological role ..... 22
1.10.2.1 The mycobacterial C*bd*O in relation to other bacteria ..... 22
1.10.3 ABC transporters ..... 25
1.10.4 Functional mechanism of ABC-type transporters ..... 26
1.10.5 The role of C*bd*O in *E.coli* ..... 28
1.10.7 C*bd*O in pathogenesis ..... 29
1.10.6 $F_1F_0$ ATP synthase ..... 29
1.11 Rationale for this study ..... 31
1.10.9 Hypothesis ..... 32
1.10.10 Aim ..... 32
1.10.11 Objectives ..... 32
2. Materials and Methods ..... 33
2.1 Bioinformatic tools and virtual software programs ..... 33
2.1.1 Databases used in this study ..... 33
2.1.2 NCBI BLAST (http://blast.ncbi.nlm.nih.gov/Blast.cgi) ..... 33
2.1.3 Clustal Omega or Clustal W2 (http://www.ebi.ac.uk/Tools/msa/clustalo/) ..... 34
2.1.4 I-TASSER (http://zhanglab.ccmb.med.umich.edu/I-TASSER/) ..... 34
2.1.5 PyMOL (https://www.pymol.org/) ..... 34
2.2 Chemicals and Reagents ..... 34
2.3 Bacterial strains and cultivation conditions ..... 34
2.4 DNA manipulation ..... 39
2.4.1 Small scale plasmid preparation (Alkaline lysis) ..... 39

`

2.4.2 Sodium acetate precipitation ..... 40
2.4.3 Bulk preparation of plasmid DNA ..... 40
2.4.4 Mycobacterial genomic DNA extraction ..... 41
2.4.5 Mycobacterial small-scale genomic DNA extraction ..... 41
2.5 Nucleic acid quantitation ..... 42
2.6 Polymerase chain reaction (PCR) ..... 42
2.6.1 Gene knockout primers ..... 42
2.6.2 Sequencing primers ..... 43
2.6.3 Primers for creating suicide constructs and complementation vectors ..... 44
2.6.4 Restriction digestion of DNA ..... 46
2.6.5 Dephosphorylation of DNA ..... 47
2.6.6 Phosphorylation of DNA ..... 47
2.6.7 Modification of DNA overhangs ..... 47
2.6.8 DNA ligation ..... 47
2.7 Bacterial transformations ..... 48
2.7.1 *E. coli* transformations ..... 48
2.7.2 Mycobacterial electroporations ..... 49
2.8 Agarose electrophoresis ..... 50
2.9 DNA purification ..... 50
2.10 Sequencing ..... 51
2.11 Preparation of freezer stocks, seed stocks and preservation of plasmids and strains 51
2.12 Construction of the *cydDC*KO constructs (Homologous recombination) ..... 51
2.13 Construction of the *cydDC*KO constructs (Recombination genetic engineering - recombineering) ..... 53
2.14 Generation of KO mutants (homologous recombination) ..... 55

`

2.15 Generation of KO mutants (Recombination genetic engineering - Recombineering) ..... 58
2.16 Southern blot analysis ..... 61
2.16.1 gDNA digestion ..... 61
2.16.2 Electro-blotting ..... 61
2.16.3 Probe synthesis and labelling ..... 62
2.16.4 Hybridization ..... 62
2.16.5 Immunological detection ..... 63
2.17 Lysis of *E. coli* cells for preparation of membrane fractions ..... 63
2.17 Lysis of *M. smegmatis* cells ..... 64
2.18 Purification of membrane fractions by ultracentrifugation ..... 64
2.19 Phenotypic characterization of Mutants ..... 65
2.19.1 Membrane spectroscopy *E. coli* and *M. smegmatis* ..... 65
2.19.2 Response to induced oxidative stress ..... 65
2.19.3 Growth curves ..... 66
2.19.4 Temperature sensitivity assays ..... 66
2.19.5 Nutrient starvation assays for *E. coli* ..... 67
2.19.6 Nutrient starvation assays for *M. smegmatis* ..... 67
2.20 Data analysis ..... 67
3. Results ..... 68
3.1 The *cydC* gene in *M. smegmatis* encodes a functional protein ..... 68
3.2 Modeling the CydDC subunits ..... 72
3.3 Construction of a plasmid carrying the Mtb *cydDC* genes for heterologous expression in *E. coli* ..... 75
3.4 Construction of a plasmid carrying the *M. smegmatis cydDC* genes for heterologous expression in *E. coli* ..... 77

`

3.5. Heterologous expression of the Mtb putative transporters restores C*bd*O biogenesis in *E*. *coli.* ..... 79

3.6 Growth kinetic analysis of *E*. *coli* and its derivative strains ..... 80

3.7 Heterologous expression to assess the stationary growth phase arrest phenotype 82

3.8. Heterologous expression to assess the temperature sensitivity defect of the *E*. *coli* Δ*cydD* strain ..... 84

3.9 Heterologous expression is able to restore sensitivity towards exposure to exogenous hydrogen peroxide ..... 86

3.10 Construction of an in-frame double deletion mutant of the *M*. *smegmatis* that lacks the *cydDC* operon. ..... 87

3.10.1 Construction generation of the double deletion of the *cydDC* operon by recombineering in *M. smegmatis* ..... 89

3.12 Selection of Single Crossover recombinants ..... 91

3.13. Genomic confirmation of the Δ*cydDC* mutant ..... 91

3.13 Construction of the M smegmatis ΔcydDC genetically complemented strain... 94

3.14. Deletion of *cydDC* leads to loss of the heme *d* peak in the membrane fraction of *M. smegmatis* ..... 95

3.16. Growth kinetic analysis of *M. smegmatis* and its derivative strains. ..... 96

3.17 The Δ*cydDC* mutant strain is sensitive to exogenous hydrogen peroxide ..... 97

3.18. The Δ*cydDC* mutant strain fails to exit stationary growth phase ..... 98

4. Discussion ..... 100

4.1 Modeling the CydDC subunits ..... 100

4.2 The presence of the *cydDC* genes is necessary for C*bd*O biogenesis ..... 103

4.3 Growth kinetics of *E*. *coli* derivative strains and the *M. smegmatis* Δ*cydDC* mutant 104

4.4 The role of C*bd*O in exit from stationary phase. ..... 106

`

4.5 Heterologous expression corrects temperature sensitivity phenotype ..... 107

4.6 Loss of C*bd*O leads to sensitivity to oxidative stress induced by hydrogen peroxide ..... 108

5. Conclusion ..... 110

6. Limitations and future studies ..... 110

7. Appendices ..... 112

8. References ..... 118

`

**Abbreviations**

| | |
|---|---|
| **ABC** | ATP-binding cassette |
| **Amp** | Ampicilin |
| **APCs** | Antigen presenting cells |
| **ART** | Antiretroviral therapy |
| **ATP** | Adenosine triphosphate |
| **BCG** | Bacille Calmette-Guérin |
| **BDQ** | Bedaquiline |
| **bps** | Base pairs |
| **BSA** | Bovine serum albumin |
| **C*bd*O** | Cytochrome *bd* Oxidase |
| **CFU** | Colony forming units |
| **CO** | Carbon monoxide |
| **CTAB** | Cetyltrimethylammonium bromide |
| **DIG-dUTP** | Digoxygenin labeled –dUTP |
| **DMSO** | Dimethyl sulfoxide |
| **DNA** | Deoxyribo-nucleic acid |
| **dNTPs** | Deoxynucleotide triphosphates |
| **DOTS** | directly observed therapy short-course |
| **dUTP** | Deoxy-Uracil triphosphate |
| ***E. coli*** | *Escherichia coli* |

`

| | |
|---|---|
| **EDTA** | Ethylenediaminetetraacetic acid |
| **EMB** | Ethambutol |
| **EPTB** | Extrapulmonary tuberculosis |
| **ESAT-6** | Early secretory antigenic target 6 **(Esx-1)** |
| **ETC** | Electron transport chain |
| **Fe** | Iron |
| **$Fe^{2+}$** | Ferric ion |
| **Fe-S** | Iron-sulfur |
| ***g*** | Gravitational acceleration |
| **g** | grams |
| **Gly** | Glycine |
| **GTP** | Guanosine triphosphate |
| **HCl** | Hydrochloric acid |
| **HCOs** | Heme copper oxidases |
| **HTR** | High temperature resistant |
| **His** | Histidine |
| **HIV** | Human Immuno-deficiency Virus |
| **hrs** | Hours |
| **Hyg** | Hygromycin |
| **IFNγ** | Interferon gamma |
| **INH** | Isoniazid |

`

| | |
|---|---|
| **Kan** | Kanamycin |
| **kbs** | Kilo base pairs |
| **KCl** | Potassium chloride |
| **kDa** | Kilo Daltons |
| **L** | Liters |
| **l** | length |
| **LA** | Luria Bertani agar |
| **LB** | Luria Bertani broth |
| **LTBI** | Latent TB infection |
| **M** | Molar |
| **MK** | Menaquinone |
| **mL** | Milli liters |
| **mm** | Milli meters |
| **MDR-TB** | Multi-drug resistant Tuberculosis |
| **$MgCl_2$** | Magnesium chloride |
| **min** | Minutes |
| ***M. smegmatis*** | *Mycobacterium smegmatis* |
| **Mtb** | *Mycobacterium tuberculosis* |
| **MTBC** | *Mycobacterium tuberculosis* complex |
| **NaCl** | Sodium Chloride |
| **NaOH** | Sodium hydroxide |

`

| | |
|---|---|
| **$NAD^+$** | Nicotinamide adenine dinucleotide |
| **NADH** | reduced form of $NAD^+$ |
| **NEB** | New England Biolabs |
| **ng** | Nanogram |
| **NO** | Nitric oxide |
| **OD** | Optical density |
| **oriM** | Origin of replication in Mycobacteria |
| **PAMPs** | Pathogen associated molecular patterns |
| **PCR** | Polymerase chain reaction |
| **PMF** | Proton motive force |
| **PRR** | Pattern recognition receptors |
| **PTB** | Pulmonary tuberculosis |
| **PZA** | Pyrazinamide |
| **Redox** | Oxidation reduction |
| **RIF** | Rifampicin |
| **RNI** | Reactive nitrogen intermediate |
| **ROI** | Reactive oxygen intermediate |
| **RPM** | Rotation per minute |
| **$sdH_2O$** | Sterile distilled water |
| **SDS** | Sodium dodecyl sulfate |
| **SDH** | Succinate dehydrogenase |

`

| | |
|---|---|
| **sec** | Seconds |
| **Ta** | Annealing temperature |
| **TB** | Tuberculosis |
| **TCA** | Tri-carboxylic acid cycle |
| **TLRs** | Toll-like receptors |
| **Tm** | Melting temperature |
| **TNF-α** | Tumor necrosis factor alpha |
| **µg** | micrograms |
| **WHO** | World Health Organization |
| **XDR** | Extensively drug resistant |

`

# 1 Introduction

## 1.1 Tuberculosis diagnosis and challenges

Tuberculosis (TB) is a deadly pulmonary disease caused by the notorious human pathogen *Mycobacterium tuberculosis* (Mtb) (Filliol et al., 2002). Although commonly associated with chronic lung damage, TB can infect other anatomical sites of the body to cause extrapulmonary TB (EPTB) disease such as disease in the lymph nodes (Kim et al., 2003). Mtb is a deadly pathogen which has historically afflicted mankind (Krause, 1927, Keshavjee and Farmer, 2012). Today, Mtb is responsible for an incidence of 9.6 million TB cases, a mortality rate of 1.4 million cases of pulmonary TB (PTB) and 0.8 million cases of EPTB cases annually across the globe (WHO, 2016) (Figure 1.1.).

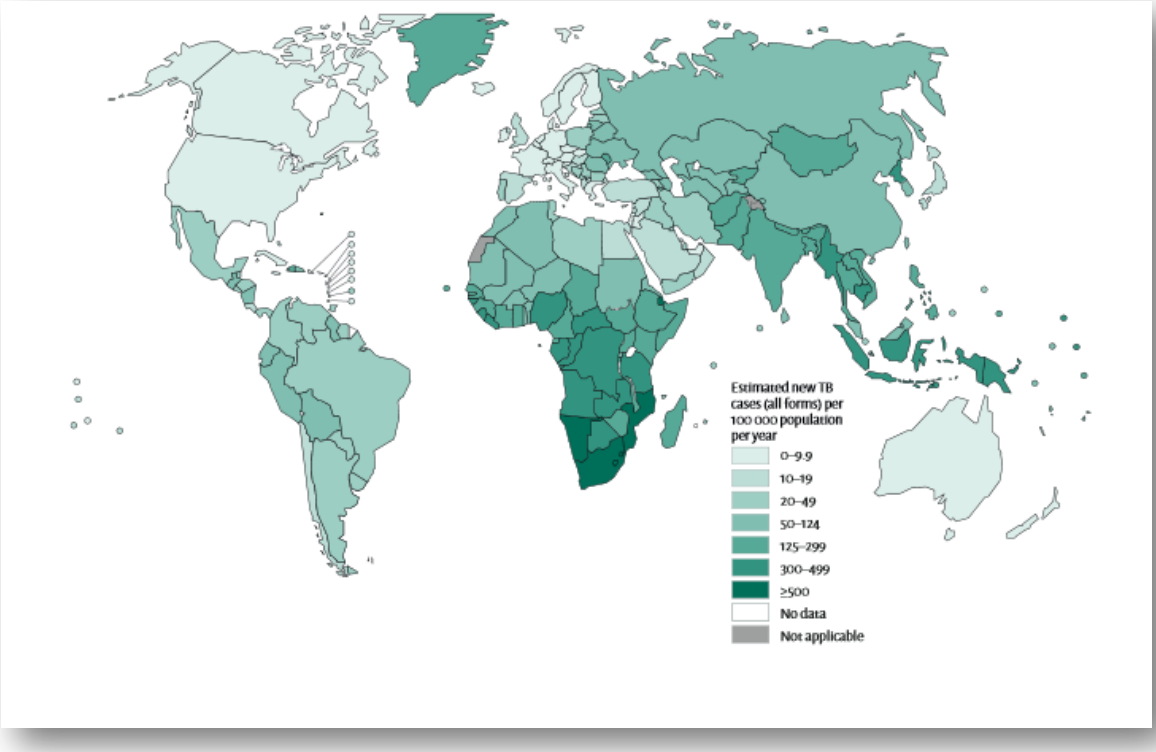


**Figure 1.1**. Diagrammatic illustration of the world map showing TB hotspots or estimated TB incidences in 2016 by of shades of green. Intense green colour corresponds to a high number of incident cases per 100 000 population annually. The African continent is the worst affected with South Africa (SA) showing the highest incidence with more than 500 new TB cases recorded each year per 100 000 population. Adapted from WHO 2016.

`

Despite being curable, TB continues to claim a massive amount of human life as exemplified by the grim statistical figures. Currently, the global TB epidemic is more intense in developing countries such as South-Africa (S.A) Figure 1.1.

Challenges that hamper the successful eradication of TB include numerous socio-economic factors and lack of innovative interventions. Poverty is a reality for many people in third world countries (DOH, 2015, Amaral et al., 1996). As a result, establishment of sporadic informal settlements are common and these are marked by problems of overcrowding, poor hygiene and malnutrition, which are thought to be key drivers of TB infection (DOH, 2015, Millet et al., 2013). Furthermore, developing countries have a vast landscape of rural land, where there is additional problems of poor sanitation and improper healthcare infrastructure (DOH, 2015, Millet et al., 2013). In TB endemic countries with such challenges, the burden of disease has increased to unprecedented levels causing rampant loss of human life due to the inability to detect and treat source cases timeously (WHO, 2016). As such, better diagnostic tools are a crucial necessity. These provide a frame work to better manage cases of outbreaks and to initiate sick individuals on chemotherapy (Yagui et al., 2006, Tenover et al., 1993, Organization and Organization, 2007). The late 19$^{th}$ and early 20$^{th}$ century saw numerous therapeutic innovations to combat TB. For instance, in 1882, Sir Robert Koch developed tuberculin as a proposed cure for TB, which saw success as a diagnostic tool rather than a curative measure (Trudeau, 1892). Tuberculin has since been repurposed for TB diagnosis under the moniker Tuberculin Skin test (TST) (Cooke, 1915). TST is in use today as pure protein derivative (PPD) and is at best useful in diagnosing latent TB infection (LTBI) (Stavri et al., 2012). Upon suspicion of TB, various tests including chest X-ray radiography and sputum smear microscopy are performed to confirm the presence of the tubercle bacilli (DOH, 2014, Rabahi et al., 2002).

In urban settlements, infrastructure is widely available but is outdated. For instance, the gold standard for diagnosis in a country such as S.A, with an annual incidence of 450 000 cases remains solid/liquid culture based methods (DOH, 2014, SSA, 2013). Although the latter are specific, they have inherent limitations such as the inability to infer drug susceptibility data which is a crucial necessity when initiating sick individuals

`

on treatment (DOH, 2014). In this regard, the advent of molecular diagnostic tools such as GeneXpert and Genotype MTBDRplus has revolutionized TB diagnosis, yielding short turnaround times, better sensitivity and providing drug susceptibility data (DOH, 2014, WHO, 2016).

Compounded to issues of socio-economic problems, is the lack of new drugs with improved killing kinetics. One of the reasons TB eradication has been challenging is the lengthy treatment duration, with a high pill burden which contributes to non-compliance, ultimately culminating in the emergence of drug resistant strains of Mtb (Adane et al., 2013). The emergence of such strains has occurred at an alarming rate globally, and threatens the eradication of TB (WHO, 2016). Finally, and arguably one of the major drivers of the TB epidemic, and deeply entrenched in TB endemic settings, is comorbidity with the human immunodeficiency virus (HIV) (Rabahi et al., 2002). The dual synergy in individuals with gradual immune decline is deadly, and increases the TB incidence toll which enhances the risk of primary infection or reactivation TB (WHO, 2016).

## 1.2 TB Transmission and Pathogenesis

Mtb is an airborne pathogen, transmitted by the inhalation of infected respiratory nuclei expelled from an individual with active PTB disease. In a new host, the infective respiratory nuclei travel via respiratory air passages to the upper or lower lobes of the lung, where there is elevated oxygen and inherent delayed immunity (Figure 1.2) (Balasubramanian et al., 1994).

`

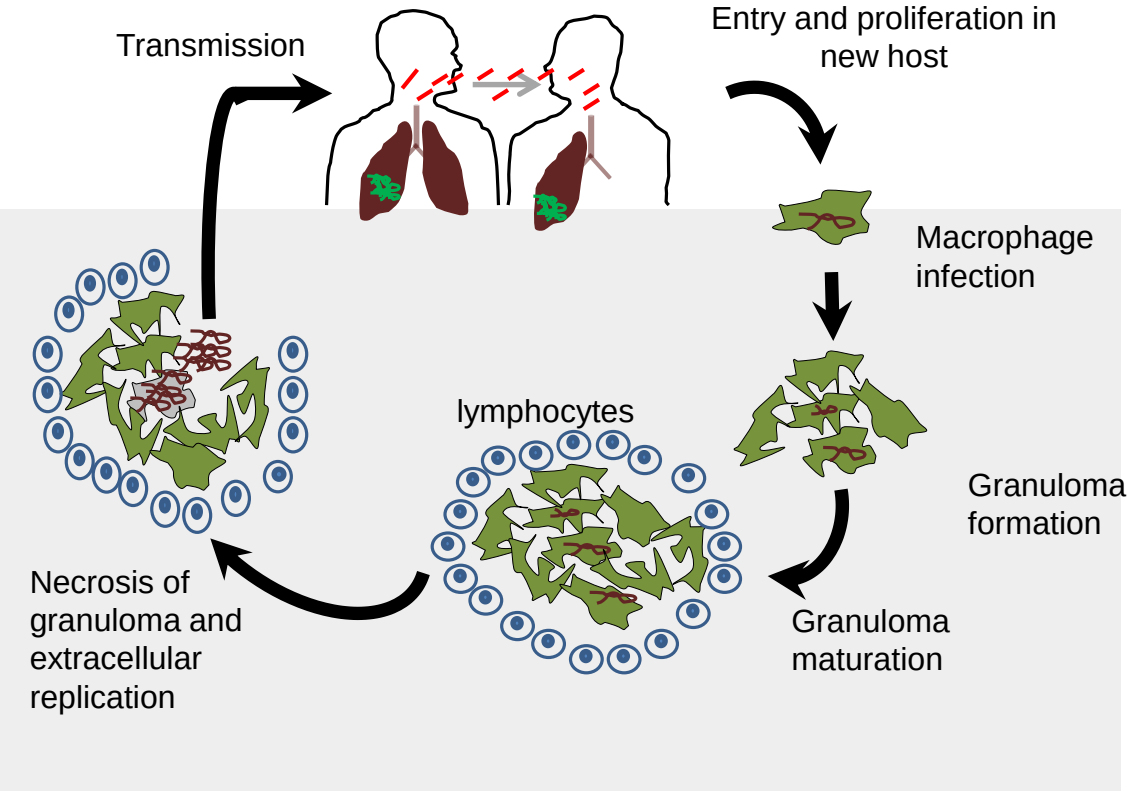


**Figure 1.2**. Schematic illustration of TB transmission and pathogenesis. Adapted from Cambier et.al., 2014. Infection is acquired when an uninfected person inhales respiratory nuclei containing Mtb. In the new host, Mtb replicates until encountered by resident alveolar macrophages (AMs) in the lung. The formation of an intact granuloma begins until it matures to form a barrier of containment. The granuloma collapses in an event of gradual immune decline releasing the Mtb which may remain localised or hematogenously disseminated. In the cycle of infection, Mtb is expectorated in the process of coughing to infect a new host.

In the lungs, Mtb is rapidly engulfed by dendritic cells (DCs), monocytes and alveolar macrophages (Sakamoto, 2012). The initial encounter of Mtb with the host is primarily mediated by alveolar macrophages (AMs) (Sakamoto, 2012). AMs recognize and interact with pathogen associated molecular patterns (PAMPs) on the surface of Mtb through a diverse group of pathogen recognition receptors (PRR) (Bafica et al., 2005, Fremond et al., 2004, Ryffel et al., 2005). Most frequently, host pathogen interaction occurs through toll like receptors (TLRs), which stimulate a chronic pro-inflammatory cytokine response that is growth restrictive for the bacilli (Bafica et al., 2005). This interaction also establishes a protective niche, wherein Mtb persists indefinitely in a metabolically quiescent state. Upon phagocytosis by alveolar macrophages, Mtb has the capacity to replicate unchecked intracellularly, inducing necrotic lesions that

`

ultimately result in the demise of the Mtb laden macrophages (Vergne et al., 2005, Ferrari et al., 1999, Chen et al., 2006). Necrosis results in death of most bacteria (Figure 1.2).

In immunocompetent individuals, bacterial cells that survive the respiratory burst are rapidly engulfed by monocytes (Gercken et al., 1994, Shi and Pamer, 2011). Monocytes induce trafficking of various cell types to the site of infection, establishing a highly structured barrier known as the granuloma to aid in containment of infection (Gonzalez-Juarrero et al., 2001). The lesion at the initial site of implantation is called the ghon focus. Tubercle bacilli may traffic via the lymphatic system to regional lymph nodes prior to the formation of the granuloma, causing lymphadenitis and granulomatous lymphaginitis. These sites colonized by Mtb are collectively referred to as the Rankes complex. Extensive dissemination of Mtb can occur via the blood stream during these early stages of infection. Approximately, 90% of infected immunocompetent individuals can resolve these lesions without progressing to active TB disease. However, in 10% of infected individuals, it is suspected that a high bacterial burden, immune decline or infection with a highly virulent strain results in primary progressive disease (Comstock, 1982). In individuals that do not clear the infection but also do not display symptoms, the tubercle bacilli are postulated to exist in a metabolically quiescent state. Studies of gene expression have shown that under these conditions, Mtb shuts down key anabolic processes, down-regulates expression of most non-essential genes and exists in a non-replicative state (Eoh and Rhee, 2013). This chronic state is diagnosed as LTBI which afflicts 2 billion individuals worldwide (WHO, 2015). In this state, a patient has no clinical manifestation of the disease and can exist in this condition for a life time, barring an event that leads to health deterioration (Corbett et al., 2003). In the event of gradual health decline, which occurs between 5-10% of individuals who relapse, the highly structured granuloma steadily collapses and forms a caseous granuloma which eventually liquefies to form a cavitary granuloma (Tufariello et al., 2003). Herein, Mtb is able to escape to other anatomical sites and cause miliary TB disease or cause further lung damage (Corbett et al., 2003). This is diagnosed as secondary TB disease and is mainly characterized by symptoms ranging from unexplained weight loss, to dyspnea (Sagbakken et al., 2008). Approximately 80% of clinical cases originate from secondary

`

TB disease (Garay, 1996). Moreover, immune compromised individuals are unable to recruit more immune cells to the site of infection due to T-cell depletion and in such cases, Mtb causes debilitating EPTB disease which accounts for 15% of secondary reactivation cases (De Backer et al., 2006). These complex clinical presentations in both immune competent and immune compromised individuals render the disease difficult to treat and manage.

### 1.3 Treatment and drug resistance

TB is a curable but challenging disease to treat, requiring protracted treatment with combinatorial therapeutic drugs (Maher et al., 2003). This is evidenced by the fact that in the post antibiotic era, TB is still associated with a high mortality rate. In S.A alone, TB claims just under 65 000 lives each year (SSA, 2013). Since the discovery of rifampicin (RIF) in 1957, multiple drug treatment was implemented for the management of drug susceptible TB due to high relapse cases and the emergence of resistance when mono-drug therapy was administered (Keshavjee and Farmer, 2012, Sensi, 1983). To increase cure rates and prevent the soaring emergence of drug resistant strains, the WHO implemented Directly Observed Short Course Therapy (DOTS) were, drugs are administered to patients under the direct supervision of a health care professional (WHO, 1995). At present, the standard treatment protocol for short course combination therapy for drug susceptible TB in SA includes a two-month intensive phase of RIF, isoniazid (INH), ethambuthol (EMB) and Pyrazinamide (PZA), followed by four months continuation phase of RIF and INH (DOH, 2014).

EPTB is associated with significant fatalities globally and treatment involves the same regimen with the same duration as PTB for the drug intensive phase, while the continuation phase can be extended up to seven months (DOH, 2014). Moreover, the treatment of TB is complicated by multiple therapeutic complexities including but not limited to a high pill burden, poor drug penetration to certain body compartments and adverse drug-drug interactions. Adding to this, is the pool of approximately 2 billion individuals with LTBI, which is difficult to treat and has rendered TB nearly impossible to eradicate. Approximately 10% of this vast population stands a life time risk of relapsing

`

to active PTB disease, of which 15% will develop EPTB (WHO, 2016). INH preventative therapy has been proven effective and is the only wide-spread therapy for LTBI (WHO, 2016). INH therapy is difficult to scale and needs protracted treatment durations, However, nine months can generally suffice to achieve bacterial clearance (Cohen et al., 2006). Comorbidity with HIV is a major factor that threatens the successful eradication of TB especially in the context of the 2 billion individuals with LTBI. The drug antagonism between anti-TB drugs and antiretroviral therapy (ART) is generally not well understood. However, it has been demonstrated that RIF gradually decreases the plasma concentration of nevirapine and efavirenz (Ngaimisi et al., 2011). This may confer resistance to ART therapy due to exposure of HIV to sub-lethal drug concentrations during therapy. As TB is an opportunistic disease in HIV infected individuals, resistance to ART results in the gradual dissolution of the solid granuloma through depletion of the CD4 T-cell population, which constitute the granuloma wall. This leads to poor containment of TB disease in the lungs of HIV infected individuals creating numerous therapeutic challenges.

The rapid emergence of drug resistant TB strains is unequivocally one of the major drivers of the TB epidemic (WHO, 1993). Multidrug resistant TB (MDR-TB) is defined as TB that is resistant to either RIF or INH (WHO, 2016). Cases of MDR-TB are a common occurrence globally, with WHO estimating 450 000 incident cases and approximately 170 000 deaths associated with MDR-TB in 2012 alone (WHO, 2013). MDR-TB is more expensive to treat and requires protracted treatment with toxic drugs (WHO, 2016). This has created an urgent need for new drugs. Recently, the food and drug administration (FDA) approved Bedaquiline, the first new TB drug in 40 years, for the treatment of MDR-TB (Mahajan, 2013). Patients with MDR-TB are elevated to a combinatorial regimen of fluoroquinolones and other second line drugs. In addition to MDR-TB, extensively drug resistant TB (XDR-TB) has been reported. This form of drug resistant TB comprises MDR-TB, with the added resistance to fluoroquinolones and aminoglycosides (Daniel et al., 2013). The prevalence of these composite forms of drug resistance in the clinic demonstrates that Mtb has the intrinsic ability to develop resistance to anti-TB agents. This can occur through multiple mechanisms such as the ability to extrude drugs using dedicated transport systems (Calgin et al., 2013).

`

Alternatively, stable chromosomally encoded resistance is acquired through exposure to sub-lethal concentrations of antimicrobial agents (Black et al., 2014). This underscores the need to develop new drug that have novelty in their action.

## 1.4 New drugs for TB

TB represents a serious challenge to global health. In recent years, various factors some of which have been described in the previous sections have contributed to TB resurgence with increased virulence due to the emergence of MDR strains. As a result, substantive effort has been directed towards the discovery of novel drugs to add to the existing antibiotic arsenal (Neres et al., 2012). New lead antibiotics that have resulted from these endeavors are described next.

### 1.4.1 Benzothiazinone

Benzothiazinone (BTZ) represents a group of new drugs in the developmental pipeline for TB treatment. BTZ043 a lead compound, is presently in the late preclinical stages of development (Lienhardt et al., 2012). BTZ043 shows a minimal inhibitory concentration (MIC) of 1 ng/mL against Mtb, making it significantly more potent than any of the currently used drugs. BTZ043 targets the DprE1 component of the mycobacterial decaprenylphosphoryl-β-D-ribofuranose-2′-epimerase encoded by the *dprE1*/*dprE2* operon (Makarov et al., 2009). These genes are essential for growth of Mtb and *M. smegmatis* (Crellin et al., 2011, Sassetti and Rubin, 2003). Expression of this operon is pre-requisite to carry out the epimerization reaction of decaprenylphosphoryl-β-D-ribofuranose (DPR) into decaprenylphosphoryl-β-D-arabinose (DPA)(Mikušová et al., 2005). DPA is the sole monomer for the synthesis of the arabinan moiety of the mycobacterial cell wall, whose unique composition renders mycobacteria insensitive to a number of antibiotics (Wolucka, 2008). Furthermore, all Mtb clinical isolates tested so far, from drug sensitive to all forms of MDR cases, were susceptible to BTZ043, making this drug a promising candidate for the treatment of all forms of TB (Wolucka, 2008).

`

### 1.4.2 Q203

Q203 is a lead compound belonging to a class of imidazopyridine amides currently under clinical development (Pethe et al., 2013). Q203 shows remarkable activity in the nanomolar range with MICs of 2.7 nM/mL for Mtb (H37Rv) and 0.28 nM/mL in macrophages. The cellular target for Q203 is the $bc_1/aa_3$ oxidoreductase, which is encoded by the *qcrCAB* operon (Pethe et al., 2013). Inhibition by Q203 is specific to Mtb and the same killing effect was observed against all forms of MDR-TB in clinical isolates. Q203 is easy and affordable to synthesize, which is an added benefit for low-income TB endemic countries. This candidate showed remarkable safety with no signs of clinical toxicity at high dosage in mice (Pethe et al., 2013). Q203 also displayed remarkable stability, suggesting that it might achieve good exposure levels in the blood (Pethe et al., 2013). As a result, Q203 is an ideal drug candidate, which also displayed compatibility with other TB drugs (Pethe et al., 2013).

### 1.4.3 Bedaquiline

As mentioned previously, Bedaquiline (BDQ) is the first drug in 4 decades to receive accelerated approval by the FDA (Cohen, 2013). BDQ belongs to the arylquinolone class of drugs and although it displayed delayed killing kinetics in the initial days of administration. It is efficacious in bacterial clearance during protracted treatment. The cellular target of BDQ is the C-ring of the $F_1F_0$ ATP synthase. BDQ achieves bacterial killing by blocking the C-ring, leading to intracellular ATP depletion, periplasmic redox imbalance and subsequent death of bacteria (Sacksteder et al., 2012). BDQ is only approved for treatment of MDR-TB and has also displayed synergy with other anti-tubercular drugs (Sacksteder et al., 2012). These advances are anectodal proof that bacterial electron transport chains (ETCs) are relatively unexplored biological pathways with untapped potential for the identification of novel drug targets. This hypothesis forms the basis of the work presented in this MSc and will be explored further below.

## 1.5 The Electron transport chain

The increase in drug resistance and therapeutic complexities that present with treating HIV-TB co-infected individuals has necessitated an urgent need for new drugs, with

`

novel modes of actions. Moreover, in Africa, to succeed in the fight against TB, solutions that are tailored to the local needs are required. For this, this study explores the mycobacterial ETC, a new and tractable area of research in mycobacteria for the identification and validation of new drug targets. The following section reviews the literature of the components of the aerobic branch of the mycobacterial ETC, their role in electron transport, and their validation in drug development.

### 1.5.1 The aerobic branch of the mycobacterial ETC

Mycobacteria occupy diverse and dynamic ecological niches which has prompted various evolutionary adaptions for survival. These adaptations include utilization of their branched ETC (also referred to as the respiratory chain), which endows them with the ability to optimize ATP yield in adverse and constantly changing environments. The modular nature of the ETC allows fine tuning of its components to best suit prevailing growth conditions and the availability of electron donors or electron acceptors, Figure 1.3.

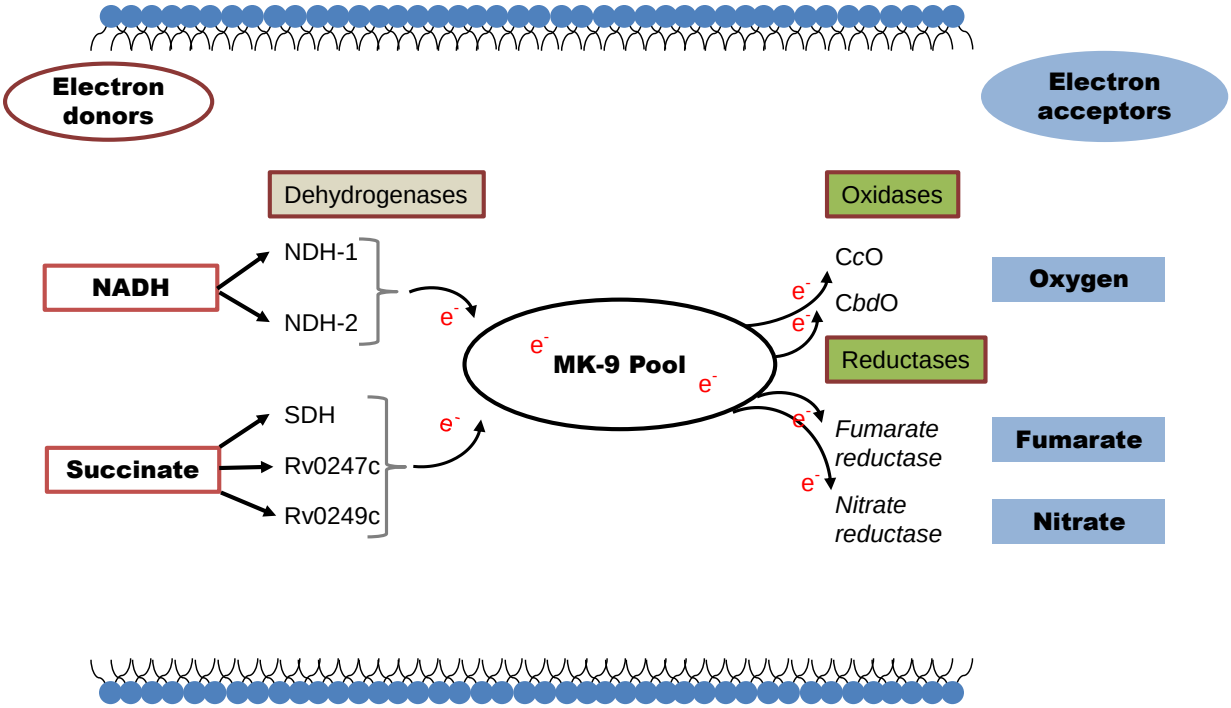


**Figure 1.3**. Schematic illustration of the branching and flexibility of Mtb showing electron donors and acceptors used by Mtb during respiration. Adapted from Hurdle et al., 2011. Electrons enter the ETC via NADH dehydrogenase (NDH) and succinate dehydrogenase (SDH) and are transferred to menaquinone (MK-9). Under aerobic conditions, electrons are transferred to oxygen via cytochrome $bc_1$ reductase-cytochrome $caa_3$ oxidase supercomplex (C*c*O) or the cytochrome *bd* oxidase (C*bd*O). Electrons can be transferred to nitrate and fumarate, when these are available, via the nitrate and fumarate reductases.

During different stages of TB pathogenesis, oxygen availability may vary widely, under aerobic conditions. To adapt to this, Mtb couples substrate catabolism to respiration using two terminal oxidases (with different affinities to oxygen), while in the absence of oxygen, electron transport is re-routed to anaerobic terminal oxidases (Figure 1.3). The ETC of bacteria is located in the plasma membrane and comprise a series of enzymes and enzyme complexes that catalyze coupled oxidation/reduction reactions.

### 1.5.2 The composition of the mycobacterial aerobic electron transport chain

The mycobacterial ETC comprises enzymes that vary in metal cofactor and heme composition in their catalytic center (Figure 1.4).

`

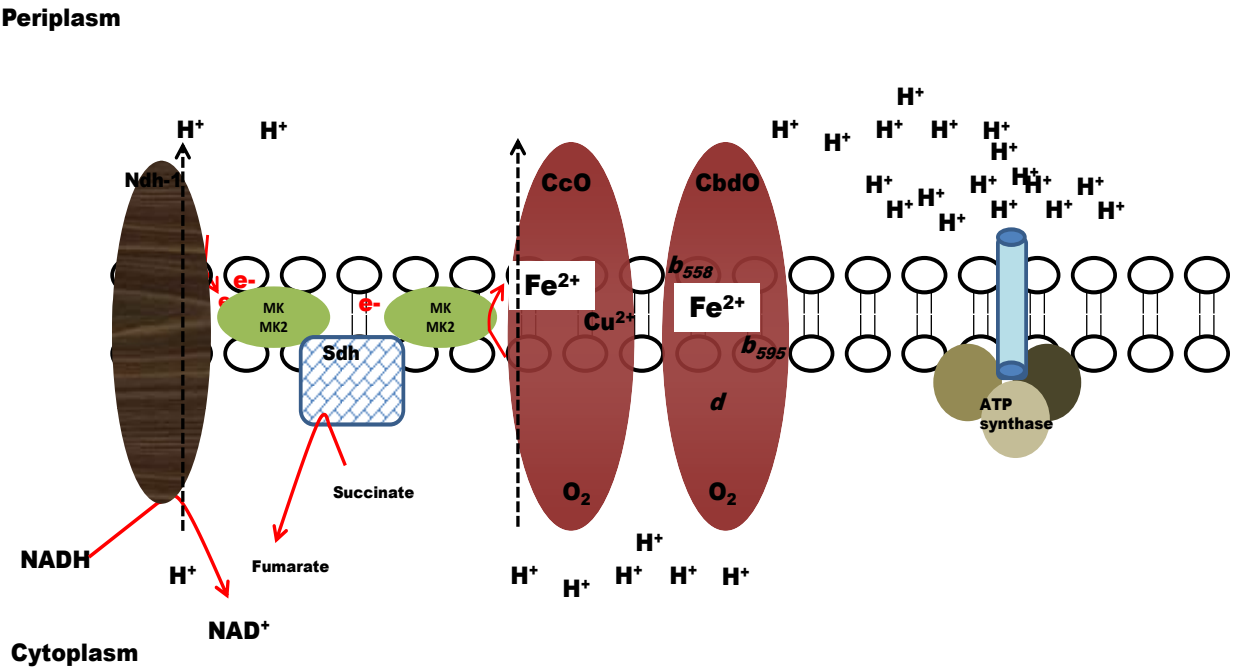


**Figure 1.4**. Schematic representation of the mycobacterial aerobic ETC. Electron flow is initiated by the oxidation of the reducing equivalents, NADH by NADH dehydrogenase (ndh-1) which is associated with the translocation of protons ($H^+$) across the cytoplasm and succinate dehydrogenase (*sdh*) respectively. The accumulation of protons in the periplasm builds a proton gradient which is used to generate ATP by the ATP synthase. The electrons that are released, are relayed through the lipid soluble menaquinol pool to one of the two terminal electron acceptors cytochrome c Oxidase (C*c*O) cytochrome *bd* Oxidase (C*bd*O) expressed under aerobic or hypoxic conditions respectively. Within the CbdO, $b_{558}$, $b_{595}$ and *d* represent heme molecules. Adapted from Hurdle et al., 2011.

Central to the ETC, is the lipophilic menaquinone pool, which is reduced by different dehydrogenases that in turn extract energy via oxidation of cytoplasmic electron donors (kana, 2009). This process is linked to the generation of periplasmic proton motive force (PMF) through proton translocation (kana, 2009). Due to the branching of the ETC, the menaquinol pool is oxidized by one of the terminal oxidases depending on oxygen tension (kana, 2009). The electrons are finally relayed to oxygen, which is the final electron acceptor under aerobic conditions. When the proton concentration in the periplasm is greater than in the cytoplasm, protons move through the membrane bound ATP synthase to synthesize ATP via oxidative phosphorylation (Chance and Williams, 1956).

The respiratory chain of Mtb has recently emerged as a previously untapped source for the identification and validation of new antitubercular drug targets. In the section below, the individual components of the aerobic branch of the mycobacterial ETC are detailed

`

further in terms of their biochemical properties, their role in electron transport, ATP synthesis and their potential as promising drug targets.

## 1.6 NADH dehydrogenase

Electron donors such as NADH and succinate are products of other metabolic pathways and enter the ETC of bacteria and mitochondria for oxidative metabolism. The initiation of electron transport depends on the action of quinone oxidoreductases, such as the NADH dehydrogenase and succinate dehydrogenase (Black et al., 2014). There are three types of NADH dehydrogenases in bacteria including the sodium pumping NADH dehydrogenase (NQR), the proton pumping NADH dehydrogenase (NDH-1) and non-proton pumping NADH dehydrogenase (NDH-2) (Kerscher et al., 2007). This classification is based principally on differences in structural complexity and their efficiency in energy conservation.

### 1.6.1 NDH-1

The type I NDH is structurally more complex and dynamic than the other two families of NADH dehydrogenases. In bacteria, NDH-1 is encoded by a 14 sub unit *nuoA-N* operon which represents the ortholog of the 45 subunit mitochondrial NADH dehydrogenase (Kerscher et al., 2007, Sazanov and Hinchliffe, 2006). Also known as complex I, this enzyme serves as the main gated channel for electrons into the ETC through the oxidation of its substrate, NADH, shown in Figure 1.5 (Kerscher et al., 2007).

`

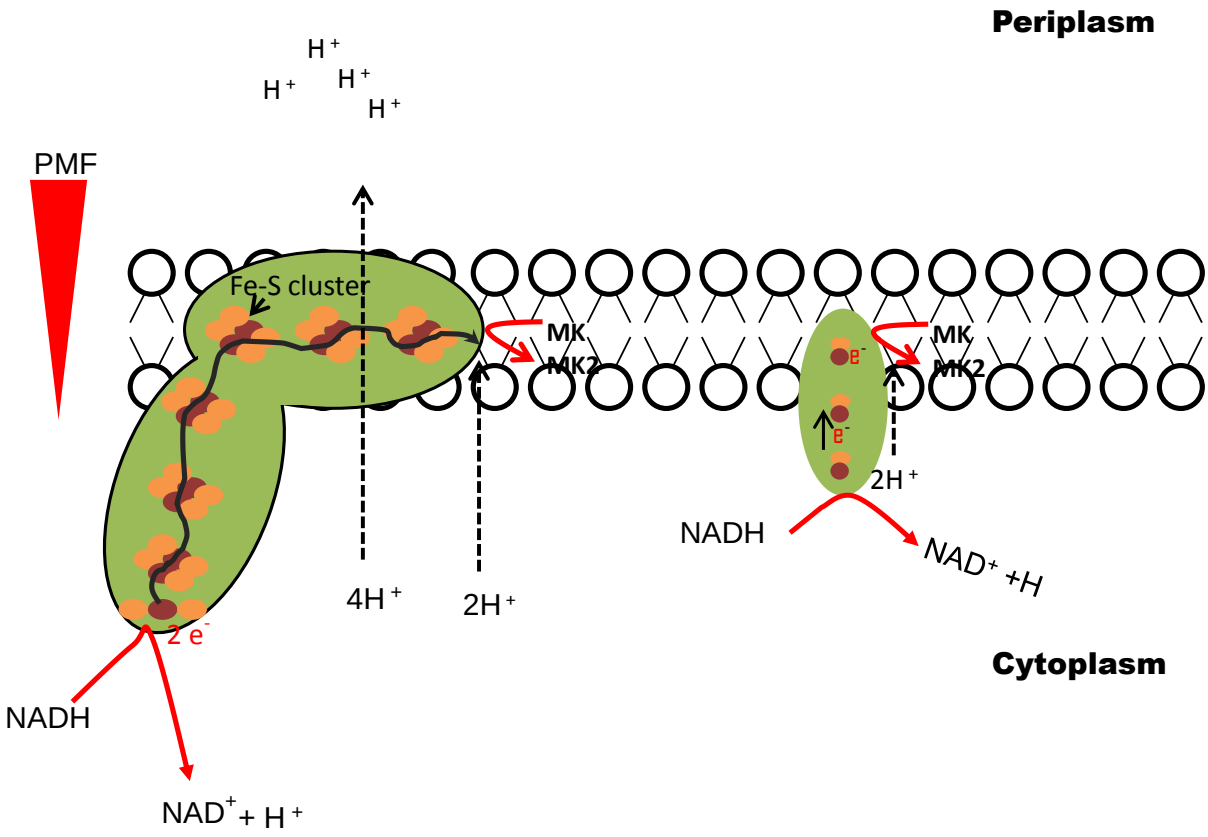


**Figure 1.5.** Diagrammatic illustration of the alternate forms of NADH dehydrogenase in Mtb. NDH-1 is involved in energy conservation through proton translocation across the cytoplasm. NDH-2 is the preferred alternate form in Mtb although it lacks proton pumping activity. In both cases type I and type II NDHs**,** facillitate initiation of the electron transport chain through the oxidation of NADH. This reaction results in recycling of redox intermediates contributing to redox homeostasis. Adapted from Sazanov and Hinchliffe, 2006.

Complex I is present in various species of mycobacteria, with an additional role of recycling the $NAD^+$ cofactor to ensure that other metabolic pathways are not negatively affected by an imbalance in the NADH/$NAD^+$ redox couple. NDH-1 is considered as the most basic form of the enzyme required to execute its holistic function. This includes NADH oxidation, quinol reduction and proton translocation (Kerscher et al., 2007). NuoB-G are cytoplasmic proteins which are associated with the membrane bound subunits and are responsible for the oxidation of NADH. NuoA, H, I J, K, L, M, and N are located in the lipid bilayer, with several predicted transmembrane domains that aid in the translocation of protons across the cytoplasm (Russell and Cook, 1995, Weinstein et al., 2005, Kerscher et al., 2007, Miesel et al., 1998). In terms of energetics, the

`

release of two electrons during NADH oxidation is coupled to the translocation of four protons, thus contributing to the conservation of energy in the form of a proton gradient in the periplasm (Figure 1.5). Proton translocation occurs through iron-sulfur (Fe-S) clusters that can interact with molecular oxygen. This Interaction contributes to the inherent low levels of oxidative radicals generated by the respiratory chain. Surprisingly, the activity of Complex I is completely abolished in *M*. *leprae* with the *nuoN* pseudo gene being all that remains of Complex I (Sassetti et al., 2003, Cole et al., 2001). Consistent with this, growth of Mtb in the *In vitro* hypoxic Wayne model has demonstrated that Complex I is dispensable for growth and is not required for persistance (Rao et al., 2008). The role of Complex I in proton translocation was determined experimentally in *E. coli*, and *Klebsiela pneumonia* through inhibition with piericidin A and the use of pH sensitive dyes (Stolpe and Friedrich, 2004). In Mtb infected macrophages, NuoG which encodes a subunit of Complex I has been implicated in the inhibition of apoptosis (Velmurugan et al., 2007). These results implicate complex I, which is highly expressed during anaerobic conditions in *E. coli* and Mtb, in virulence (Unden and Bongaerts, 1997, Shi et al., 2005).

### 1.6.2 NDH-2

Type II NDH also known as the alternative NADH dehydrogenase, is a single subunit flavoprotein that lacks the ability to translocate protons (Kerscher et al., 2007) (Figure 1.5). Besides its role in recycling $NAD^+$, which is a cellular oxidant in bacteria, this simple enzyme carries out the oxidation of NADH and reduces the quinone pool (Kerscher et al., 2007). NDH-2 is also present in mycobacteria and seems to be the preferred NADH:menaquinone oxidoreductase in several mycobacterial species. This is evidenced by the observation that the genome of *M*. *leprae*, which has undergone extensive reduction, retains a functional NDH-2 for oxidation of NADH (Sassetti et al., 2003, Cole et al., 2001). Furthermore, NDH-2 activity in *M*. *smegmatis* is 5-fold higher than NDH-1 activity (Miesel et al., 1998, Vilcheze et al., 2005). This enzyme is ubiquitous in prokaryotes and its expresion in *E. coli* occurs mainly under aerobic conditions (Unden and Bongaerts, 1997, Pereira et al., 2004). NDH-2 is present in Mtb in alternate forms as Ndh and NdhA (Pereira et al., 2004). Optimal *In vitro* growth of Mtb

`

requires the expression of NDH-2 while its expression in immune compromised mice shows that it is not required for pathogenesis (McAdam et al., 2002, Sassetti and Rubin, 2003). The presence of two forms of NDH-2 does not seem to be due to genetic redundancy as one copy appears to be more important than the other (Lin et al., 2011, Griffin et al., 2011). NDH-2 enzymes are the simplest NADH dehydrogenases and encode a short polypeptide (463 amino acids) with two **G**X**G**XX**G** motifs for NADH oxidation and flavin (FAD) binding for menaquinone reduction (Melo et al., 2004, Weinstein et al., 2005). Type II NDHs have been explored for drug development by screening a variety of inhibitors. As proof of the principle, *In vitro* screening studies with phenothiazines demonstrated mycobactericidal activity with these compounds, albeit at very high minimum inhibitory concentrations (MICs). Chlorpromazine and other related drugs have also been shown to have bactericidal effect against MDR-TB (Amaral et al., 1996). For instance, trifluoperazine (TPZ), a derivative of phenothiazines, displayed activity in a macrophage model and compatibility with other antitubercular drugs (Reddy et al., 1996). Mechanistic studies also unraveled the mode of inhibition of phenothiazines, which includes uncompetitive inhibition of Complex I (Yano et al., 2006). The consequences of uncompetitive inhibition in mycobacteria may include an imbalance in the redox carriers (NADH/$NAD^+$ couple), reduced electron flux and reduced PMF resulting in a decrease in ATP yield (Katoch et al., 1998). These advances illustrate the unique mycobactericidal activity of phenothiazines through disruption of ATP synthesis and impeding cofactor recycling.

### 1.7 Succinate dehydrogenase (SDH)

Also known as Complex II, SDH is also capable of initiating the ETC in both bacteria and mitochondria. SDH is a flavoprotein with a dual role in the ETC and the tricarboxylic acid cycle (TCA) through the oxidation of succinate to fumarate and the concomitant transfer of two electrons to the menaquinone pool to generate menaquinol (Black et al., 2014). Quinol fumarate reductase also known as fumarate dehydrogenase (FDH), is an enzyme that is functionally and structurally similar to the SDH, and for this reason, it is annotated as Complex II as well (Cecchini et al., 2003). During anaerobic conditions, FDH catalyzes the oxidation of quinol to reduce fumarate to succcinate (Cecchini et al.,

`

2003). SDH are generally multi-subunit enzymes that do not couple succinate oxidation to proton translocation (Figure 1.6).

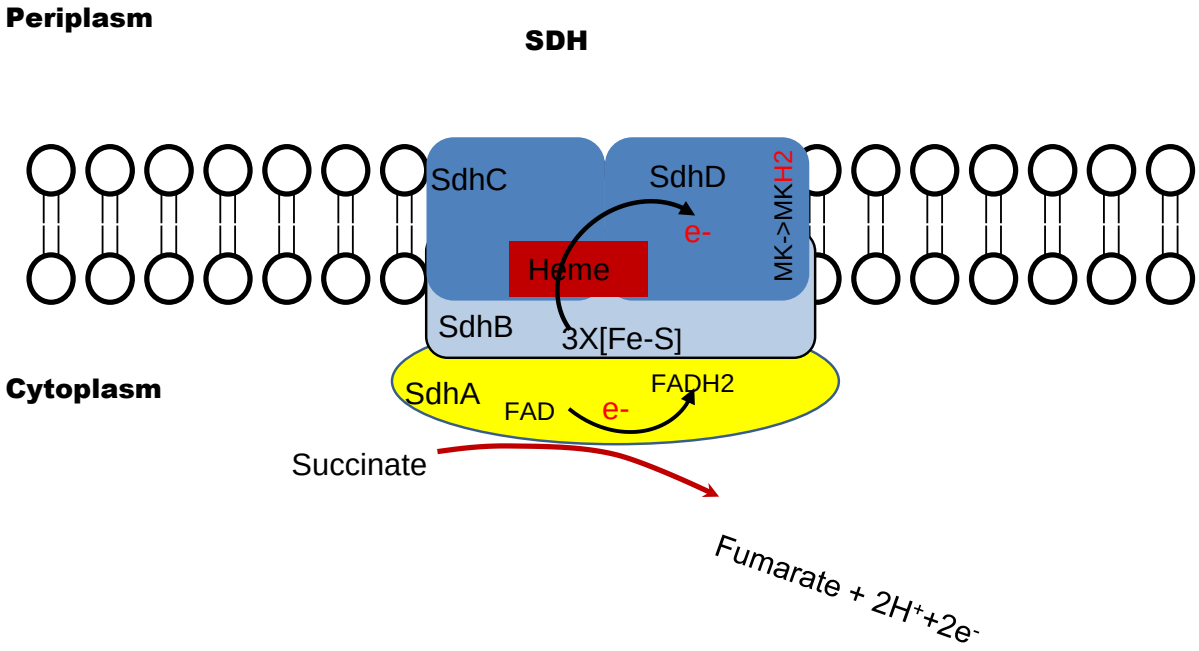


**Figure 1.6**. Schematic illustration of succinate dehydrogenase also known as Complex II. In Mtb SDH is encoded by four subunits: SdhA, SdhB, SdhC and SdhD. SDH reduces the menaquinol pool but is not associated with energy conservation through proton translocation. Adapted from (Huang and Millar 2013.)

In mycobacteria, SDH is present as SDH-1 and SDH-2. SDH-2 is encoded by *sdhA*, *sdhB*, *sdhC* and *sdhD*. Subunits of *sdhA* and *sdhB* are hydrophillic and form the cytoplasmic domains of SDH-2. *SdhA* contains the substrate binding site and the FAD prosthetic group (Cecchini et al., 2003, Lancaster, 2002). Subunit B of SdhB contains three distinct Fe-S clusters for electron transport and is sandwiched between SdhA and the membrane. SdhC and SdhD constitute integral membrane domains with variable number of *b*-type cytochromes and quinone binding sites, which are responsible for the two electron transfer and subsequent reduction of menaquinone (Cecchini et al., 2003, Lancaster, 2002). The reaction entailing the oxidation of succinate and the concomittant reduction of menaquinone is biochemically unfavourable due to the low reduction potential of menaquinone relative to that of the oxidation of succinate. This reaction would result in the reversal of electron transfer. Thus to circumvent this, it is proposed that the membrane reduction potential is used to drive the reaction forward, where the

`

electrons from the cytosol pass through cytochrome *b* via the Fe-S clusters until deposited into the menaquinone pool (Schirawski and Unden, 1998). Alternate forms of the SDH enzyme are differentially expressed depending on the culture conditions. For instance, SDH-1 was upregulated 4-fold under energy limiting conditions while SDH-2 was significantly downregulated under the same conditions (Berney and Cook, 2010). Conversely, SDH-2 was upregulated 2-fold while SDH-1 was significantly downregulated under high oxygen tension (Berney and Cook, 2010). Therefore, it is tempting to speculate that these expression profiles implicate SDH-1 as a dedicated enzyme, which is adapted to functioning at high oxygen tension while its counterpart essentially functions as FDH during hypoxia. The SDH complex is dispensable for growth in Mtb (Sassetti et al., 2003) and as such, the true role of this enzyme is not thoroughly understood and requires elucidation.

### 1.8 Menaquinone

Isoprenoid quinones form part of bacterial plasma membranes (Lester and Crane, 1959) and are pivotal in electron transport, oxidative phosphorylation and possibly active transport (Dunphy and Brodie, 1971, Redfearn, 1967, Taber, 1980). Quinones are lipophillic proteins that facilitate electron transport in the inner membrane during energy metabolism (Hedrick and White, 1986) and have been used as taxonomic markers in bacteria (Bragg and Hou, 1967). There are various types of quinones which differ in number and side chain position of the encoded structural subunits. Ubiquinones, menaquinones and desmethyl menaquinones are widespread bacterial quinones (Hedrick and White, 1986). Ubiquinones predominate in eukaryotes and some gram negative bacteria while menaquinones are widespread among gram positive, gram negative bacteria and archaeabacteria (Hedrick and White, 1986). Desmethyl menaquinones are not common and have been reported mainly in pathogenic enterobacteria (Hedrick and White, 1986). Mycobacteria employ MK, an inner membrane confined lipid soluble electron carrier for electron transport (Yassin et al., 1988). MK is a derivative of 2-methyl-1.4-naphthoquinone and contains variable lengths of repeating units of isoprenoids and its biosynthesis entails a range of enzymes. MK biosynthesis in Mtb is mediated by at least six genes encoded by the *menABCDEH*

`

gene cluster (Cole et al., 2001). Mtb and *M. smegmatis* rely exclusively on MK-9 as a redox intermediate (Collins and Jones, 1981, Collins et al., 1977, Yassin et al., 1988). MK-9 is reduced by both the NADH dehydrogenase and SDH to form menaquinol. In the presence of oxygen, the menaquinol pool terminates at one of the two terminal oxidases which subsequently oxidizes the reduced menaquinol pool (Yassin et al., 1988). The enzymes involved in the biosynthesis of MK-9 represent ideal drug targets for TB drug development as MK-9 is not homologous to the mitochondrial ubiquinone electron carrier. Hence, cross-reactivity with the human enzymes is not expected.

### 1.9 Cytochrome $bc_1aa_3$ super complex

Bacterial oxidases catalyze approximately 90% of molecular oxygen reduction estimated to occur in the biosphere (Norman et al., 1965). Unlike the mitochondrial ETC which has a single terminal cytochrome *c* oxidase, bacterial respirasomes are branched, harboring distinct terminal oxidases for the reduction of electron acceptors under specific conditions. Bacterial terminal oxidases are generally grouped into two super families; the heme copper oxidase (HCO) and the cytochrome *bd*-type oxidase super families. Whilst the latter will be discussed in more detail in the following section, HCOs are by far the largest super family of respiratory oxidases (García-Horsman et al., 1994). HCOs are ubiquitous in nature, virtually present in all domains of life. This super family also encompasses terminal oxidases that generally exist in complexes with other enzymes and collectively function in unison (García-Horsman et al., 1994). HCOs are characterized by the presence of multiple redox centers such as the presence of different types of cytochromes, Rieske Fe-S clusters (carried in the reductase component of the supercomplex) and multiple subunits encoded by the oxidase component of the supercomplex (Kitagawa and Ogura, 2007, Calhoun et al., 1994). Furthermore, HCOs are optimally expressed under normoxic growth conditions and couple quinol oxidation to the generation of a proton gradient across the cytoplasmic membrane (Matsoso et al., 2005). Their catalytic site, where oxygen reduction occurs, contains a copper atom and a cytochrome composed of a *b* type heme molecule. This binuclear catalytic center is notably different from the hetero-di-heme catalytic composition of the *bd*-type oxidase (Matsoso et al., 2005, García-Horsman et al., 1994).

`

The diagrammatic representation of the HCO found in Mtb, that is the Cytochrome $bc_1$ reductase-cytochrome *c* oxidase super complex, comprising cytochrome $bc_1$ reductase and cytochrome *c* oxidase components, is shown (Figure 1.7).

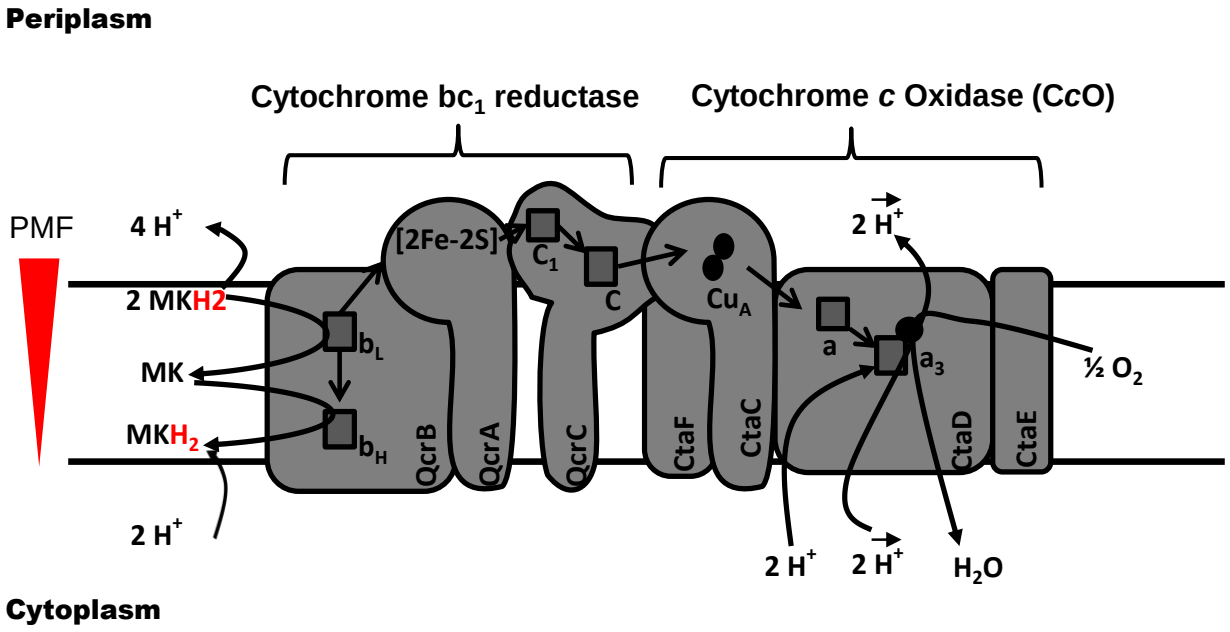


**Figure 1.7**. Cytochrome $bc_1/aa_3$ super complex. This oxidoreductase is composed of two enzyme complexes, namely: cytochrome $bc_1$ reductase and cytochrome *c* oxidase (C*c*O). The $bc_1$ complex is encoded by the *qcrCAB* operon while C*c*O is encoded by the *ctaBCDEF* operon. This super complex serves as the main aerobic branch for respiration under high oxygen tension. It catalyzes the reduction of oxygen to water and conserves energy through the formation of a proton motive force (PMF) in the process. Adapted from Graf et al., 2016.

In *Corynebacterium glutamicum*, the cytochrome $bc_1$ reductase is responsible for the oxidation of the menaquinol pool, a reduced electron carrier in gram positive bacteria (Megehee et al., 2006, Megehee and Lundrigan, 2007, Graf et al., 2016).The cytochrome $bc_1$ reductase of *C. glutamicum* and that of mycobacterial species is encoded by the *qcrCAB* operon (Pethe et al., 2013, Matsoso et al., 2005, Niebisch and Bott, 2001) Figure 1.7. Cytochrome *c* oxidase (C*c*O) is separately encoded by the *ctaBCDEF* operon (Figure 1.7) (Pethe et al., 2013, Matsoso et al., 2005, Niebisch and Bott, 2001). Bioinformatic analysis of the $bc_1$ reductase and C*c*O by Black and co workers revealed that both these components are conserved across the mycobacteria (Black et al., 2014, kana, 2009). The *qcrC* gene encodes a unique cytochrome comprising two *c*-type hemes with quinol binding sites, a typical feature of actinomycetes (Matsoso et al., 2005). The *qcrB* gene encodes cytochrome *b* and *qcrA*

`

encodes the Fe-S cluster subunit. In C*c*O, *ctaB* encodes an assembly factor while *ctaC-F* encode subunit II, III, IV and V respectively (Matsoso et al., 2005, Black et al., 2014), which form the transmembrane domains for proton translocation and a catalytic redox center comprising a copper ion, a high spin *b*-type heme, a tyrosine residue coordinated to histidine that in turn binds the heme for the reduction of dioxygen to water (Sousa et al., 2012). Due to the high degree of homology of the $bc_1$ complex in mycobacteria and in *C*. *glutamicum,* it has been proposed that the same structural integrity is preserved in Mtb (Niebisch and Bott, 2001) and *M. smegmatis* (Kana et al., 2001). Indeed, the presence of the $bc_1$ complex was since verified by two studies in Mtb and *M*. *smegmatis* (Matsoso et al., 2005, Megehee et al., 2006). Since this terminal oxidase plays a vital role in the growth of Mtb (Sassetti et al., 2003, Matsoso et al., 2005), it has been targeted for drug development by Q203 for which clinical trials are underway (Pethe et al., 2013, Kang et al., 2014). Serious growth defects have been reported upon inactivation of the $bc_1$ complex in *M*. *smegmatis* (Matsoso et al., 2005). Furthermore, disruption of this complex was accompanied by an increase in the expression of cytochrome *bd* oxidase (C*bd*O), suggesting that the two aerobic branches of the ETC in Mtb can accommodate changes in electron flux. Conversely, the opposite was not observed when C*bd*O was inactivated by targeted disruption (Megehee and Lundrigan, 2007). These advances in targeting terminal respirisomes involved in the production of ATP comprise a promising strategy for the eradication of TB. This MSc further explores the possiblity of targetting the assembly of the C*bd*O for TB drug development. For further context, the relevant literature pertaining to C*bd*O is discussed below.

## 1.10 Cytochrome *bd* Oxidase (C*bd*O)

### 1.10.1 Distribution and evolution

C*bd*O is widely distributed among prokaryotes, moreover, its distribution seems to be limited to prokaryotes that respire anaerobically (Brochier-Armanet et al., 2009, Baughn and Malamy, 2004). It has been shown that prokaryotes can encode one or more C*bd*O

`

family member and as a rule, microorganisms that encode multiple members of C*bd*O also harbor at least one HCO reductase (Borisov et al., 2011). C*bd*O is more common in proteobacteria and actinobacteria and has also been detected in 18 other bacterial phyla (Brochier-Armanet et al., 2009). C*bd*O is an ancient enzyme with a progenitor in both bacteria and the archaea. This unique enzyme may have originated in bacteria and acquired through horizontal gene transfer by various members of the archaea (Brochier-Armanet et al., 2009).

### 1.10.2 Genetics and physiological role

#### 1.10.2.1 The mycobacterial C*bd*O in relation to other bacteria

The ETC of mycobacterial species like of many bacteria terminate at the $aa_3$-type C*c*O or C*bd*O under aerobic conditions (Kana et al., 2009). The expression level of each terminal oxidase is dictated by $O_2$ abundance. For instance, C*c*O is highly active under oxystatic conditions whilst the expression of C*bd*O increases under microaerophillia (Kana et al., 2001, Aung et al., 2014, Matsoso et al., 2005). This is consistent with expression kinetics in *Azotobacter vinelandii* and *Klebsiella pneumoniae*, where C*bd*O deficiency severely impairs nitrogen-fixing ability under microaerobic conditions (Kelly et al., 1990, Juty et al., 1997, Edwards et al., 2000). As with C*c*O, C*bd*O functions as a terminal electron acceptor under aerobic conditions and generates 2 moles of water for each mole of $O_2$ reduced (Kana et al., 2009). This process is associated with conservation of energy in the form of periplasmic PMF which is later used by the rotary ATP synthase to generate metabolic energy in the form of ATP (Kana et al., 2009). In *M*. *smegmatis*, two subunits encode C*bd*O, the larger subunit I (53.96 KDa) encoded by the *cydA* gene and the smaller subunit II (37.95KDa) encoded by the *cydB* gene (Kana et al., 2001) (Figure 1.8). Inactivation of these subunits by mutagenesis results in the spectroscopic loss of a diagnostic peak associated with C*bd*O biogenesis (Kana et al., 2001). It has been established that subunit I is axially coordinated to a low spin *b*-type hemoprotein ($b_{558}$) by Histidine and Methionine residues at position 186 and 393 respectively (Osborne and Gennis, 1999).

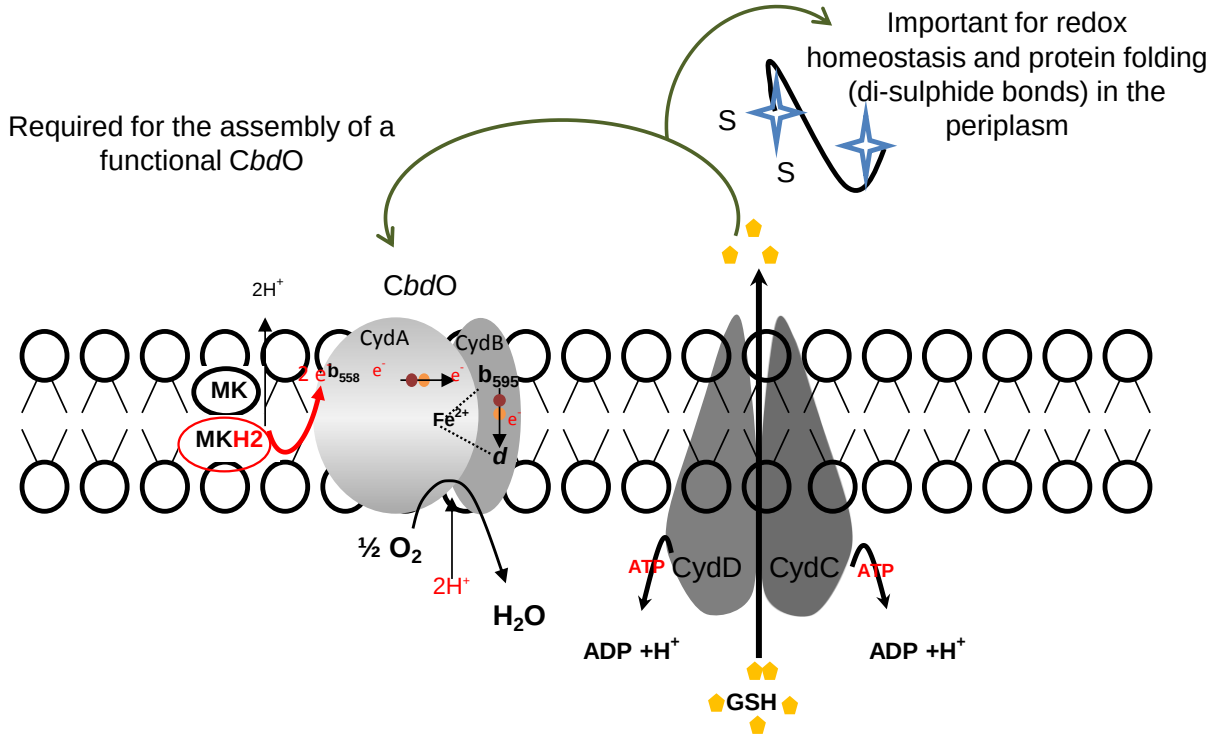


**Figure 1.8**. Schematic illustration of Cytochrome *bd* Oxidase (C*bd*O) one of the terminal branches of aerobic respiration in Mtb. C*bd*O comprises two structural proteins namely CydA and CydB but requires the presence of the unlinked *cydDC* operon which encodes a transporter necessary for biogenesis of a functional C*bd*O. C*bd*O catalyzes the reduction of oxygen to water and lacks proton pumping activity. The CydDC function as exporters of thiol (GSH) compounds which reduce periplasmic proteins to restore redox homeostatic poise in the periplasm. Adapted from Pittman et al 2002.

Subunit II is bound by two high spin hemoproteins, namely $b_{595}$, a *b*-type hemoprotein, and a chlorin type- *d* hemoprotein, which are coordinated by Histidine and Glutamine residues at position 19 and 99 respectively (Borisov et al., 2008, Yang et al., 2007). *In vitro* studies reveal that in *M smegmatis,* C*bd*O is upregulated more than 50-fold in response to 0.6% air saturation with increased generation time (Berney and Cook, 2010). Also, it has been established that the expression of the structural genes increases at least 3 fold in response to a decrease in $O_2$ saturation between 5 to 0.5% (Kana et al., 2001). Furthermore, *In vivo* studies reveal that in Mtb, transcript levels of both *cydA* and *cydC* increase during chronic infection in mouse lungs and that mutations in *cydC* result in impaired growth of Mtb in mice (Shi et al., 2005). Additionally Mtb mutants of *cydC* exposed to INH therapy have a growth defect during persistence

`

(Dhar and McKinney, 2010). All of these observations point to C*bd*O being important for virulence of Mtb.

Notably in *M*. *smegmatis*, biogenesis of a functional C*bd*O under microaerophillia requires the synthesis of two other proteins downstream of the *cydAB* operon, namely the CydD and CydC transporters (Aung et al., 2014). The *cydDC* genes are transcribed as an operon, separately from the *cydAB* operon. In 2014, Aung and co-workers mapped the transcriptional start site (TSS) of *cydD* and identified a genetic region -68 bp upstream of the TSS, essential for transcriptional regulation of the *cydDC* operon (Aung et al., 2014). Consistent with this, bioinformatics analyses from this MSc reveals a spacer region of 95 bp between *cydB* and *cydD*. This DNA spacer region potentially represents binding sites for transcriptional regulation of the *cydDC* operon. The regulatory mechanism for the *cydAB* operon has been reported both for Mtb and *M*. *smegmatis* and is facilitated by the cyclic AMP receptor protein (Aung et al., 2014). Regulation of the *cydDC* operon is yet to be reported in any mycobacterial species. However, it is likely that regulation is facilitated by the two component system *Arc*AB and the FNR system as in *E*. *coli* (Iuchi and Lin, 1991, Fu et al., 1991). The two component *Arc*AB system functions by responding to changes in $O_2$ tension (Iuchi and Lin, 1991). Consistent with this, the *M*. *smegmatis cydDC* operon is reported to be induced optimally at a dissolved $O_2$ concentration of 0.7% (Aung et al., 2014). However, it is unclear whether this induction is due to microaerophilia only as the *Arc*AB two component system and FNR systems in *E*. *coli* do not necessarily respond to $O_2$ levels but may be indirectly sensing the redox poise of cell (Iuchi et al., 1990, Lynch, 1996).

Based on amino acid homology, the *M*. *smegmatis cydDC* operon and its homologs in Mtb are predicted to encode subunits characteristic of the ATP Binding Cassette (ABC) domain, suggesting that they are ABC transporters (Black et al., 2014, Aung et al., 2014). These proteins are discussed further below

`

### 1.10.3 ABC transporters

ATP Binding Cassette (ABC) type transporters are ubiquitous in nature and constitute one of the largest of all protein families (Linton and Higgins, 1998). Members of this family couple energy of ATP hydrolysis to a wide variety of solute translocation across cellular membranes. ABC-type transporters share a common architectural organization comprising two hydrophilic ABC and two hydrophobic transmembrane domains (TMDs)(Szmelcman et al., 1976) (Figure 1.9). The hydrophilic ABC domain is characterized by the presence of a conserved ATP hydrolyzing domain of approximately 215 amino acids called the ABC or nucleotide binding domain (NBD). The archetypal ABC domain has remarkable conservation of primary sequence of the cassette and is characterized by several short motifs, namely: the presence of the Walker A and Walker B motifs, which are indicative of the NBD and the signature motif, located upstream of the Walker B motif. Other motifs diagnostic of the ABC domain include the Q-loop, consisting of a conserved glutamine residue located upstream of the Walker A motif. Also, downstream of the Walker B motif is the H-loop consisting of a conserved Histidine residue (Szmelcman et al., 1976). The organization of this domain is also remarkably conserved across many ABC transporters.

The TMDs preserve the substrate translocation passageway. Unlike the NBD of different ABC transporters, the translocation pathway exhibits extreme variability in conservation (Hiles et al., 1987). This enables ABC transporters to translocate a wide variety of substrates in and out of the cell membrane. Additionally, ABC transporters have a variety of physiological roles not limited only to transmembrane passage. For instance, ABC transporters are of high medical and economic relevance often implicated in antimicrobial resistance and chronic diseases such as cystic fibrosis (Gerlach et al., 1986, Gros et al., 1986).

`

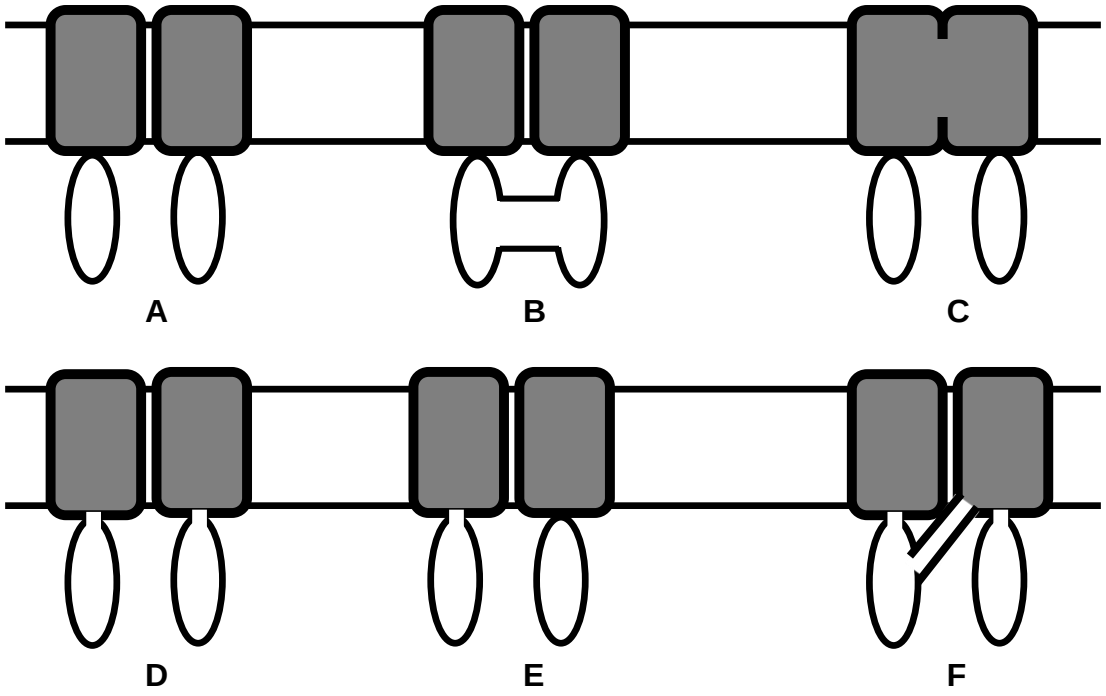


**Figure** 1.9. Schematic illustration of gene fusion events culminating in multidomain proteins which is a prominent feature of ABC transporters. The archetypal ABC transporter contains four domains. The two transmembrane domains (TMD) can be hetero-or homodimeric domains (Shaded squares). Similarly, the 2 **A**TP **B**inding **C**assette domains (Ovals) (ABCs) can be encoded as hetero- or homodimeric subunits. The domains can exist in various associations: A) Four separate domains B) Fused ABC domains with heterodimeric TMDs C) Fused TDMs with homodimeric ABC domains D) One TDM fused to one ABC domain (as in CydDC), E) One TDM fused to one ABC but also including separate TDMs and ABCs and F) All four domains in a single protein. Adapted from Linton and Higgins 2001.

ABC transporters belong to three main classes based on functional category. The first class comprise importers, which include all members that mediate the uptake of nutrients, Second, is the functional class of exporters, which refers to all members that secrete various molecules and the third functional category includes non-transport related functions such as translation of mRNA and DNA repair (Doolittle et al., 1986).

### 1.10.4 Functional mechanism of ABC-type transporters

Crystallization of certain ABC members has allowed elucidation of the functional mechanistics associated with ABC proteins. All ABC transporters contain the larger

`

transmembrane domain and the smaller ABC helical domain, with 3-4 helices (Linton and Higgins, 1998). The two domains are connected by two flexible loops such as the Q-loop, which mediates the connection between TMDs and ABC domains (Hollenstein et al., 2007, Dawson and Locher, 2006). For transport to occur, irrespective of whether the protein is an importer or an exporter, oligomerization of the polypeptides must first occur. It has been established that during transport, the Walker A motif of one subunit interacts with the Walker B of the other subunit. ATP is required for dimerization. This was shown by mutagenesis of essential residues in the protein crystal or by employing EDTA to prevent ATP hydrolysis in the co-purification of the dimer (Hollenstein et al., 2007). In both cases, 2 molecules of ATP were observed in association with the dimer interface. More specifically, one ATP molecule interacts with the Walker A motif of one subunit, and another molecule with the signature motif of the other subunit (Hollenstein et al., 2007). ATP hydrolysis requires stabilization of the adenosine group in ATP. The adenosine group is stabilized by a group of conserved aromatic residues preceding the Walker A motif. A conserved lysine residue within the Walker A motif forms a hydrogen bond with the oxygen atoms of the adenosine group and the two phosphates thus spatially orientating both phosphates (Geourjon et al., 2001). A conserved histidine of the H-loop is also necessary for ATP hydrolysis and plays a major role in the stabilization of the adenosine ring by forming a hydrogen bond with the last phosphate group (Geourjon et al., 2001).

For transportation of nutrients into the cell, the periplasmic binding protein releases the substrate into the TMDs which are capable of binding and transporting 2 substrates concurrently. Substrate binding induces conformational changes in the TMDs that relay signals to the ABC domains for ATP hydrolysis-facilitated translocation (Senior et al., 1995). For exporters such as the CydDC, once the substrate binding occurs, the re-orientation of the substrate binding site on the inside of the membrane, with the concomitant reduction in its affinity for the substrate, must first occur. This conformational change culminates in ATP hydrolysis and substrate extrusion into the periplasm (Senior et al., 1995).

`

### 1.10.5 The role of C*bd*O in *E.coli*

*E. coli* respires using two membrane-bound terminal oxidases under aerobic conditions namely: cytochromes *b*o and C*bd*O (Kita et al., 1984, Anraku and Gennis, 1987). The *cydAB* operon encoding C*bd*O is expressed both aerobically and anaerobically (Cotter et al., 1990, Poole and Cook, 2000). Consistent with this, the expression of C*bd*O is remarkably high under hypoxia, with the enzyme having extraordinary affinity for $O_2$ (D'mello et al., 1996). Loss of C*bd*O results in complex phenotypic defects. Phenotypic consequences of loss of C*bd*O in *E. coli* includes the inability to exit stationary phase at high temperatures under aerobic conditions (Siegele et al., 1996); sensitivity to high temperature (Delaney et al., 1992), hypersensitivity to $H_2O_2$ (Delaney et al., 1992); sensitivity to several metal ions (Cook et al., 1998, Poole et al., 1989); loss of motility and increased benzylpenicillin sensitivity (Pittman et al., 2002).

In *E. coli*, the *cydD* and *cydC* genes are transcribed as a separate operon from the *cydAB*, and are necessary for C*bd*O assembly (Georgiou et al., 1987, Poole et al., 1989, Poole et al., 1993, Delaney et al., 1993, Bebbington and Williams, 1993, Aung et al., 2014). These genes encode heterodimeric components of the ABC domain similar to those of ABC transporters (Poole et al., 1993) as shown in Figure 1.8 and Figure 1.9. *E. coli* encodes approximately 80 ABC transporters (Linton and Higgins, 1998). It was proposed that the substrate of the CydDC might be heme (Poole et al., 1993, Poole et al., 1994). However, Goldman and coworkers later proved that the export of heme to the periplasm and its assembly into heterodimeric apoproteins does not require *cydC* (Goldman et al., 1996b). More importantly, transport studies using everted membrane vesicles revealed no significant differences between wild-type and *cydD* mutant strains (Cook and Poole, 2000). Intriguingly though, overexpression of CydDC results in the synthesis of a novel heme pigment in anaerobically grown cells, suggesting a link with heme metabolism (Cook et al., 2002).

A quantum leap in understanding the functioning of CydDC was the observation that the periplasm of a *cydC* mutant is more oxidizing than that of wild-type (Goldman et al., 1996b). This, and the observation that CydC deficiency can be corrected by exogenous

`

reducing agents, suggested that CydDC exports a reducing molecule to the periplasm for maintenance of redox homeostasis (Goldman et al., 1996a, Pittman et al., 2002). It was further demonstrated that CydDC exports reduced GSH and cysteine to the periplasm in an ATP-dependent manner (Pittman et al., 2005, Pittman et al., 2002). The sensitivity of a *cydD* mutant to benzylpenicillin and dithiothreitol, and the loss of motility, were all reversed by addition exogenous (Pittman et al., 2002) cysteine. The addition of cysteine also increased cytochrome *c* levels in the periplasm of a *cydD* mutant, however, did not correct the biogenesis (Poole et al., 1994) defect. Consistent with the CydDC being a cysteine exporter, a *cydD* mutant displayed hypersensitivity to high cysteine concentrations in the medium and accumulated higher cytoplasmic cysteine levels. CydDC overexpression confers resistance to high extracellular cysteine concentrations.

### 1.10.7 C*bd*O in pathogenesis

The presence of C*bd*O in pathogenic bacteria is associated with virulence in humans and livestock. For instance, all members of the Mtb complex, which includes genetically related pathogens associated with TB pathology, possess C*bd*O (Kana et al., 2009). Furthermore, in *Shigella flexneri* and *Brucella abortus*, the loss of C*bd*O resulted in attenuation of intracellular survival and virulence (Way et al., 1999, Endley et al., 2001). Therefore, the need to understand C*bd*O assembly is critical to developing drugs that will target this respiratory complex.

### 1.10.6 $F_1F_0$ ATP synthase

ATP is the biological currency of every living cell. Cells obtain energy through various metabolic pathways including substrate level phosphorylation, a process that does not depend on the reducing potential of external electron donors for ATP synthesis (black et al., 2014). On the contrary, microorganisms that depend on the presence of oxygen for growth, produce the bulk of their ATP through oxidative phosphorylation (OxPhos). The ATP synthase is a highly conserved and widely distributed energy generating enzyme in both prokaryotes and eukaryotic mitochondria (Elston et al., 1998). During the terminal

`

step of OxPhos, the membrane bound $F_1F_0$ ATP synthase dissipates the free energy of the electrochemical gradient to synthesize ATP through the phosphorylation of ADP (Weber and Senior, 2003). The $F_1F_0$ ATP synthase is an extremely small rotary engine which is composed of the peripherally located, aqueous soluble $F_1$ rotary motor and the membrane confined $F_0$ rotary motor (Weber and senior 2003, black et al 2014 and dimroth et al 200). The $F_1$ motor is encoded by the $\alpha_3\beta_3\gamma\delta\varepsilon$ subunits while the $F_0$ segment is encoded by $ab_2Cn_{(10\text{-}15)}$ (Weber and Senior, 2003, Black et al., 2014). Collectively, the γεCn unit is called the central or rotor stalk while $b_2$ and δ is called the stator stalk which prevents rotation of both the $F_1$ and $F_0$ motors. Rotation of the central stalk relative to the hexagonic $F_1$ motor induces torque in the $F_0$ motor, which allows proton translocation through the C-rings which engages the three functional catalytic sites on the $F_1$ segment for ATP synthesis (Figure 1.10).

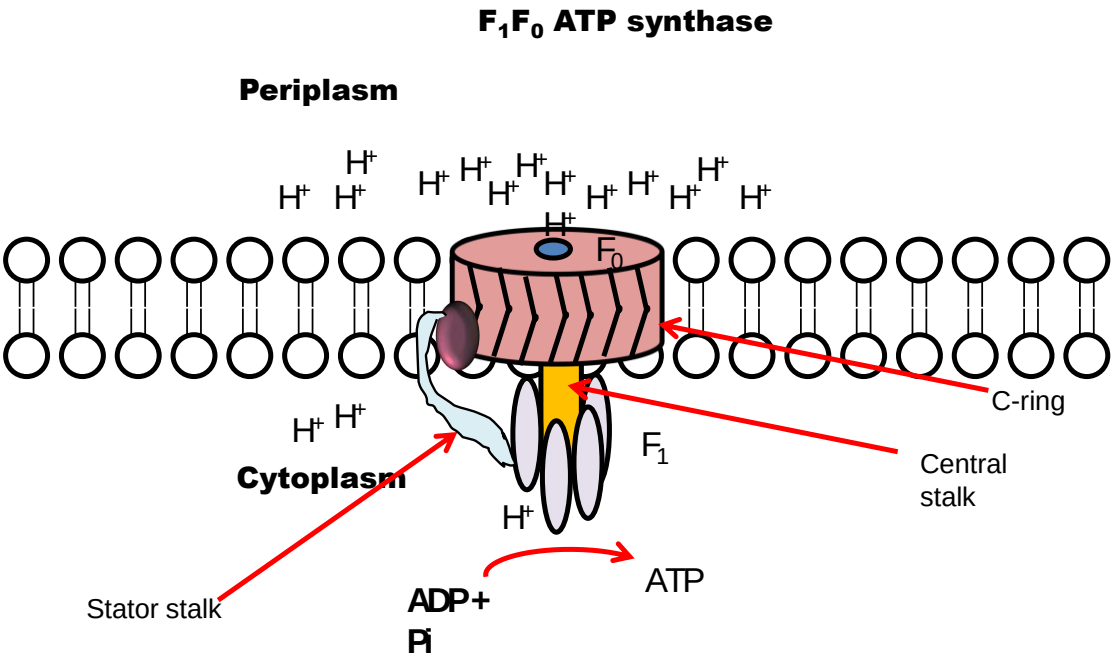


**Figure 1.10**. Schematic representation of the $F_1F_0$ ATP synthase. The ATP synthase has ATPase activity as well. The ATP synthase is composed of the membrane bound $F_0$ region and the hydrophillic $F_1$ region. ATP is synthesized by utilizing the free energy of the proton gradient. Adapted from Kana et al., 2009.

`

Conversely, evidence of ATP hydrolysis mediated torque of the three functional catalytic sites on the $F_1$ rotor, induces proton translocation across the cytoplasm (Weber and Senior, 2003). The ATP synthase forms an essential component for synthesis of metabolic energy in Mtb (Berney and Cook, 2010, Black et al., 2014). This enzyme complex is conserved across the mycobacteria and is encoded by the *atpBEFHAGDC* operon and functions essentially the same as described above during aerobic conditions. Furthermore, during hypoxic growth, another enzyme that mimics the functioning of the ATP synthase called the methylmalonyl-CoA decarboxylase, generates ATP through dissipating the $Na^+$ gradient generated by fermentation of succinate (Becher and Müller, 1994). However, this has not been demonstrated in any species of the mycobacteria.

### 1.11 Rationale for this study

During TB pathogenesis, Mtb is engulfed by alveolar macrophages which eventually are surrounded by other immune cells to form a barrier of containment. This barrier also provides a protective niche for Mtb to survive indefinitely under immune pressure. In such a granulomatous environment, Mtb is subjected to suboptimal hypoxic conditions were its active growth is kept in check by the immune response. We hypothesize that under these conditions, the biological role for C*bd*O switches from being supportive to critically essential for survival. It is expected that during hypoxic growth, the levels of expression of C*bd*O is elevated and this contributes towards pathogenesis as demonstrated previously (Way et al., 1999, Endley et al., 2001) in *B. abortus* and *S. flexinerri*. Furthermore, it has been established in various model and pathogenic microorganisms that during hypoxic persistence and stationary growth phase, C*bd*O provides for energetic requirements and protects from various environmental stresses while electron flux through the main aerobic branch is reduced by low oxygen tension. To further explore C*bd*O biology, this MSc will focus on the *cydDC*-encoded ABC transporter.

`

### 1.10.9 Hypothesis

It is our hypothesis that the *cydDC* operon encodes a heterodimeric ABC type transporter, whose substrate is a thiol containing compound (reduced glutathione) which maintains a balanced redox poise in the periplasm and thus contributing to the biogenesis and functioning of C*bd*O in Mtb. Hence, in the absence of CydDC, we expect that C*bd*O will not assemble properly and the spectroscopic features of this respiratory enzyme will be missing from membrane preparations of *M. smegmatis*.

### 1.10.10 Aim

To investigate the function of the *cydDC* encoded ABC type transporter in *M. smegmatis.*

### 1.10.11 Objectives

- The sequenced genome of *M. smegmatis* suggests that the *cydC* gene contains a SNP that would render it non-functional. We propose that this is a sequencing mistake, as the spectroscopic features of C*bd*O are present in wild type *M. smegmatis* (Kana et al., 2001) , suggesting that this organism has a functional *cydDC* operon. We will prove this by sequencing the *cydC* locus.
- Prove the functionality of the *M. smegmatis cydDC* genes by heterologous expression in an *E*. *coli cydD* mutant.
- To construct a suicide vector for the deletion of the *cydDC* operon in *M smegmatis.*
- To use this above mentioned suicide vector for allelic exchange mutagenesis in *M. smegmatis.*
- To characterize the resulting mutant for C*bd*O assembly by assessing membrane fractions for spectral features associated with C*bd*O.
- To phenotypically assess the mutant strains under various stress conditions

`

# 2. Materials and Methods

## 2.1 Bioinformatic tools and virtual software programs

Several in silico tools were used to view, analyze, design, compare, edit and manipulate bacterial gene sequences of interest and their homologs. These are outlined below.

### 2.1.1 Databases used in this study

**Table 2. Database and their application in this study**

| Name | Website address | Application |
|---|---|---|
| Smegmalist | http://mycobrowser.epfl.ch/smegmalist.html | Nucleotide or protein sequences of specific genes were downloaded from Smegmalist. |
| EcoCyc | http://www.ecocyc.org/ECOLI/organism-summary | Sequences of *E. coli* were obtained from this website. |
| Tuberculist | http://tuberculist.epfl.ch | Sequences of interest (nucleotide or protein) of Mtb were obtained from Tuberculist. |

### 2.1.2 NCBI BLAST (http://blast.ncbi.nlm.nih.gov/Blast.cgi)

The **B**asic **L**ocal **A**lignment **S**equence **T**ool was used to identify sequences of proteobacterial and actinobacterial microorganisms encoding the *cydDC* type ABC

`

transporter homologs. This online tool is also a comparative genomics tool that allows the alignment of nucleotide or amino acid sequences. This tool was used to align sequences of Mtb, *M. smegmatis, E. coli* and various other microorganisms.

### 2.1.3 Clustal Omega or Clustal W2 (http://www.ebi.ac.uk/Tools/msa/clustalo/)

Clustal Omega suite was utilized to align multiple sequences in high throughput or in pairs, in an attempt to identify regions of homology of the ATP binding cassette of different microorganisms. Both of the clustal suites were used.

### 2.1.4 I-TASSER (http://zhanglab.ccmb.med.umich.edu/I-TASSER/)

As the crystal structure of the *cydDC* is yet to be determined, a protein threading tool (**I**terative **T**hreading **ASSE**mbly **R**efinement server) was used to predict the structure of the *M*. *smegmatis cydD* and *cydC* subunits.

### 2.1.5 PyMOL (https://www.pymol.org/)

Pymol allows for the visualization of Protein data bank files. The *M. smegmatis cydD* and *cydC* predicted structure was visualized and manipulated using this software.

## 2.2 Chemicals and Reagents

All chemicals, reagents and primers used in this study, except when stated, were procured from Sigma Aldrich and Inqaba biotech while enzymes and buffers were procured from Roche, Fermentas and New England Biolabs (NEB). For an in depth list, refer to Appendix A.

## 2.3 Bacterial strains and cultivation conditions

For plasmid propagation, the laboratory stock of *E. coli* DH5$\alpha$, strain K12 and derivative strains were cultivated in selective broth: (Luria Bertani [LB]/ 2XTY) or selective Luria agar media (LA) supplemented appropriately with antibiotics at the following concentrations: 200 $\mu$g/mL hygromycin (Hyg), 200 $\mu$g/mL ampicillin (Amp), 50 $\mu$g/mL kanamycin (Kan), 50 $\mu$g/mL and streptomycin (Strp). Bacteria were propagated in broth

`

in a shake flask incubator overnight. Broth cultures with recombinant plasmids > 8 KB were propagated at 30 °C (New Brunswick Scientific Innovar™ 4000) with shaking at 100 rpm, while those carrying plasmids < 8 KB were grown at 37 °C with shaking at 100-250 rpm. Strains with plasmid sizes > 8 KB or <8 KB were propagated in solid media at 30 °C and 37 °C respectively. *E. coli* strains used and/or generated in this study are outlined below

**Table 2.1. List of plasmids and strains used and generated in this study**

| Name | Description | Source |
|---|---|---|
| **Plasmids** | | |
| p2NIL | Cloning vector; $Km^R$ | Parish *et al.*, 2000 |
| pGOAL17 | Plasmid carrying , *lacZ, and sacB* genes as a *Pac*I cassette; | Parish *et al.*, 2000 |
| pBlueScript | *E. coli* cloning vector; $amp^R$; *lacZ*-alpha; *ori*E | Promega |
| pSE_100 | *E. coli-Mycobacterium* shuttle vector carrying Pmyc1tetO; HygR | (Ehrt et al., 2005) |
| pMAS | Derivative of pBlueScript. Plasmid carries the *aadA* cassette encoding, $Strp^R$ | CBTBR |
| pMV306H | pMV306 derivative carrying $Hyg^R$ marker L5 integrating proficient *E. coli–Mycobacterium* shuttle vector integrating at $tRNA^{Gly}$ ; $Hyg^R$. | H. Boshoff |

`

| | | |
|---|---|---|
| pOTB*cyd* | Plasmid carrying the whole Mtb *cyd* operon; $Hyg^R$ | Kana *et al*., 2001 |
| pGEM29M | Plasmid carrying *M. smegmatis cyd* operon | Kana *et al*., 2001 |
| pBlueScriptΔ*cydDC* | Plasmid carrying 1176 bp upstream sequence including 24 bp sequence of *cydD* to create an inframe deletion and 864 bp of downstream sequence of *cydC*, including 36 bp of *cydC* sequence to generate an inframe double deletion allele of the *cydDC* $Amp^R$ | This study |
| p2NILΔ*cydDC* | Suicide plasmid carrying a *cydDC* truncation excised from pBlueScriptΔ*cydDC* as 2007 bp *Hin*dIII fragment, $Kan^R$ | This study |
| pSE**:**pOTBcyd | Episomal overexpression construct, carrying the whole Mtb *cyd* operon. $Hyg^R$ | This study |
| pTweety**::***cydDC* | Cloning of the *cydDC* operon in a shuttle vector $kan^R$ | This study |
| pTweety | Complementation vector carrying an integrase gene. $Kan^R$ | (Pham et al., 2007) |
| pNIT | Mycobacterial replication plasmid that allows the inducible expression of the | (Murphy et al., 2015) |

`

| | | |
|---|---|---|
| | phage Che9c RecET recombination system, and constitutive expression of the *sacB* gene. $Kan^R$ | |
| *Escherichia coli* DH5α | Host strain for cloning and sub cloning. *supE44 ΔlacU169 hsdR17 recA1 endA1 gyrA96 thi-1 relA1* | Hanahan (1983) |
| *Escherichia coli* wildtype K12 (3561) | Wildtype *E. coli* K12 strain | Robert K Poole , 1993 |
| 3562 K12 | *E. coli* Δ*cydD* strain | Robert K Poole , 1993 |
| Δ*cydD***(**pSE**:**pOTB*cydABDC*) | Overexpression construct transformed into *E*. *coli cydD* deficient strain | This study |
| $mc^2$ 155**::**Δ*cydDC*_ pMVp*cydDC* | Complementation of *M*. *smegmatis cydDC* mutant strain using an integrating plasmid $Hyg^R$ | This study |
| *M. smegmatis* $mc^2$ 155 | Electrocompetent High frequency transformation mutant of *M. smegmatis* ATCC 607 strain | Snapper et al. (1990) |
| *M. smegmatis***::** *pTweety* p*cydDC*_ | Complementation of *M*. *smegmatis cydDC* mutant strain using an integrating shuttle vector. $Kan^R$ | This study |
| *M. smegmatis* Δ*cydDC* | *M. smegmatis* with an inframe double deletion allele of the *cydDC* operon. | This study |

`

*M. smegmatis* $mc^2$ 155 and its derivative strains, were cultivated either in Middlebrook 7H9 broth media (Difco), supplemented with 0.2% glycerol, 0.05% tween 80, 0.085% NaCl, 0.2% glucose and 0.5 % glycerol (referred to as 7H9 media) and 7H10 solid media supplemented with 0.085% NaCl, 0.2% glucose and 0.5 % glycerol (referred to as 7H10 media) with and without shaking respectively. Where necessary, derivatives of *M. smegmatis* $mc^2$ 155 were cultured in selective media with antibiotics at the concentration of 25 μg/mL Kan or Strp or 50 μg/mL Hyg.

For growth under defined oxygen tensions, *M. smegmatis* was cultivated in a bioreactor as described by (Kana et al., 2001). Briefly, batch cultures of *M. smegmatis* $mc^2$ 155 and its derivative strains, were carried out in a New Brunswick BioFlow fermentor 110. The 2L bioreactor vessel had a 1L working volume and the following mechanical features:

- Two, six bladed axial flow impellers mounted on a stirring shaft that was controlled by an over-head rotor, connected to the control box for electronic speed adjustment.
- The reactor was equipped with a temperature blanket with a water cooling coil circuit system and a temperature probe to monitor and maintain a heat stable environment
- A pH probe to monitor and adjust changes in pH
- A Mettler Toledo dissolved oxygen probe dipped inside the cultivation media to detect fluctuations in dissolved oxygen. Oxygen was supplied by passing compressed air through the ring sparger by means of an external, manually controlled rotometer which had a capacity between 0-400 mL/min of air supply.
- The unit also had a foam probe and a sampling port.

The electric heat blanket and all probes were linked to the control unit which kept tight regulation of the selected variables within set limits when the cruise/cascade mode was selected. Agitation ranged between 50-650 rpm and was set to cascade mode in order to control air saturation, which allowed the unit to modulate impeller speed for maintaining the set point dissolved oxygen. For growth of *M. smegmatis* cultures, the

`

vessel was sterilized with 1L 7H9 containing 3 mL glycerol. Upon cooling, 7H9 was supplemented with 2 mL 25% tween 80, 0.6 mL antifoam and 10 mL 100X glucose/salt mix (0.085% NaCl and 0.2% glucose). The vessel was equilibrated overnight and the $dO_2$ probe calibrated to 0% air, by sparging the media with compressed nitrogen, then to 100% by introducing compressed air. A stationary phase pre-culture (100 mL) was inoculated into the vessel and the cultures cultivated at 21, 10, 5, 1, and 0.7% $dO_2$ in cascade mode. At 21 and 0.7% $dO_2$ tension, a sample was withdrawn through a vacuumed sampling port. Cells were harvested through centrifugation.

## 2.4 DNA manipulation

### 2.4.1 Small scale plasmid preparation (Alkaline lysis)

Plasmid extraction was carried out as described by (Sambrook et al., 1989). A single colony was inoculated in a culture flask containing 2 mL LB supplemented appropriately with antibiotics. 1 mL freezer stock of the pre-culture was prepared and cryogenically preserved at -80 °C, the remainder was precipitated at 16162 x g for 1 min and the pellet was re-suspended in 100 μL ice cold solution I (50 mM glucose, 25 mM Tris-HCl [pH 8.0] and 10 mM EDTA). Subsequently, 200 μL of room temperature solution II (1%SDS and 0.2 M NaOH) was added, and the suspension thoroughly mixed by gentle inversion (6-8 times). The suspension was incubated at room temperature for approximately 5 min, followed by the addition of 150 μL ice cold solution III (3 M potassium acetate and 11.5% acetic acid). The suspension was mixed and incubated on ice for 5 min. Thereafter, centrifugation at 16162 x g for 10 min at room temperature was carried out and the clarified supernatant decanted into a sterile 1.5 eppendorf tube containing 5 μL RNAse A (10 mg/mL), followed by incubation at 42 °C for 15 min. Isopropanol (600 μL) was added to the suspension and the DNA was collected by centrifugation at 12470 x g for 20 min. The supernatant was discarded and the transluscent pellet was washed twice with 500 μL of 70% ethanol at 12470 xg for 5 min and dried in an Eppendorf concentrator at 60 °C for 12 min. The pellet was re-suspended in 30 μL of nuclease free water by incubating the tubes at 37 °C for 15 min,

`

gently flicking the side of the tubes and centrifuging for 10 sec at maximum speed in a microfuge.

### 2.4.2 Sodium acetate precipitation

To remove excess salts that might interfere with the activity of restriction enzymes, plasmid extracts were purified as follows: one tenth 3M sodium acetate (pH 5.3) of the total volume and 3X the total volume of 100 % ethanol were added to the DNA. The sample was mixed and incubated at -20 °C for 15 min. Subsequently, centrifugation at 12470 x g for 20 min at ambient temperature was carried out and the translucent pellet was washed, dried and re-suspended as previously described (see 2.4.1)

### 2.4.3 Bulk preparation of plasmid DNA

For bulk preparation of DNA, the small-scale protocol (described in section 2.4.1) was scaled-up. Bulk extraction of plasmid DNA was carried out from 50 mL of overnight culture and the volumes of all solutions were increased ten-fold. For sequencing and electroporation purposes, the Nagel-Macherey nucleobond kit was used for plasmid bulk preparation, following the manufacturer's specifications. Briefly, an overnight culture (50 mL) was precipitated by centrifugation at 3901 x g for 10 min. The pelleted cell mass was thoroughly re-suspended in 4 mL cold buffer S1 (50 mM Tris-HCl, 10 mM EDTA, 100 µg/mL RNAse pH 8.0) by vortexing. After the addition of 4 mL room temperature buffer S2 (200 mM NaOH, 1% SDS), the suspension was incubated at ambient temperature for approximately 5 min, followed by the subsequent addition of 4 mL cold buffer S3 (2.8M potassium acetate pH 5.1), and incubation on ice for a further 5 min. To clarify the cell lysate, the suspension was centrifuged at 3901 x g for 20 min and the supernatant transferred to a column with a silica membrane, equilibrated with 2.5 mL buffer N2 (100mM Tris, 15% ethanol, 900mM KCl, 0.15% triton X-100 pH adjusted to 6.3 with $H_3PO_4$). This was accompanied by two wash steps with 10 mL Buffer N3 (100mM Tris, 15% ethanol, 1.15 M KCl and pH adjusted to 6.3 with $H_3PO_4$). Solution N5 (5 mL) (100mM Tris,15% ethanol, 1. M KCl and pH adjusted to 8.5 with $H_3PO_4$) was used to elute the DNA into a 50 mL conical tube, containing 4 mL room

`

temperature isopropanol. One mL aliquots of this suspension were immediately centrifuged at 12470 x g for 20 min in 1.5 eppendorf tubes. The pellet was washed and dried as previously described (2.4.1), re-suspended in elution buffer (15 μL) and pooled into one tube.

### 2.4.4 Mycobacterial genomic DNA extraction

DNA from *M*. *smegmatis* and its derivative strains was isolated following the modified Cetyl trimethyl ammoniumbromide (CTAB) DNA extraction protocol described by (Somerville et al., 2005). Mycobacterial cultures were propagated in 7H9 broth to an optical density of ($OD_{600)}$ of 2. A 1 mL freezer stock of this culture was prepared and cryogenically preserved at -80 °C. Bacterial culture (2 mL) was precipitated by centrifugation at 16162 x g for 2 min. The cell pellet was re-suspended in 500 μL of 0.01M TE buffer (pH 8.0) and incubated at 65 °C for 20 min. Thereafter, 70 μL of lysozyme (10 mg/mL) was added to the heat killed suspension, thoroughly mixed by gentle inversion and incubated at 37 °C for 60 min. Following the addition of 6 μL proteinase K and 70 μL 10% SDS, the suspension was mixed and incubated at 65°C for 120 min after which, 100 μL of 5M sodium chloride and 80 μL pre-warmed CTAB/NaCl were added to the suspension, followed by incubation at 65 °C for 10 min. Thereafter, 750 μL of chloroform/isoamyl [ratio of 24:1 (v/v)] was added and the suspension mixed vigorously by inversion. The suspension was centrifuged at 12470 x g for 10 min and 800 μL of the top aqueous layer transferred to a sterile 1.5 mL eppendorf tube containing 450 μL chilled isopropanol. The suspension was centrifuged at 12470 x g for 20 min and the pellet washed, dried and re-suspended as previously described (see 2.4.1).

### 2.4.5 Mycobacterial small-scale genomic DNA extraction

For screening purposes, genomic DNA was isolated as follows: five hundred (500 μL) of overnight culture was harvest by centrifugation at 16162 x g for 2 min (2.4.4) and re-suspended in 100 μL of distilled water. Chloroform (100 μL) was added to the, and the suspension was mixed by inversion. The suspension was heat killed by incubation at 65

`

°C for 15 min, followed by centrifugation at 12470 x g for 15 min. The top aqueous layer containing DNA was transferred to a sterile labelled eppendorf tube and stored at 4 °C for later use.

### 2.5 Nucleic acid quantitation

Quantification of nucleic acids (DNA and RNA) is important in processes such as restriction digests, cloning and southern blot analysis. To measure the quantity of DNA in a sample, a property of light absorption by DNA is exploited. DNA absorbs light at a wavelength of 260 nm. Quantification of DNA or RNA was facilitated by the use of the Nanodrop ND-1000 spectrophotometer (Nanodrop Technologies) used in conjunction with software from the manufacturer (Coleman Technologies). Alternatively, a standard volume of DNA was visualized on a 1% agarose gel parallel to a molecular weight marker and the concentration of the DNA was inferred by comparing the intensity of the bands relative to Roche DNA ladder II.

### 2.6 Polymerase chain reaction (PCR)

Amplification of genomic DNA was facilitated by PCR. For this, primers homologous to the genomic region of interest were designed by the Clone Manager suite of programs.

#### 2.6.1 Gene knockout primers

Genome editing was accomplished by the design of primers for gene knockout. Primers had the 21 bp of sequence homologous to regions upstream and downstream of the gene of interest, a GC clamp and restriction sites were incorporated to facilitate cloning. The primers were thus engineered to generate a truncated version of the original gene. Amplification of PCR amplicons for cloning was facilitated by a high fidelity DNA-dependent DNA polymerase with proofreading activity. A gradient PCR (to determine the optimum annealing temperature for primers) was initially set up to a final volume of 25 μL according to the manufacturer's specification with the following components in the master mix: dNTPs were added to a final concentration of 0.2 mM, 5X recommended buffer was included in the reaction mixture, the forward and reverse primers were added to a final concentration of 1 μM each, template DNA between 50-150 ng/μL, 1% DMSO,

`

2 units of DNA polymerase and the volume topped up to 25 μL with $sdH_2O$. Cycling conditions for amplification were typically as follows: 1 cycle of denaturation at 98 °C for 3 min; 1 cycle of denaturation at 98 °C for 30 sec; 30 cycles of the following steps: annealing at 50-70 °C for 1 min, extension at 72 °C for 1 min; 1 cycle final extension at 72 °C for 10 min and 1 hold cycle at 12 °C, overnight.

For screening of potential mutants by PCR, a DNA polymerase with no 3`-5` exonuclease activity was employed. The PCR master mix was prepared according to the manufacturer's recommendations except that DMSO was replaced with 1 X GC buffer and 2 mM $MgCl_2$ was used. With regards to the cycling conditions, 95 °C of denaturation was used instead for 3 min. The rest of the cycling conditions are as stated above.

### 2.6.2 Sequencing primers

Overlapping primers (between 18-24 bp) for sequencing, were designed at least a 100 bp upstream and downstream from the genomic region of interest for every 350 bp. In some instances, bidirectional sequencing was done with several reverse primers spanning the region of interest. See below for primers used for sequencing

**Table 2.2 *cydC* sequencing primers**

| Primer name | Sequence 5`-`3 | Position |
|---|---|---|
| *cydC*_Fwd | ATGATCCGTTGCTCCGCCTGA | Binds 100 bp upstream *cydC* |
| *cydC* Int Fwd_ | ACCTTCGAGCGTCATCACCGC | Binds inside *cydC* |
| *cydC*_Rvs | CGGTACAGCGAACAAAATCGG | Binds 100 bp downstream *cydC* |

`

### 2.6.3 Primers for creating suicide constructs and complementation vectors

Primers to amplify the full length gene/s of interest were designed, and engineered as previously described **(see 2.6.1)**. A high fidelity polymerase was used to generate the fragment according to the cycling conditions already described **(see 2.6.1)**. Primers for creating gene knockouts are given in Table 2.4 and for sequencing the construct, primers are given in Table 2.5. Primers for genetic complementation are given in Table 2.6.

**Table 2.3 Gene knock out primers**

| Region targeted | Primer name | Sequence 5`-`3 | Amplicon | Position |
|---|---|---|---|---|
| *cydD* upstream region | *cydD* upstream Fwd | **GCGCGC**AAGCTTGGCTTC TTCCTGCTGGAG *Hin*dIII | 1176 bp | From position 1197 bp inside *cydB* to 21 bp into *cydD* |
| | *cydD* upstream Rvs | **GCGCGC**CAGCTGCGACG ATGTGGGCGAGCA *Pvu*II | | |
| *cydC* downstream region | *cydC* downstream Fwd | **GCGCGC**CAGCTGCGGCC GTCTCGCGGTG *Pvu*II | 864 bp | From position 885 downstream of *cydC* to 21 bp into *cydC* |
| | *cydC* downstream Rvs | **GCGCGC**AAGCTTCGTCCG CGACACGCCGGT *Hin*dIII | | |

Restriction sites are underlined and the GC clamp is indicated in bold.

**Table 2.4 Suicide construct sequencing primers**

| Sequencing primer | | Primer Sequence (5`-`3) | amplicon |
|---|---|---|---|
| Upstream | Original | GCGCGCAAGCTTGGCTTCTTCCTGCTG | 420 bp |

`

| | | |
|---|---|---|
| Forward | GAG | |
| Upstream new reverse | TCCCGCCACGGCGCTGGTAGC | |
| Upstream new forward | TCCGTGCGCCACCTGTGTCCA | 540 bp |
| Upstream original reverse | GCGCGCCAGCTGCGACGATGTGGGCGAGCA | |
| Downstream Original Reverse | GCGCGCAAGCTTCGTCCGCGACACGCCGGT | 460 bp |
| Downstream new forward | CGATGCCCAGCCCATTGCGCG | |
| Downstream new reverse | CGGGTCTGGTGCTGTGCTGGT | 510 bp |
| Downstream original forward | GCGCGCCAGCTGCGGCCGTCTCGCGGTG | |

Restriction sites are underlined

**Table 2.5. Primers for genetic complemention**

| Primer name | Sequence 5`-`3 | Position | Amplicon |
|---|---|---|---|
| *cyd* comp Fwd | GCGCGCAAGCTTTGAACCTCTGGCGTGCGC *Hin*dIII | 100 bp upstream of *cydD* | 3150 bp |
| *cyd* comp Rvs | GCGCGCCAGCTGACTCACCGGATCGGGTCG *Pvu*II | 100 bp downstream of *cydC* | |

Restriction sites are underlined

For preliminary screen of the potential mutants and for complementation of the mc$^2$ 155 Δ*cydDC*::*cydDC*, the following primers were used.

`

**Table 2.6 Mutant screening primers**

| Primer name | Sequence 5`-`3 | Position |
|---|---|---|
| US_Fwd | TACCTGATCGCTGCGGTC | Binds 52 bp upstream *cydD* |
| DS_Rvs | GTGTCTGACGACTCGGTCGAC | Binds inside *cydC* |
| *cydC* Int Fwd_ | TTTCCGGTGGTCCTGCTCGAC | Binds 168 bp downstream *cydC* |

### 2.6.4 Restriction digestion of DNA

Restriction enzymes and buffers were procured from Fermentas, Roche or NEB. Restriction digests were carried out following the manufacturer's instructions. Restriction digests of PCR amplicons, plasmid DNA or genomic DNA were set up in a final volume of 10-30 μL. An eppendorf tube containing sd$H_2O$, 1X buffer, at least 1 μg of (amplicon, plasmid) DNA and 1U enzyme (diluted in enzyme buffer to a ratio of 1:2) constituted the reaction mixture which was incubated at 37 °C for 60 min. Buffers containing Bovine Serum Albumin (BSA) were utilized when a restriction enzyme had a dependency on BSA. For double digests, enzymes that were compatible in one buffer were preferred, if enzymes were not compatible in the same buffer, the enzyme that required a low ionic strength buffer took first preference, followed by digestion with an enzyme that required incubation in a high ionic strength buffer. When necessary, enzymes were heat inactivated at 65 °C for 20 min. For southern blot analysis, at least 3 μg of genomic DNA was digested in a final volume of 20 μL with overnight incubation at 37 °C.

`

### 2.6.5 Dephosphorylation of DNA

To reduce background due to re-ligation of vector during cloning, removal of phosphate groups in a linearized vector is necessary. For this, Antarctic phosphatase (NEB) was used (diluted in a ratio 1:2) to the buffer in the reaction mixture which contained 1X reaction buffer and was incubated at 37 °C for 60 min, depending on the amount of DNA cut. The enzyme was heat inactivated at 65 °C for 20 min.

### 2.6.6 Phosphorylation of DNA

For blunt end cloning, PCR amplicons were phosphorylated using polynucleotide kinase (PNK) (NEB) in 10-30 μL reaction volumes containing the following constituents: $dH_2O$, 1X PNK buffer, 1 μg DNA and 1U PNK. The buffer was always used in 1:10 ratios of the total volume while the enzyme/buffer ratio was always 1:2. The reaction was incubated at 37 °C for 60 min.

### 2.6.7 Modification of DNA overhangs

Klenow (Thermofisher Scientific) was used to blunt overhangs generated during digestion of DNA with restriction endonucleases. The enzyme was used by following the manufacturer's instructions and retains the capacity to fill in overhangs in the 5` direction in the presence of dNTPs. The reaction was incubated at 37 °C for 15 min and the enzyme was heat inactivated at 65 °C for 20 min.

### 2.6.8 DNA ligation

Cloning involved ligation of either two or three DNA fragments. The T4 DNA ligase kit (NEB) was used according to the manufacturer's specifications for all cloning strategies. For this, a ligation reaction was set up in a final volume of 20 μL with the following components, sdH2O, 1:10 enzyme buffer of the total volume, 1:1 volume ratios of the insert(s) and vector DNA and 1:2 enzyme to the buffer ratio (buffer component contains ATP). The reaction was incubated at room temperature overnight and was transformed into *E. coli* calcium chloride/ rubidium chloride competent cells. For the ligation reaction to be a success, optimum insert to vector concentrations are required. A standard

`

concentration of 50 ng/μL for the vector was always used. The amount of insert necessary for a 1:1 ratio of vector to insert was calculated as follows:

$$\text{Amount of insert} = \frac{50\ \text{ng (vector)} * \text{size of insert (bp)}}{\text{size of vector (bp)}}$$

## 2.7 Bacterial transformations

### 2.7.1 *E. coli* transformations

*E. coli* DH5α (1 mL freezer stock) was cultivated in 20 mL LB or 2XTY. A pre-culture (1 mL) was inoculated in fresh 2XTY and incubated at 37 °C with shaking at 250 rpm to $OD_{600}$ of 0.5. Cells were cooled on ice for 15 min and harvested by centrifugation at 3901 x g for 10 min at 4 °C. Cells were re-suspended in 10 mL ice cold 0.1 M calcium chloride ($CaCl_2$) and washed twice by centrifugation at 3901 x g for 10 min at 4 °C in the same solution. Washed cells were re-suspended in 1 mL 0.1 M $CaCl_2$ and incubated on ice for 30 min before use. For transformations, 100 μL of competent cells were aliquoted into eppendorf tubes containing plasmid DNA (100-1000 ng/μL). The tubes were incubated on ice for 15 min. The suspension was heat shocked at 42 °C for 90 sec for transformations and subsequently incubated on ice for 3 min. Cells were rescued in 800 μL 2XTY and incubated at 30 °C or 37 °C, depending on the size of the recombinant plasmid with shaking at 100 rpm. Transformants were plated on LA supplemented appropriately with antibiotic **(see 2.3)**. Plates were dried in a biosafety cabinet level II (BSC II) and subsequently incubated as previously described **(see 2.3)** without shaking.

Alternatively, chemically competent *E. coli* cells were prepared as previously described (Sambrook et al., 1989). Briefly, *E. coli* DH5α (1 mL freezer stock) was cultivated in 20 mL LB or 2XTY at 37 °C with shaking at 250 rpm to stationary phase. This pre-culture (1 mL) was inoculated into fresh 2XTY (100 mL) and incubated at 37 °C with shaking at 250 rpm to $OD_{600}$ = 0.5. Cells were cooled on ice for 15 min and harvested by

`

centrifugation (Beckman Coulter Allegra™ X-22R centrifuge) at 3901 x g for 10 min at 4 °C. The cell mass was re-suspended in 0.4 volumes TfbI (30 mM potassium acetate, 100 mM rubidium chloride, 10 mM calcium chloride, 50 mM manganese chloride, 15 % v/v glycerol). After being chilled on ice for 12 min, cells were harvested as before and the cell pellet re-suspended in 0.04 original volumes of TfbII (10 mM MOPS, 75 mM, 10 mM rubidium chloride, 15 % v/v glycerol). The solution was chilled on ice. Aliquots of this suspension (400 μL) were used immediately. Alternatively, the cells were snap frozen in ethanol and stored at -80 °C. For transformations, 100 μL of competent cells were aliquoted into eppendorf tubes containing 100-1000 ng/μL plasmid DNA. Tubes were incubated on ice for 15 min. The cell suspension was heat shocked at 42 °C for 90 sec for transformations and subsequently incubated on ice for 3 min. Cells were rescued in 800 μL 2XTY and incubated at 30 °C or 37 °C with shaking at 100 rpm. Transformants were plated on LA supplemented appropriately with antibiotic **(see 2.3)**. Plates were dried in a BSC II and subsequently incubated at 30 °C or 37 °C without shaking. For recipes of all solutions, refer to Appendix A

### 2.7.2 Mycobacterial electroporations

For electroporations, 100 mL of *M. smegmatis* $mc^2$ 155 was propagated in a shake flask at 37 °C as previously described **(see 2.3)** to $OD_{600}$ = 0.8-1. Cells were harvested by centrifugation (Beckman Coulter Allegra™ X-22R centrifuge) at 3901 x g for 10 min at 4 °C. The pellet was re-suspended in ice cold 10% glycerol (v/v). The washing procedure was repeated twice and cells re-suspended in a final volume of 1 mL 10% glycerol (v/v) and used immediately. At least 1μg of plasmid DNA was mixed with 300 μL competent cells in a 0.2 cm electroporation cuvette kept on ice. The BioRad Gene Pulser XCell™ system was employed for electroporations with the following settings: 2500 V, 25 μF, 1000 Ω and 0.2 cm. Cells were immediately rescued with 800 μL 2XTY. For generation of knock out mutants via the recombineering strategy, rescue media was supplemented with isovaleronitrile (1 μL for every 1 mL of media). Following overnight phenotypic expression of marker genes, the transformants were harvested, re-suspended in fresh media and subsequently propagated for 3-7 days as previously described **(see 2.3)**

`

## 2.8 Agarose electrophoresis

Following plasmid extraction, PCR amplification, restriction profiling, genomic DNA digestion and cloning, separation of fragments on agarose gel was routinely done by agarose gel electrophoresis and visualized under UV. The principle of agarose electrophoresis is based on separation of DNA according to size. Agarose dissolved in 45 mL 1X TAE buffer (40 mM Tris-acetate and 1 mM EDTA) and supplemented with 1.5 μL ethidium bromide (0.5 μg/mL) was left to solidify with an 8 or 16 well comb in the casting tray, before being immersed in an electrophoretic tank containing 1X TAE. Samples were mixed with 3 μL loading dye (containing glycerol and bromophenol blue) and were loaded alongside a molecular weight marker and separated at 80-100 V for 50 min. DNA was visualized under UV and images saved using a GBox SynGene hardware operated by SynGene software (v7.1.2). A low percentage agarose gel (0.8-1%) was prepared for the separation of high molecular weight DNA fragments.

## 2.9 DNA purification

DNA fragments of interest were excised from agarose gel for downstream processes such as cloning. The Nucleospin DNA extraction and purification kit (Macherey and Nagel) was employed for all gel purification purposes following the manufacturer's instructions. The DNA fragments of interest were first visualized as previously described **(see 2.8)** and the bands were excised using a heat sterilized scalpel. Appropriate protective gear was adorned while excising fragments on the illuminated bench top panel of the transilluminator in the dark room. Excised fragments were transferred to a sterile eppendorf tube and subsequently weighed on a bench top scale. For every 100 mg of gel, 200 μL buffer NTI was added and the tubes were incubated at 50 °C for 10 min. Once the gel was completely dissolved, the suspension was transferred to a column and centrifuged at 11000 x g for 30 sec. Following binding of DNA to the column, the flow through in the collection tube was discarded and the column washed twice at 11000 x g for 30 sec in 700 μL buffer NT3. The membrane on the column was dried by centrifugation at 11000 x g for 60 sec. Buffer NE (30 μL) was added to the columns fitted with sterile eppendorf tubes and incubated at ambient temperature for 5

`

min. DNA was eluted by centrifugation at 11000 x g for 60 sec and visualized as previously described **(see 2.8).**

### 2.10 Sequencing

All constructs generated via amplification of genomic regions of interest by PCR were sequenced. Sequencing primers **(see 2.6.2)** were designed and aliquots of constructs shipped to the Central Analytical Facility at the University of Stellenbosch. All sequences were analyzed with Seqman™or clustal suite of programs. For *In silico* tools used in this study, refer to section **2.1**

### 2.11 Preparation of freezer stocks, seed stocks and preservation of plasmids and strains

At least 3 freezer stocks (0.5 mL) of each cloning vector, final knockout construct and strain were prepared in sterile 66% glycerol and cryogenically preserved at -80 °C for reference purposes. Similarly, 1 mL of cultures with the plasmids of interest were aliquated into several eppendorf tubes and were cryogenically preserved as previous. These were used as seed stocks to use in experiments.

### 2.12 Construction of the *cydDC*KO constructs (Homologous recombination)

Primers to generate a knockout construct of the *cydDC* operon were designed as previously described in Table 2.4 **(see 2.6.1)**. A set of primers were designed to amplify 1176 bp upstream of *cydD*. A GC clamp and *Hin*dIII site was engineered in the forward primer of the upstream region of *cydD* while a GC clamp and a *Pvu*II restriction site was engineered into the reverse primer of the upstream region. Similarly, primers to amplify 854 bp downstream of *cydC* were designed and had a *Hin*dIII restriction site in the forward primer, with a GC clamp and a *Pvu*II restriction site engineered in the reverse primer, See Figure 2.1 below.

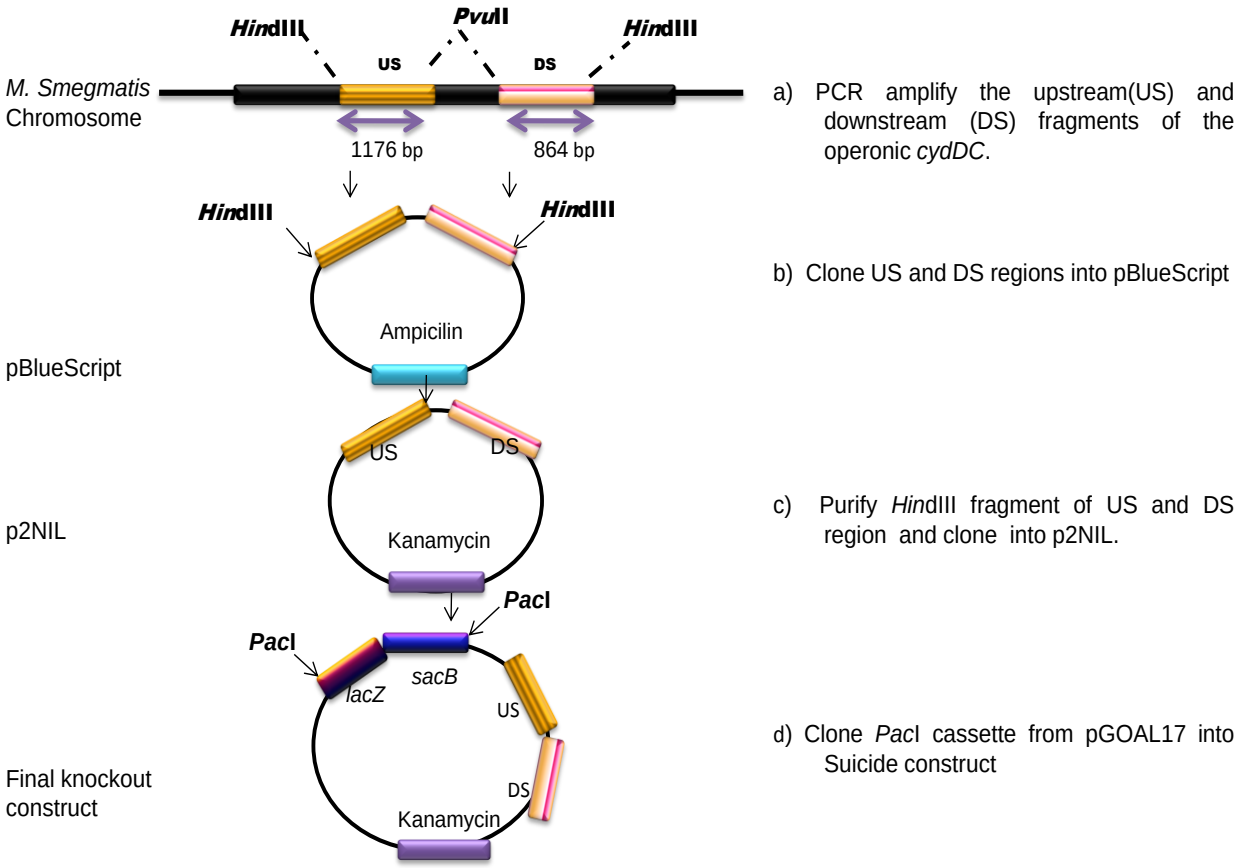


**Figure 2.1**. Diagrammatic illustration of the construction of the *cydDC* suicide construct for use in homologous recombination. Both the upstream and down stream of the operonic *cydDC* were PCR amplified and cloned into pBlueScript via the three way cloning strategy. The fragment was purified as a *Hin*dIII fragment and a two way cloning stategy into p2NIL was carried out. Selectable marker genes were cloned from pGOAL 17 into the suicide construct which was used to knock out the the *cydDC* in *M. smegmatis*.

Primers were procured from Inqaba biotech. Amplification of both the upstream and the downstream regions was done by PCR as previously described **(see 2.6.1)**. The amplicons were separated and visualized on a 1% agarose gel by electrophoresis at 80 V for 50 min. To ensure the right fragment was amplified, a restriction enzyme that cut both the upstream and downstream regions asymmetrically was used for verification. The digests were separated by gel electrophoresis on a 1% agarose gel for 50 min and visualized under UV and images saved using a GBox SynGene hardware operated by SynGene software (v7.1.2). Both the upstream and the downstream amplicons were digested as previously mentioned **(see 2.6.4)** in a sequential digest of *Hin*dIII and *Pvu*II. The *Hin*dIII enzyme was heat inactivated at 65 °C for 20 min. The cloning vector (p2NIL) was also digested with *Hin*dIII and the enzyme heat inactivated after one hour of

`

digestion at 37 °C. The p2NIL was dephosphorylated as previously described **(see 2.6.5)** and all fragments separated by gel electrophoresis. The fragments were gel purified as previously described **(see 2.9)**. A ligation reaction was prepared as previously described **(see 2.6.8)** and the potential recombinants transformed as previously mentioned **(see 2.7.1)**. Recombinant plasmids were extracted as previously described and verified by restriction profiling as previously mentioned **(see 2.6.4)**. The suicide construct was sequenced as previously mentioned **(see 2.10)** and plasmid containing selectable marker genes digested with *Pac*I and cloned. The final construct was transformed into the surrogate strain as previously described (see 2.7.1) and propagated at 30 °C for 48 hours. Blue colonies that emerged were inoculated in broth and the plasmid subsequently extracted for profiling. Freezer stocks of this construct were prepared as previously mentioned **(see 2.11).** This construct was electroporated into *M. smegmatis* $mc^2$ 155.

## 2.13 Construction of the *cydDC*KO constructs (Recombination genetic engineering - recombineering)

A substrate for the deletion of the *cydDC* operon was designed using the clone manager suite of programs and synthesized by GeneScript. The linear substrate contained the following genetic elements: Upstream sequence of *cydD* (350 bp) flanked by a *Pac*I site in the upstream position, a *Hpa*I restriction site flanked by a 34 bp LoxP sequence separated from another 34 bp LoxP sequence by an *EcoR*V restriction site (Figure 2.2). At the terminal end of the second LoxP sequence, a *Hpa*I restriction site was inserted, flanked by a downstream sequence of 350 bp) with a *Pac*I site incorporated at the downstream terminal end. The linear substrate was synthesized by GeneScript and cloned into pUC57, encoding ampicillin resistance. Plasmid DNA (2 μL) was transformed into the surrogate DH5α strain and the plasmid verified by restriction profiling as previously described **(see 2.6.4).** The plasmid (3404 bp) was linearized with *EcoR*V. A plasmid (pMAS 4306 bp) harbouring the 1.4 kbp Strp marker cassette was extracted, profiled using restriction enzymes and digested with *EcoR*V to release the 1.4 kbp Strp cassette, which was subsequently gel purified **(see 2.9)**. The linearized vector was dephosphorylated using NEB Antarctic phosphatase as previously described **(see**

`

**2.6.5)** and the 1.4 kbp Strp cassette was phosphorylated with NEB PNK for blunt end cloning as previously described **(see 2.6.6).** Both the insert and the vector were separated and visualized on a 1% agarose gel **(see 2.8)** and gel purified **(see 2.9)**.

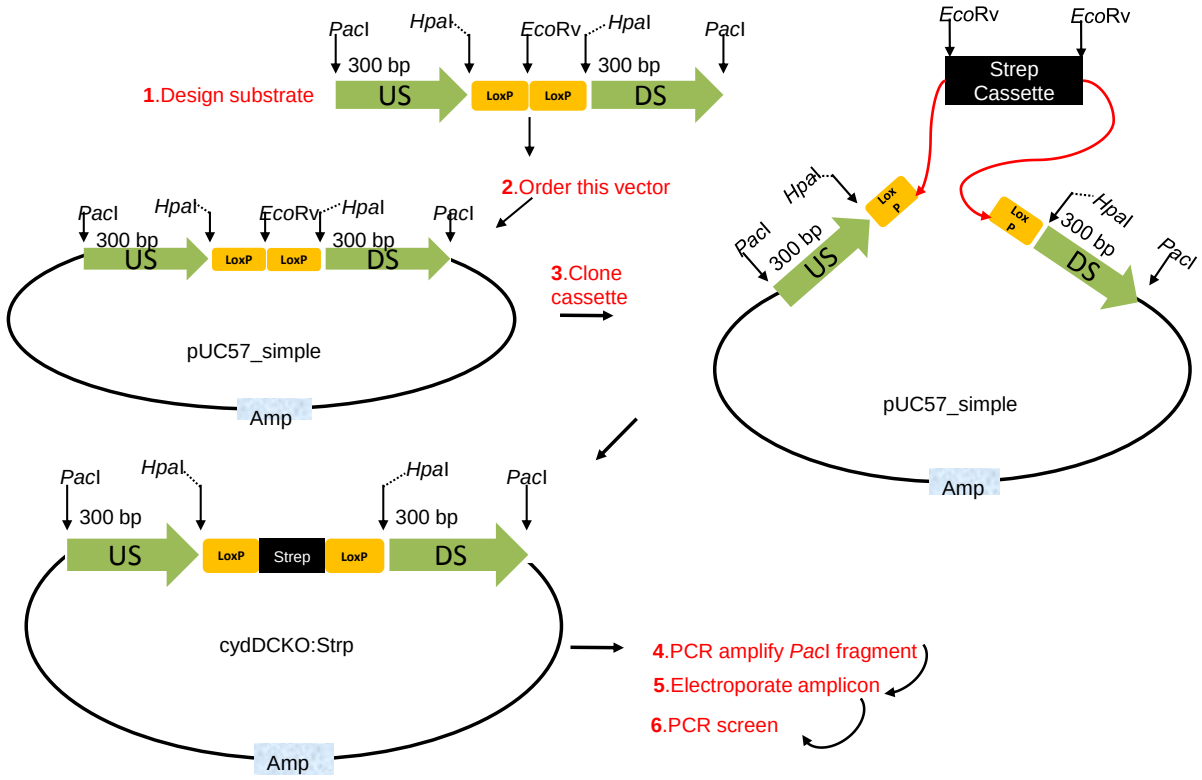


**Figure 2.2**. Diagrammatic illustration of the design of the recombineering substrate. Three hundred base pairs (300 bp) was selected upstream of *cydD* and downstream of *cydC* with *Pac*I restriction sites engineered in the upstream of *cydD* and downstream of *cydC*. A blunt cutter (*Hpa*I) was engineered immediately downstream and upstream of *cydD* and *cydC* respectively to enable the removal of the LoxP-LoxP sequence which was separated by another blunt cutter (*Eco*Rv). Following cloning of the selectable marker cassette, primers specific for the substrate were used to amplify the substrate which was later electroporated in *M. smegmatis* $mc^2$ 155 for allelic exchange by recombineering. Electroporations were plated in 7H10 strep and incubated until colonies emerged. These were screened by PCR.

The gel purified fragments were visualized once more before cloning to confirm integrity and concentration. A ligation reaction using NEB ligase was performed overnight as previously described (see 2.6.8). The ligation mixture was transformed into 100 µL of $CaCl_2$ competent cells as previously described **(see 2.7.1)** and selected on LA, supplemented with Strp for growth at 37 °C. Recombinant plasmids were extracted and screened as previously described **( see 2.4.1 and 2.6.4)**

`

## 2.14 Generation of KO mutants (homologous recombination)

Reverse genetics allowed for the functional analysis of the *cydDC* encoded exporter in *M. smegmatis*. This involved creating a truncated version of the *cydDC* operon through homologous recombination, a technique described by (Gordhan and Parish, 2001). The final Kan marked Δ*cydDC* construct with selectable marker genes was mixed with 300 μL electrocompetent *M. smegmatis* cells while on ice and transformed as described previously **(see 2.7.2)**. Cells were rescued in 2XTY and incubated with shaking overnight (30 °C) for phenotypic expression of marker genes. Cells were harvested and re-suspended in 500 μL of 7H9 and propagated on 7H10 supplemented with Kan and Xgal. Plates were incubated at 30 °C for 4 days and blue colonies were picked and propagated in 7H9 with Kan. The culture was propagated to $OD_{600}$ =2 and 70 μL diluted serially in 7H9 (700 μL) from $10^{0}$-$10^{-9}$. Dilutions were plated in duplicate on 7H10 (2% sucrose and 2% Xgal) and incubated at 37 °C**.** White colonies were picked and spotted in 7H10 (XGal) and 7H10 (Kan, Xgal). Cells that appeared white on 7H10 (Xgal) and perished on 7H10 (Kan, Xgal) were taken forward as possible mutants for preliminary screen by PCR. This procedure is outline in Figure 2.3.

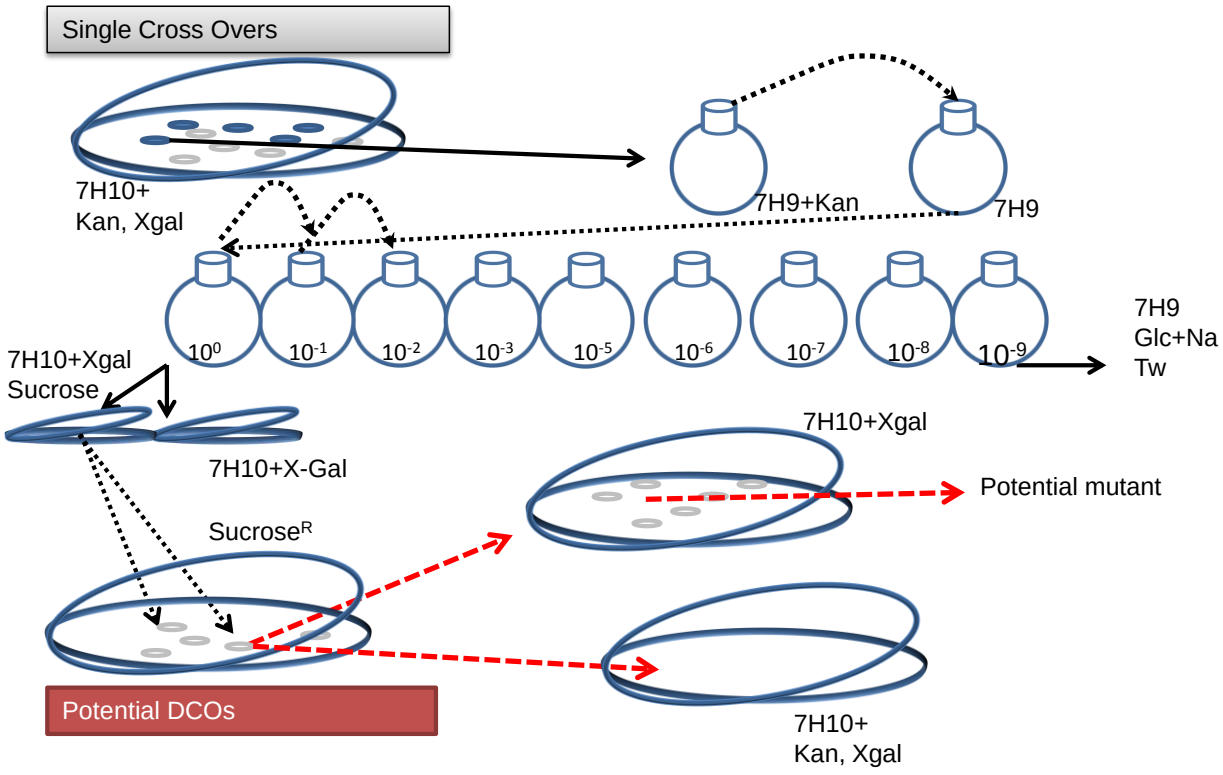


**Figure 2.3**. Schematic illustration of the generation of knock out mutants by homologous recombination. Blue colonies were cultured in 7H9 with Kan and cultivated to stationary phase. One mL of this culture was sub-cultured in 7H9 and propagated to stationary phase. A ten fold serial dilution of this culture was prepared and plated on 7H10 with and without sucrose. White colonies on 7H10 with sucrose were further patched on 7H10 supplemented with Kan, Xgal and 7H10 without kan. Colonies that appeared white on 7H10 Xgal and die on Kan were potential mutants and were taken forward for screening. (Adapted from Gordhan and Parish 2001)

Primers for screening were designed such that one amplifies a portion of the upstream region, one amplifies portion of the downstream region while the third amplified a region within *cydC,* see Figure 2.4 below.

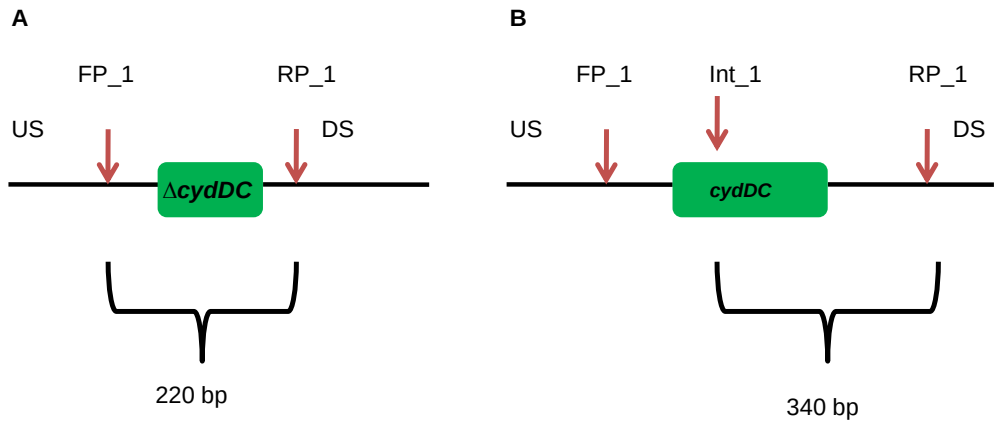


**Figure 2.4**. Diagrammatic illustration of the primer binding sites for preliminary screening of potential mutants by PCR. A) Forward Primer 1 (FP_1) that binds upstream of the truncation pairs with Reverse primer 1 (RP_1) to yield an amplicon of 220 bp. B) a primer that binds within *cydC* pairs with RP_1 to yield an amplicon size of 340 bp. This region for binding of Int_1 is missing from the *cydDC* deletion mutant.

A schematic illustration of how homologous recombination occurs in the chromosome is depicted below in Figure 2.5.

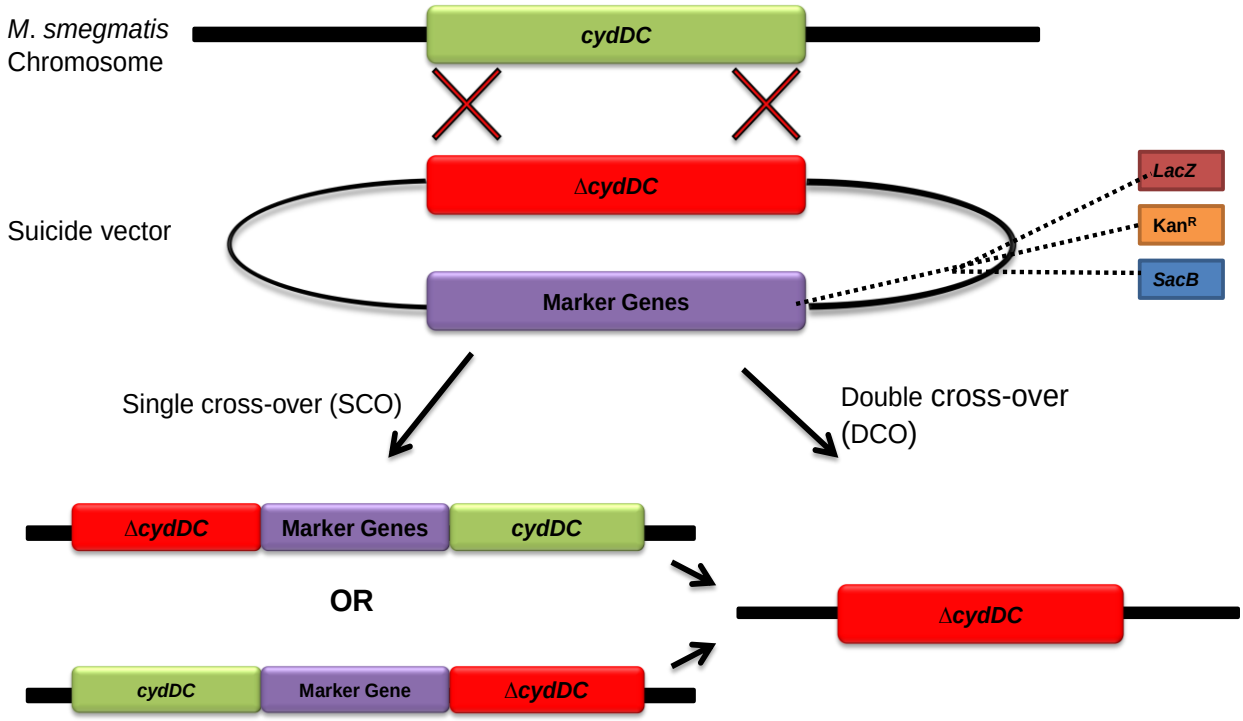


**Figure 2.5**. Diagrammatic illustration of the two step allelic exchange. A vector that carries the upstream sequence of *cydD* and the downstream sequence of *cydC* and additionally lacks the ability to replicate on its own is introduced *M. smegmatis* $mc^2$ 155 by electroporation. Regions of homology hybridize leading to the generation of single cross overs (SCO) which contains both the mutated allele, the wild-type allele and the selectable marker cassette. A double cross over (DCO) event leads to the loss of the wild-type allele and selectable marker genes. (Adapted from Gordhan and Parish 2001)

`

## 2.15 Generation of KO mutants (Recombination genetic engineering - Recombineering)

A plasmid (pNIT) encoding proteins for the RecET system needed for recombineering was extracted and profiled using restriction enzymes as previously described **(see 2.4.1, and 2.6.4).** Wild type *M. smegmatis* was cultivated at 37 °C overnight and prepared for transformations. Electro-competent *M. smegmatis* cells were transformed with atleast 1 µg of the pNIT plasmid as previously described **(see 2.7.2)**. Transformations were incubated at 30 °C, overnight to allow phenotypic expression of selectable marker genes. Transformations were plated on 7H10 Kan and incubated at 30 °C for 4 days. A single colony was cultivated in 2 mL 7H9 Kan to $OD_{600}$ 2. A 100 µL of this culture was inoculated in a 100 mL 7H9 Kan and propagated to $OD_{600}$ 0.4 at which point the recombinase machinery was induced by adding iso-valero nitrile (1 µL per 1 mL media). The culture was allowed to reach $OD_{600}$ 0.8-1, and harvested at 3901 x g for 10 min. The culture was subsequently washed three times with 10% glycerol (v/v). Primers to amplify regions of homology in the substrate were designed and procured as previously mentioned **(see 2.2)**. Amplification with the synthesized primers was performed by PCR as previously described **(see 2.6.1)** and a 2111 bp fragment was separated and visualized as previously described **(see 2.8)**. The amplicon was concentrated and approximately 1 µg of linear amplicon was electroporated as previously described **(see 2.7.2)**. The electroporations were incubated at 37 °C overnight for phenotypic expression of selectable marker genes. The transformants were harvested at 16162 x g for 2 min and re-suspended in 500 µL sterile 7H9. The transformants were cultivated in 7H10, supplemented appropriately with Strp and incubated at 37 °C for 4 days. Colonies were screened by PCR (Table 2.8) for sequencing and screening respectively. One primer, placed further upstream of the upstream region was designed and an internal reverse primer that binds within the streptomycin cassette was also designed.

`

**Table 2.7 Mutant screening primers for homologous recombination strategy**

| Primer name | Sequence 5`-`3 | Position |
|---|---|---|
| US_Fwd | TACCTGATCGCTGCGGTC | Binds 52bp upstream *cydD* |
| DS_Rvs | GTGTCTGACGACTCGGTCGAC | Binds inside *cydC* |
| *cydC* Int Fwd_ | TTTCCGGTGGTCCTGCTCGAC | Binds 168bp downstream *cydC* |

**Table 2.8 Recombineering sequencing and screening primers**

| Primer name | Sequence 5`-`3 | Position |
|---|---|---|
| Fwd_1 | ATGTGCTGCAAGGCGATTAAG | 100 bp upstream of the 350 bp of the upstream of the *cydD* sequence |
| Fwd_2 | TGCGGCGCTACCTGATCGCTG | Binds within the 350 bp of the upstream region |
| Fwd_3 | ACTTCGCTGCTGCCCAAGGTT | Overlaps the |

`

| | | |
|---|---|---|
| | | 350 bp region |
| Strp within | GCCGAAGTATCGACTCAACTA | Binds inside Strp cassette |
| Strp_R | GCT TCC CCT GGA GAG AGC GAG A | 100 bp downstream of the *cydC* downstream sequence |
| Screening primers | | |
| **Gene Specific_F (Recomb)** | GTTCGTGTCGCTGAAGACCT | 1058 bp |
| **Gene Specific_R (Recomb)** | GGTGCTGTACTCGACCACCT | |

`

## 2.16 Southern blot analysis

### 2.16.1 gDNA digestion

Genomic DNA of wild type *M. smegmatis*, single cross over and potential mutants was digested overnight in a volume of 20 μL with *Aat*II and *Pst*I respectively. Digests, including λ marker IV, were separated in a 0.8% agarose gel prepared in 1X TAE at 80 V for 120 min and visualized as previously described alongside a ruler.

### 2.16.2 Electro-blotting

The gel was soaked in a receptacle containing depurination solution (Solution I) made up of 0.2 M HCl and subsequently left to stand for 15 min with mild shaking every 5 min. Solution I was decanted into a waste bottle and the gel washed twice (mild shaking) for 5 min with distilled water. The gel was then soaked in denaturation solution (Solution II) composed of (0.5M NaOH/1.5M NaCl) for 30 min with mild shaking every 5 min. Solution II was decanted into a waste bottle and 1X TBE used to equilibrate the gel (50 mL 10X TBE + 950 mL $dH_2O$). A nylon membrane was cut to the following dimensions: 6.5 cm X 9.5 cm for DNA transfer. A transfer cassette was placed inside a glass dish and a sandwich set up as follows: first, two TBE soaked sponges were laid down followed by two TBE soaked filter papers, the gel was placed on the filter paper with wells facing up. The nylon membrane was properly aligned with the gel and two TBE soaked filter papers placed on the nylon membrane. A TBE soaked sponge was placed on top of the membrane followed by the top cover. The clips were engaged to close the cassette. The sandwich was transferred to a tank. Transfer was performed at these parameters: 90 V, current 600 A and time 120 min. Following transfer, the sandwich was dismantled and the membrane transferred to dry filter paper and crossed linked in a UltraViolet crosslinker for 2 min at 2470 kJ. Membranes were immediately hybridized.

`

### 2.16.3 Probe synthesis and labelling

Probes were synthesized using primers that were used to generate the upstream region of the p*cydDC*KO knockout construct. The PCR probe synthesis kit (Roche) was employed to synthesize labelled probes by incorporating a labelled dioxygenin UTP. Fast start taq DNA polymerase was used to generate probes using the same cycling conditions as described before **(see 2.6.1)**. An unlabeled probe amplicon was loaded alongside the labelled probe amplicon as a control to observe the increase in molecular weight due to incorporation of the DIG nucleotide. Probes were used immediately for hybridization.

### 2.16.4 Hybridization

Nylon membranes with DNA facing up were transferred to hybridization bottles (Hybaid HB-OV-BM) containing 10 mL pre-hybridization solution (DIG-EASY-HYB). The bottles were gently swirled to remove air bubbles and placed inside the hybridization oven (Hybaid Micro-4) at a hybridization temperature of 56°C for 30 min. The hybridization temperature was calculated using the equation:

$$T_m = 49.82 + 0.41(\%GC) - 600/L$$

$$T_{opt} = Tm - 20\ ^{\circ}C$$

**Where Tm = Melting temperature**

**L =length of the probe**

**GC= % of Guanine to Cytosine**

The PCR synthesized probe was denatured at 95 °C for 5 min and immediately placed on ice. The probe was then added at a v/v of 2 μL per 1 mL pre-hybridization solution. Hybridization was done overnight at 56 °C. The spent hybridization solution with probes was decanted into a falcon tube and stored at -20 °C for future use. Membranes were carefully removed from the hybridization bottles and subjected to 15 min of two stringent washes with 20 mL solution I at 56 °C (10 mL of 20X SSC, 1 mL 10% SDS and 89 mL

`

$dH_2O$) and 20 mL solution II at 68 °C (2.5 mL, 20X SSC, 1 mL 10% SDS and 96.5 mL $dH_2O$).

### 2.16.5 Immunological detection

Membranes were rinsed in wash buffer for 5 min **(**100 mL 20X maleic acid, 3 mL Tween 20 in 1L of $dH_2O$) and were subsequently incubated in 25 mL blocking solution for 30 min with intermittent shaking (90 mL wash buffer + 10 mL 10X blocking solution). The blocking solution was decanted and the membranes incubated in 25 mL antibody solution (50 mL blocking solution + 5 μL anti-digoxygenin antibody) for 30 min. The membranes were washed twice in wash buffer for 15 min and equilibrated in 20 mL detection buffer (0.1M Tris HCL, 0.1M NaCl pH 9.5) for 5 min. The membranes were then transferred to hybridization bags (DNA facing up) and 1 mL substrate (CSPD) added and spread over the surface. Excess CSPD was squeezed out and the hybridization bags were sealed and incubated in the dark for 10 min at ambient temperature. The blots were exposed to X-ray film for 10 min in the dark and developed by washing the film in developing solution for 30 sec, in $dH_2O$ for 30 sec, in fixative solution for 30 sec and again in $dH_2O$ for 30 sec. The films were allowed to air dry for 2 min.

## 2.17 Lysis of *E. coli* cells for preparation of membrane fractions

To establish the functionality of the *cydDC* operon, heterologous expression of Mtb genes in *E. coli* was performed. Lysis of *E. coli* cells was performed as previously described (Cox et.al., 1973). The *E. coli* K12 strain and its derivatives were homogenized using a sonicator. For this, the probe of the sonication system was first washed in 100% ethanol by pulsing for 5 min and the probe rinsed with $dH_2O$ for an additional 5 min. Cells (4g wet weight) were washed twice in 0.1 M Tris-HCl pH, 7.4 were re-suspended in 20 mL of the same buffer. The 50 mL falcon tube containing cells were placed in a small beaker with crushed ice and 100% ethanol. Cells were placed inside a soundproof booth with the probe sonicator. The probe was dipped into the falcon tube containing cells and ultrasonic wave parameters set as follows for lysis: time-20 min, cycle-6, power, 0.99. Cells were subsequently homogenized at these

`

parameters and cooled on ice for 10 min between each lysis step. 8-10 steps of lysis were performed before membrane fractions were extracted.

### 2.17 Lysis of *M. smegmatis* cells

*M. smegmatis* cells were lysed for extraction of membrane fractions as previously described (Guttman., et.al 2009). For the functional analysis of the *cydDC*, *M. smegmatis* and its derivatives were homogenized using a French Press. Parts of the FrenchPpress system were washed with $dH_2O$ and allowed to chill at 4 °C. The piston was inserted up to the “Max fill” into the cylinder, which was turned upside down and place into the tripod. The needle valve was screwed into the piston head and the flow through pipe tightly screwed on. Cells were transferred to the cylinder leaving a 1 cm head space and an empty 50 mL falcon tube was connected to the cap of the flow through tube. The piston head was fitted over the filled cylinder while supporting the piston handle with the other hand. The cylinder, held in the correct position, was then transferred to the pressure chamber. The needle valve on the piston head was tightened and the device was turned on. The lever was engaged to the medium position and the right side dial was used to adjust the pressure to 2.7 kpsi. A small drizzle into the falcon tube was observed and the entire complex was lowered down by pushing the lever to the down position. The falcon tube was unscrewed and placed on ice. The complex was removed from the French press and the piston pulled to the “max fill” mark. Membrane fractions were extracted from lysed cells by ultracentrifugation (**see 2.18**).

### 2.18 Purification of membrane fractions by ultracentrifugation

Alternatively, 100 mL of cells were harvested and re-suspended in 20 mL EDTA wash buffer (50 mM HEPES-KOH, containing 20 mM EDTA and 10% glycerol pH7.0) and cells were homogenized using a sonicator. Cells were incubated at room temperature (30 min) with casual stirring. Cell were harvested at 5755 x g for 10 min and re-suspended in 10 mL lysis buffer, supplemented with 0.1 mM PMSF and proteinase inhibitor cocktail (50 mM HEPES-K, containing 150 mM KCl, 10% glycerol pH 7.0) and homogenized in a sonicator (max power, 20 min and 4 cycles). The cell lysate was

`

incubated at 37 °C for 120 min with gentle stirring and sonicated as follows (On for 1 min (as previously described 2.17), and placed on ice for 3 min) for 20 cycles. The supernatant was harvested at 7 674 x g for 20 min at 4 °C and pooled into ultracentrifuge tubes. The supernatant was clarified at 17 266 x g for 20 min at 4 °C. The centrifugation step was repeated. The resulting supernatant was ultracentrifuged at 38 369 x g for 60 min at 4 °C. The reddish transluscent pellet was re-suspended in membrane purification buffer (50 mM HEPES-KOH, containing 300 mM KCl, 2 mM $MgCl_2$ and 20% glycerol pH 7.0) and was subsequently centrifuged at 38 369 x g for 40 min at 4 °C. The membranes were re-suspended in minimal volume of membrane purification buffer.

Alternatively, membrane fractions obtained by lysis with a French press were purified as described by (Kana et al., 2001). Membrane fractions were collected by ultracentrifugation at 17 266 x g. The supernatant was further clarified by ultracentrifugation at 47 962 x g. The supernatant from this preparation was used as membrane containing fraction and was used for membrane spectroscopy.

## 2.19 Phenotypic characterization of Mutants

### 2.19.1 Membrane spectroscopy *E. coli* and *M. smegmatis*

To determine the presence of the spectroscopic features associated with a functional C*bd*O, membrane spectroscopy was performed. The Cary4E dual beam spectrophotometer was first blanked with two cuvettes containing re-suspension buffer. Membrane fractions (3 mL) were transferred to an electroporation cuvette and were oxidized with potassium ferricyanide and reduced with grains of sodium dithionate. The reduced minus oxidized spectra were recorded at room temperature using the Cary4E spectrophotometer.

### 2.19.2 Response to induced oxidative stress

Response to oxidative stress was tested using a modified protocol described by (Poole et al., 1989). *M. smegmatis* $mc^2$ 155 and its derivatives were assayed for survival upon

`

exposure to 2% exogenous hydrogen peroxide ($H_2O_2$). For this, *M. smegmatis* $mc^2$ 155, *M. smegmatis* Δ*cydDC*, Δ*cydDC*::pMV*pcydDC* were cultured (see 2.3) in a shake flask to $OD_{600}$ = 0.1 and a 10-fold serial dilution performed on each strain in triplicate and plated on plain 7H10 media for unmarked strains and selective 7H10 for the complemented strains. The plates were incubated at 37 °C for 48-72 hrs. CFUs were enumerated to assess survival upon exposure to exogenous $H_2O_2$. Similarly *E. coli* and its derivative strains were cultured to an $OD_{600}$ 0.2 and assessed for the ability to survive exposure to 2% exogenous $H_2O_2$. A 10 fold serial dilutions of the peroxide exposed culture were plated on LA supplemented appropriately with Hyg for marked strains and on plain LA for unmarked strains. Plates were incubated at 30 °C for 24 hrs and CFUs were enumerated to assess survival.

### 2.19.3 Growth curves

Growth trend analysis was performed as described by (Kana et al., 2001). Growth trends of *M. smegmatis* and its derivatives were assessed in 7H9 in a Bioflow 110 fermenter at 21 % and 0.7% dissolved oxygen as previously described (see 2.3) for 24 hrs. For every strain, growth was first monitored at 21 % dissolved oxygen. The fermenter was allowed to stabilize at the set dissolved oxygen limit for atleast one hour before decreasing the oxygen tension to 5% and finally to 0.7%. OD readings were taken every three hours and viable counts were determined by plating dilutions of a certain range as determined by OD readings. The plates were allowed to dry in a class II biosafety cabinet and incubated at 37 °C for atleast three days. Plates were observed for growth and CFUs were enumerated.

### 2.19.4 Temperature sensitivity assays

The temperature sensitivity assay was done as described by (Kana et al., 2001). The ability of *E. coli* and its derivative strains to grow at high temperatures was investigated. *E. coli* and its derivative strains were cultivated to stationary growth phase ($OD_{600}$ 2) by incubating at 37 °C with spinning (110 rpm). A 10-fold dilution series of the stationary phase cultures was performed. Dilutions were plated with and without selection. Plates were allowed to dry in a Class II biosafety cabinet and subsequently incubated at 42 °C.

`

Plates were examined for growth and CFUs were enumerated. A student T test was employed to determine statistical difference between the data set.

### 2.19.5 Nutrient starvation assays for *E. coli*

The nutrient starvation assayed was done as initially described by (Siegele and Kolter, 1993). The ability of *E. coli* and its derivatives to exit from stationary phase was investigated. The premise here is that at stationary phase, the bacteria experience nutrient runout. A seed stock of *E. coli* and its derivatives were cultured M63 glucose minimal media. The cultures were incubated at 37 °C with spinning (110 rpm) for up to 10 days. A 10-fold dilution series of the starved cultures was performed and the dilutions were plated on M63 agar. Plates were allowed to dry in a class II biosafety cabinet and incubated at 37 °C for 24 hrs. Plates were observed for growth and CFUs were enumerated from dilutions $10^{-6}$ to $10^{-8}$. A student T test was employed to determine statistical significance between the data set.

### 2.19.6 Nutrient starvation assays for *M. smegmatis*

The ability of *M. smegmatis* and its derivatives to exit from stationary phase was investigated as described by (Siegele and Kolter, 1993). The premise here is that at stationary phase, the bacteria experience nutrient depletion. Cultures of *M. smegmatis* and its derivatives were cultured in sautons media which is a minimal concoction for mycobacterial growth. The cultures were incubated at 37 °C with spinning (100 rpm) for up to 10 days. A 10-fold dilution series of the starved cultures was performed and the dilution series plated on 7H10 with 0.05% glucose. Plates were allowed to dry and incubated at 37 °C for 24 hrs. CFUs were enumerated from dilutions $10^{-6}$ to $10^{-8}$. A student T test was employed to determine statistical significance between the data set.

## 2.20 Data analysis

The student t-test was used to analyze data. A p-value less or equal to 0.05 was considered statistically significant.

`

# 3. Results

## 3.1 The *cydC* gene in *M. smegmatis* encodes a functional protein

Upon retrieving the nucleotide sequence of *cydC* to use for targeted gene deletion, it was noted according to the Smegmalist database, that *cydC* did not encode a functional subunit due to a point mutation in the open reading frame. Previous work from our laboratory on C*bd*O suggested that our laboratory strain of high electroporation efficiency, *M*. *smegmatis* $mc^2$ 155, encodes a functional holo-enzyme for C*bd*O (Kana et al., 2001, Snapper et al., 1990). To further substantiate this, the relevant region in *cydC* was amplified by PCR (with genomic DNA from the laboratory $mc^2$155 wild type strain) and digested with an enzyme that cuts asymmetrically to confirm that region specific amplification occurred, Figure 3.

`

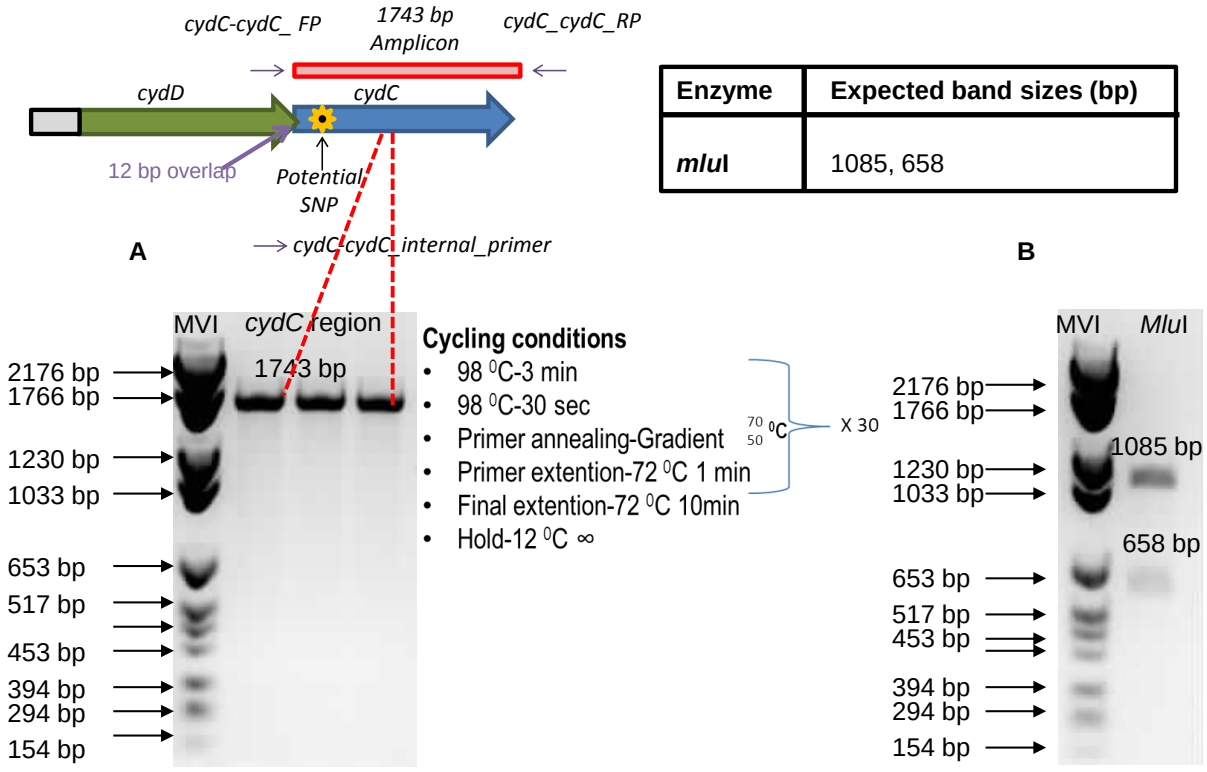


| Enzyme | Expected band sizes (bp) |
|---|---|
| ***mlu*I** | 1085, 658 |

**Figure 3.** (**a)** PCR amplification of full length *cydC* including a 100 bp of upstream and downstream sequence using a high fidelity polymerase. Amplicon (1743 bp) was separated on a 1% agarose gel by electrophoresis for 50 min and visualized under ultra violet light. There is a twelve bp region of overlap between *cydD* and *cydC* indicating that they are operonic. The three lanes represents three replicate PCRs. (**b)** Restriction digest of *cydC* amplicon with *Mlu*I to confirm gene targeted amplification. Restriction digest gave expected band sizes.

The amplicon was sequenced and sequence data was analyzed with a multiple sequence alignment tool, Clustal Omega. The reference sequence used was the *cydC* nucleotide sequence retrieved from the Smegmalist database designated, *M. smegmatis* _*cydC*_ref, in Figure 3.1. The reference sequence was aligned against the sequences generated by designing primers that span the *cydC* genetic region denoted as *cydC_cydC_* forward primer (FP), *cydC_cydC*_internal primer and *cydC_cydC*_reverse primer (RP), the positions of which are shown in Figure 3. The multiple alignment revealed that the sequence resulting from the genomic DNA of our laboratory strain harbor no point mutations and as such, mc$^2$155 encoded a functional *cydC* gene, the function of which could be interrogated further in this study (Figure 3.1).

`




**Figure 3.1**. Multiple sequence alignment using Clustal Omega to prove that *cydC* encodes a functional polypeptide. The nucleotide sequence of *cydC* was retrieved from Smegmalist and aligned with a template sequence generated from primers designed every 500 bp to span the entire gene (1543 bp). Sequence data suggests that there is a cytosine and guanine insertion (circled in red) which is not present from the template synthesized with a high fidelity polymerase from our laboratory stock of high efficiency *M. smegmatis* wild-type cells.

Notably, both the internal primer and the reverse primer had numerous errors at position 146, however, the FP had consistent correct read outs. To substantiate sequencing data, the *cydC* region was edited and translated using Exparsy translate tool to determine if the removed insertions encoded a functional polypeptide (Figure 3.1.1).

`

**A** *cydC* with insertion mutations

```
1     ttgttgcgccatgatccgttgctccgcctgaccctcgagctgttgcgtccccggctcgggcggttcctgctggccgcggc   80
81    gctcggggtgctctcgctgggcagcgcactggcgttggcggggatctcggcgtggctgatcacccggcgcctggcagatg   160
161   ccgcccgtgctggatttgaccgtcgcggtggtggcggtgcgcgcgctgggcatctcccgcggcgtcctgggctactgcca   240
```

**B** *cydC* insertions removed

```
1     ttgttgcgccatgatcgttgctccgcctgaccctcgagctgttgcgtccccggctcgggcggttcctgctggccgcggc   80
81    gctcggggtgctctcgctgggcagcgcactggcgttggcggggatctcggcgtggctgatcacccgcgcctggcagatg   160
161   ccgcccgtgctggatttgaccgtcgcggtggtggcggtgcgcgcgctgggcatctcccgcggcgtcctgggctactgcca   240
```

**C** Translation of the *cydC* region with exparsy

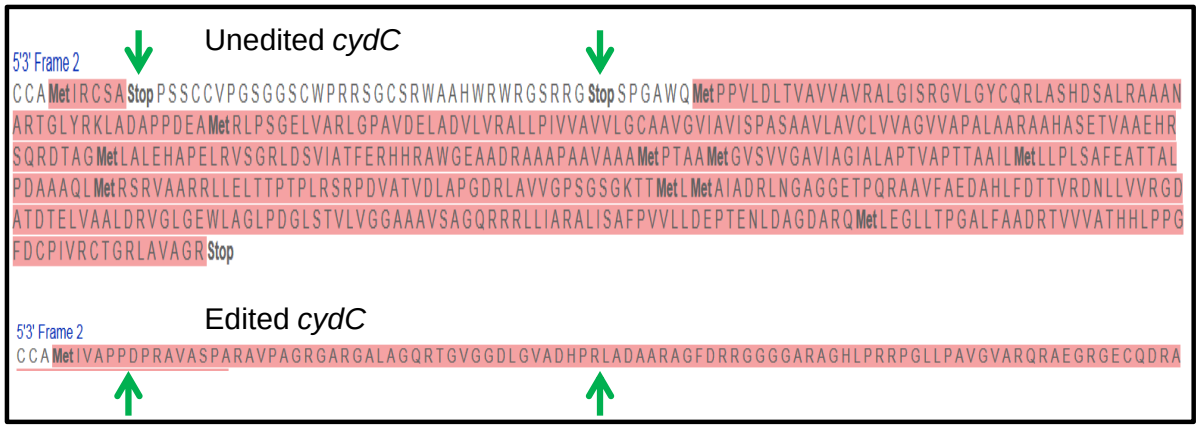


**Figure 3.1.1.** Bioinformatic analysis on the *cydC* region. Nucleotide sequence of *cydC* was retrieved from Smegmalist and mapped for nucleotide insertions identified using sequencing. According to sequence data, several primers report a cytosine and a guanine insertion at position 16 and 146 which creates a frameshift mutations resulting in stop codons that affect the encoded polypeptide. **(A )** Unedited *cydC* region showing in green Methanione signalling translation start site and in red, reported insertions. **(B**) Edited *cydC* region with insertions removed and **(C)** translation of both the edited and unedited *cydC* region using exparsy. This data proves that our laboratory strain of wildtype *M. smegmatis cydC* open reading frame encodes an intact subunit.

This yielded the necessary evidence to confirm that our laboratory strain of wild-type *M. smegmatis* encodes a functional protein thus providing the opportunity to study the function of this transporter in *M. smegmatis*. The *cydC* and *cydD* genes are operonic in *M. smegmatis* as the stop codon for *cydD* overlaps with the start codon for *cydC* (information obtained from Smegmalist) (Aung et al., 2014). Studies in the published literature on various microorganisms report only on single deletions of the ABC

`

transporter pair (*cydD* or *cydC*) (Georgiou et al., 1987, Poole et al., 1989). In addition, the phenotypes associated with these deletions are variable and sometimes difficult to explain (Georgiou et al., 1987, Poole et al., 1989). Based on this, it was decided in this study to generate a double deletion of the putative ABC transporter for functional analysis in *M*. *smegmatis*. However, before embarking on this, we first did modeling of the three-dimensional structure of the CydDC-encoded ABC-type transporter using online modeling tools (see section 2.1) to further understand the topology of these subunits.

### 3.2 Modeling the CydDC subunits

The first task of this study was to understand the structure and the configuration of the conserved residues within the helical ABC domain of the putative *cydDC*-encoded ABC-type transporter in *M. smegmatis*. Protein sequences of both CydD and CydC were retrieved from Smegmalist and deposited into ITASSER for structural threading, which was carried out with 100% confidence for 95% of the modeled residues. Conserved residues associated with the ABC domain were identified and labeled (Figure 3.2).

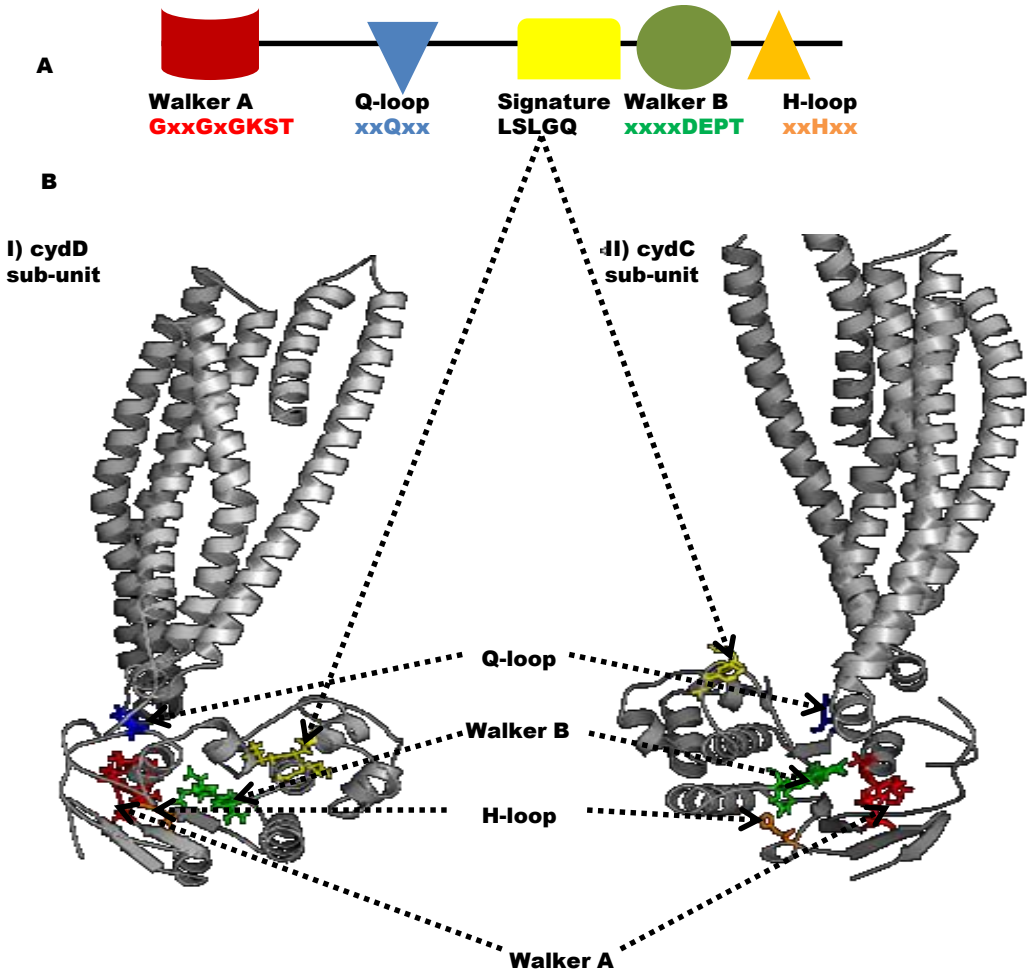


**Figure 3.2**. Structural prediction of subunit III (CydD) and subunit VI (CydC) encoding the putative **A**TP **B**inding **C**assette (ABC) type transporter in *M*. *smegmatis* using ITASSER. The conserved residues in the helical domain as outlined in the colour coded scheme, were identified to verify that the *cydDC* indeed encode members of the ABC type transporter. A) Structural configuration of conserved residues within the helical ABC domain. B) Structural prediction and mapping of conserved residues within the helical ABC domain.

The identification of conserved residues proved irrevocably that in mycobacteria, the CydDC retained conserved residues in the helical domain, which define ABC-type transporters. All of the conserved residues in the helical domain were easily identified. However, the signature motif, designated the LSGGQ motif in most bacteria was missing in both the CydD and CydC. This prompted us to do a multiple alignment with at least 10 unique CydD protein sequences from different bacteria, Figure 3.3. Four of these ten sequences were from the actinobacteria phylum and three belonged to the genus mycobacteria.

`

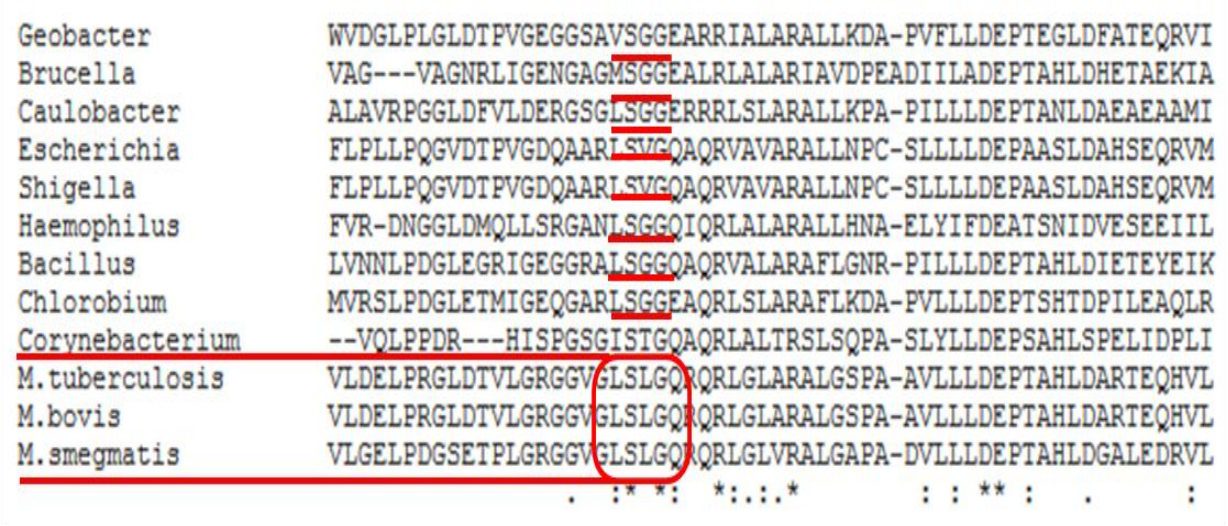


**Figure 3.3**. Multiple alignment of ten CydD protein sequences from unique microorganisms using Clustal Omega. The alignment shows that sequences encircled in red from three mycobacterial species are orthologous and have collectively preserved the **LSLGQ** signature motif which is slightly deviant from the prevalent **LSGGQ** signature motif present in a vast number of microorganisms.

The alignment revealed that the highly conserved LSSGQ motif in other bacteria was indeed present in mycobacteria, but had evolved to an LSLGQ variation of the conserved motif. As this represented a relatively minor change with the prevailing consensus sequence, we propose that this motif is indeed conserved in mycobacteria and we have modeled it on to the three dimensional structure (yellow color in Figure 3.3). Collectively, these observations with the sequence information from our laboratory stock confirmed that *M. smegmatis* encodes a functional CydDC ABC-type transporter in mycobacterial species.

To interrogate the function of the CydDC subunits in *M. smegmatis*, we adopted the heterologous expression approach in *E. coli* where the transporter is best characterized.

`

### 3.3 Construction of a plasmid carrying the Mtb *cydDC* genes for heterologous expression in *E. coli*

To provide preliminary evidence and to further probe the function of this putative exporter, an over-expression system carrying the whole Mtb *cyd* operon was constructed. The approach in this case was to use the Mtb and *M. smegmatis cydDC* genes to complement the phenotypic defects of an *E. coli* Δ*cydD* mutant. The ability of the mycobacterial genes to reverse the defects of the *E. coli* mutant would provide further evidence that these genes indeed encode a functional ABC-type transporter. Hence, the homologous Mtb region was digested from a cosmid library (pOTBcyd) to yield a fragment carrying the entire Mtb *cyd* operon. The plasmid was digested with *Bam*HI and *Hin*dIII as previously described (See 2.6.4) to release the entire *cyd* operon which was subsequently cloned into an over-expression vector (pSE100) which was initially verified by restriction profiling and linearized with *Bam*HI and *Hin*dIII. A ligation reaction was carried out including the following controls: cells only control, linearized vector control, and the uncut vector control. The ligations were transformed in *E*. *coli* DH5α and plated on LA supplemented with Hyg. A few colonies were screened by restriction digest for recombinant plasmid (data not shown). The final complementation construct (clone 5) was profiled with several enzymes to verify the integrity of the plasmid (Figure 3.4).

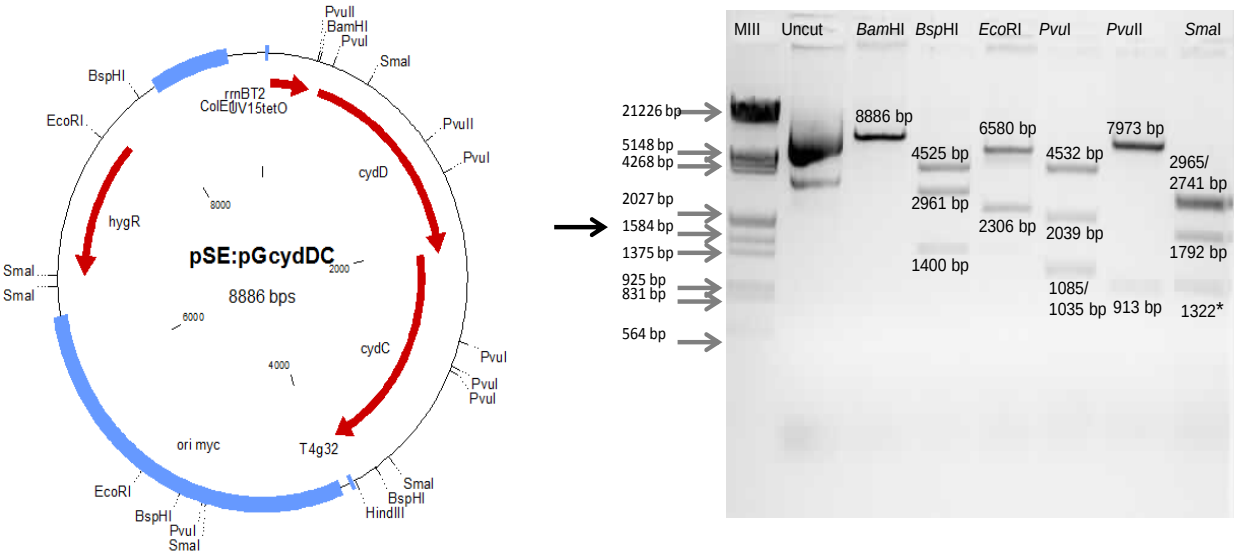


| Enzyme | Expected band sizes (bp) |
|---|---|
| ***Bam*HI** | 8886 |
| ***Eco*RI** | 2306, 6580 |
| ***Bsp*HI** | 1400, 2961, 4525 |
| ***Pvu*I** | 1085, 1035, 165 2039, 4532 |
| ***Pvu*II** | 913, 7973 |
| ***Sma*I** | 2965, 2741, 1792, 1322, 66 |

**Figure 3.4**. Restriction profile of the overexpression construct to be used for heterologous expression separated on a 1% agarose gel. From left to right: Lane 1-2, Marker III and uncut pSE control respectively. Lane 3-8 *Bam*HI, *Bsp*HI, *Eco*RI, *Pvu*I, *Pvu*II and *Sma*I digests respectively. All digest except for the *sma*I digest marked with an asterix gave the expected band sizes. This band was slightly lower than it should be.

A pre-culture of *E. coli* Δ*cydD* (1 mL) was inoculated in fresh LB and cultivated to $OD_{600}$ 0.5. The culture was washed twice in 0.1 M calcium chloride. At least 1 µg of clone 5 was subsequently transformed in calcium chloride competent *E. coli* Δ*cydD* culture. The transformants were selected in LA supplemented with Hyg as previously described (See 2.7.1). The colonies were propagated in LB supplemented with Hyg and the episomal overexpression vector was extracted as previously described (See 2.4.3) and the recombinant plasmid was digested with a few restriction enzymes for verification purposes (Appendix A10).

`

### 3.4 Construction of a plasmid carrying the *M. smegmatis cydDC* genes for heterologous expression in *E. coli*

The *M*. *smegmatis cydDC* operon was also assayed for heterologous expression in *E. coli cydD* null mutant. The *cydDC* operon was excised from a plasmid designated as "clone 29". *Sma*I restriction sites were identified as suitable for excising the *cydDC* operon including up to 300 bp of upstream nucleotide sequence of *cydD.* Blunt cloning into pMV306H was carried out using *Eco*RV to linearize the vector. The fragments were separated by agarose gel electrophoresis in a 1% agarose gel. Before cloning, gel purified fragments were separated and visualized once more to estimate the amounts needed for cloning. As routine, experimental controls that enabled effective troubleshooting included cells only, uncut plasmid and cut and ligate control. The cloning procedure was carried out overnight at ambient temperature using the NEB cloning kit as previously described see 2.6.8. Ten (10 µL) the cloning reaction was transformed in calcium chloride competent *E*. *coli* DH5α cells as previously described see 2.7.1 and the remaining stored at -20 °C. Single colonies that emerged were sub-cultured in LB supplemented appropriately with Hyg and cultivated overnight at 30 °C. Plasmid DNA was extracted following the mini prep protocol as previously detailed see 2.4.3. The extracts were profiled with two enzymes to screen for recombinants (data not sown). Clone 12 was taken forward for large-scale DNA extraction and profiled thoroughly with various restriction enzymes (Figure 3.5). All digests gave corresponding band sizes (Figure 3.5).

`

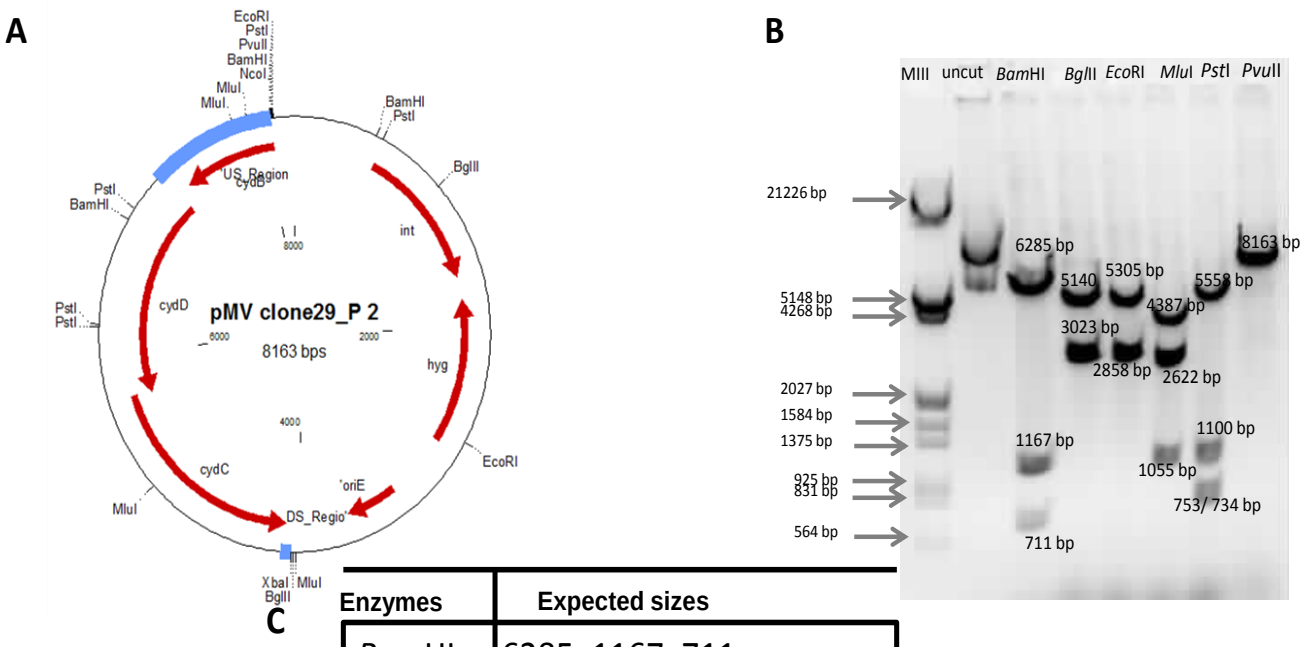


C

| Enzymes | Expected sizes |
|---|---|
| *Bam*HI | 6285, 1167, 711 |
| *Bgl*II | 5140, 3023 |
| *Eco*RI | 5305, 2858 |
| *Mlu*I | 4387, 2622, 1055, 99 |
| *Pst*I | 5558, 1100, 753, 734 |
| *Pvu*II | 8163 |

**Figure 3.5**. Restriction profile of Δ*cydDC* complementation construct designated clone 12 with various restriction enzymes. **(A)** Clone manager map for the virtual construction of "clone 12". **(B)** Restriction profile of clone 12 with various restriction enzymes. Fragments were separated on a 1% agarose gel by electrophoresis and visualized by the GeneSnap software. Loaded from left to right: lane 1&2 Marker III and uncut respectively, lane 3-8 *Bam*HI, *Bgl*II, *Eco*RI, *Mlu*I, *Pst*I and *Pvu*II digests respectively. All digests yielded expected band sizes as annotated. **(C)** Selected enzymes for digestion and expected band sizes.

Restriction mapping confirmed that plasmid was correct and could be used for subsequent heterologous expression experiments. It should be noted that this plasmid was generated after the Mtb heterologous complementation vector. As a result the first two experiments to test heterologous complementation (growth kinetics and membrane spectroscopy) and was done only with the Mtb genes. Thereafter, both the Mtb and *M. smegmatis* genes were tested by heterologous expression in the *E. coli* Δ*cydD* mutant.

`

### 3.5. Heterologous expression of the Mtb putative transporters restores C*bd*O biogenesis in *E. coli.*

The *E. coli* Δ*cydD* strain was complemented with the previously described Mtb genes. The resulting Δ*cydD*(pSE**:**pGcyd) complemented strain was assayed for the ability to restore the loss of C*bd*O associated spectral features in the *ΔcydD E. coli* strain. *E. coli* strains were grown in the Bioreactor at 1% air saturation as growth under hypoxic conditions allows for maximal biosynthesis of the C*bd*O, making is easier to detect by membrane spectroscopy (Kana et al., 2001). A diagnostic feature for the presence of a functional C*bd*O is the chlorin heme *d* molecule, which can be detected at a wavelength of 628-630 nm in the α-band by membrane spectroscopic analysis (Kita et al., 1984). As expected, this peak was absent in the *ΔcydD E. coli* strain, (Figure 3.6.)

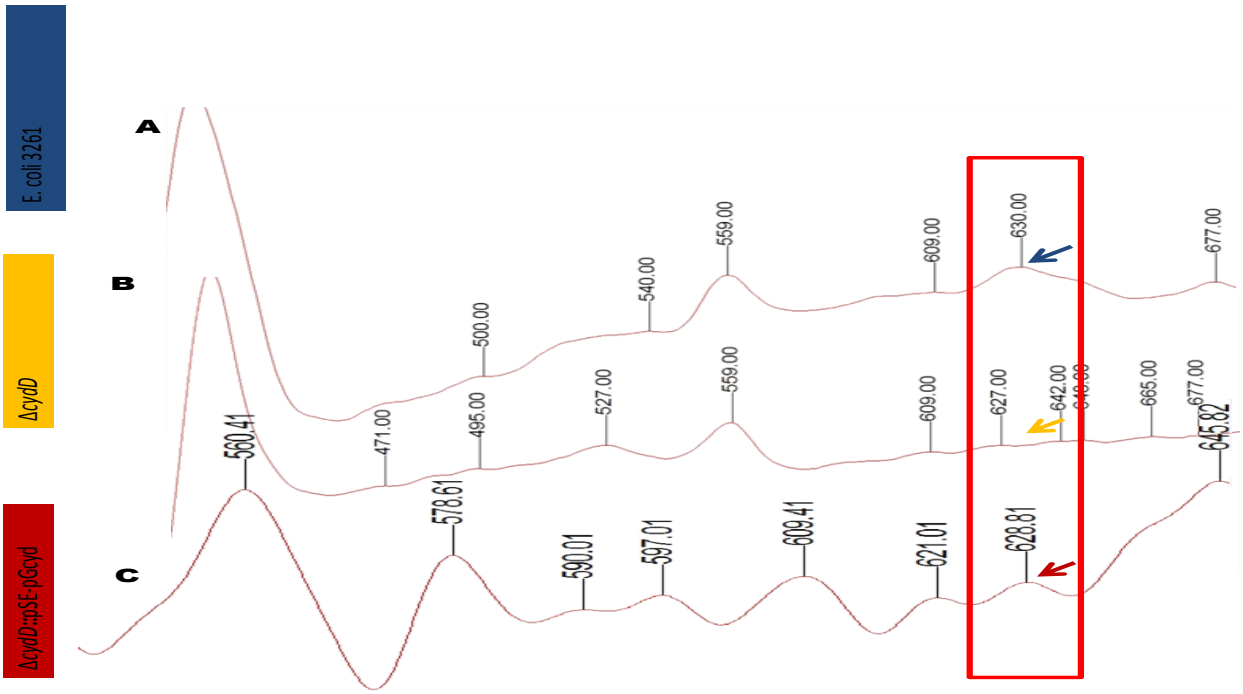


**Figure 3.6**. Absorption difference spectroscopy using the Cary 4E spectrophotometer. Reduced minus oxidized spectra of *E. coli* membrane fractions purified by ultracentrifugation. From top to bottom, aligned spectra of: **(A)** wild-type showing the presence of the heme *d* peak at 630 nm (pointing blue arrow) **(B)** Δ*cydD* characterized by the spectral loss of the chlorin heme *d* peak (yellow arrow) and **(C)** Δ*cydD*(pSE**:**pGcyd) reconstitution of *cydD* with an episomal plasmid carrying the entire Mtb *cyd* operon (red arrow). The data show that spectral features associated with the holoform of C*bd*O is present in **(A)**, wild-type *E. coli* and **(C)**, Heterologously expressed Mtb Δ*cydD*(pSE**:**pGcyd) showing that Mtb *cyd* genes are able to restore the loss of C*bd*O.

`

Ectopic over-expression of the Mtb putative ABC transporter-encoding *cydDC* genes restored diagnostic the heme *d* peak in the membrane spectrum, thus confirming functional C*bd*O biogenesis (Figure 3.6). The reduction in the expression of other cytochromes was also restored by heterologous expression.

### 3.6 Growth kinetic analysis of *E. coli* and its derivative strains

Following spectroscopic analysis of heterologously expressed putative ABC type transporters, we assessed the growth rates of the *E. coli* strains to ensure the increased expression of the mycobacterial genes did not adversely affect the growth of the Δ*cydD E. coli* strain. This was necessary as some of the experiments to test heterologous complementation could be affected by defective growth of the heterologous strain. To investigate this, the growth of *E. coli* and its derivative strains under normoxic conditions was assessed by growth curve analysis. Cells were inoculated either from a seed stock or from a single colony to prepare a pre-culture from which the experiment was performed. *E. coli* and its derivative strain were inoculated from an overnight pre-culture to an $OD_{600}$ 0.01 and OD readings were determined at 30 min intervals. Each strain was assayed in triplicate and each graph represents a mean of three independent experiments (Figure 3.7).

`

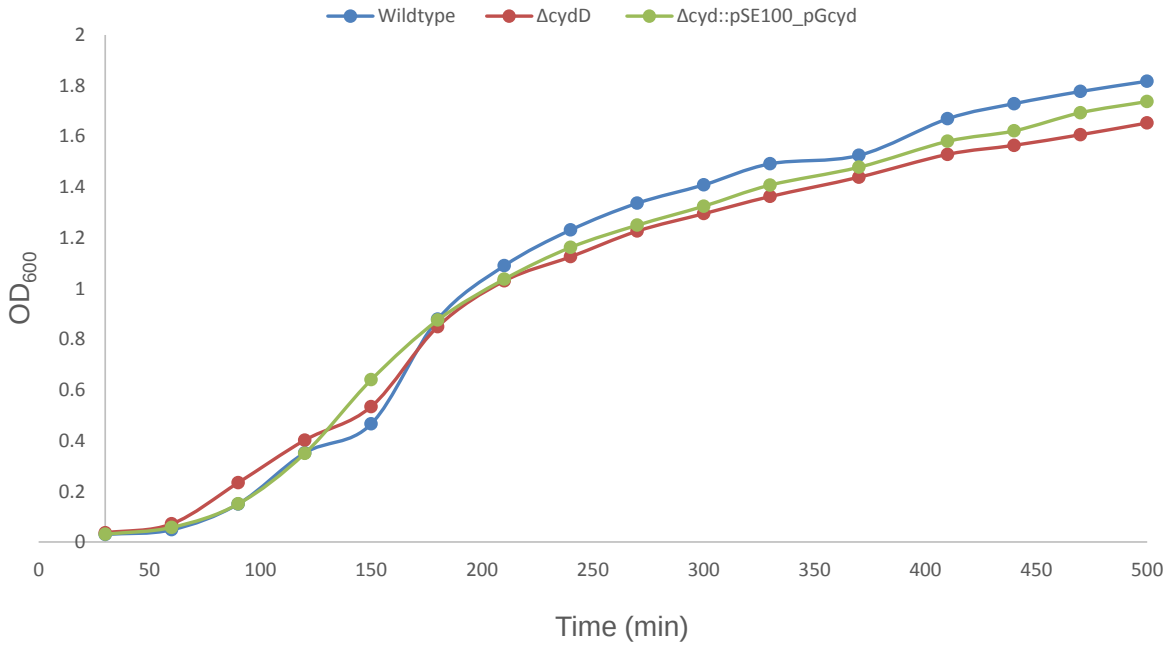


**Figure 3.7**. Growth kinetics of *E. coli* and its derivative strains for 8hrs30 min. **(A)** wild-type (Blue trendline) **(B)** Δ*cydD (*Red trendline) and **(C)** Δ*cydD*(pSE**:**pGcyd) (Green trendline). Notably, Δ*cydD* experiences a growth defect as the cultures approach stationary growth phase as noted by the failure to significantly increase in biomass over time. On the other hand, the Mtb complement displays a similar growth trend to wild-type. However, no statistical difference was observed between the growth of *E. coli* and its derivatives when the data were analyzed by the student t-test. P value= 0.16. This data represents one experimental replicate of each strain performed in the bioreactor.

Ectopic expression of the Mtb genes in *E. coli* yielded similar growth patterns to wild-type under normal growth conditions and as cells entered stationary growth phase (Figure 3.8). However, as the cell population increased and nutrients got depleted, the *cydD* null mutant exhibited what appeared to be a growth defect phenotype (Figure 3.7) as exemplified by poor turnover in biomass at the onset of stationary phase. This reduced biomass was not statistically different to the wild type with a p-value of 0.16 determined by the student t-test.

`

### 3.7 Heterologous expression to assess the stationary growth phase arrest phenotype

To further probe the growth defect observed in the *E. coli* Δ*cydD* strain during growth analysis, further analysis of growth recovery in stationary phase was carried out. It was previously reported that strains lacking CydC (previously isolated as SurB$^-$) experienced stationary growth phase arrest and as such could not exit from stationary phase at higher temperatures (Siegele and Kolter, 1993). At this point, a plasmid for heterologous expression of the *M. smegmatis cydDC* genes (pMV**::***cydDC*) was generated and included in the analysis. Hence, we asked the question: can heterologous expression of Mtb or *M*. *smegmatis* putatitve ABC type exporters rescue the stationary arrest phenotype? This would unequivocally prove that the both transporters phenocopy their counterparts found in *E. coli*. For this, a seed stock of *E*. *coli* and its derivative strains were inoculated in glucose minimal media and cultivated to stationary phase as detailed in (2.19.5). The cultures were incubated at 30 °C for up to 10 days. A 10 fold serial dilution of each strain was performed and plated on M63 plates. The plates were incubated for 24 hours at 37 °C and assessed for growth (Figure 3.8).

`

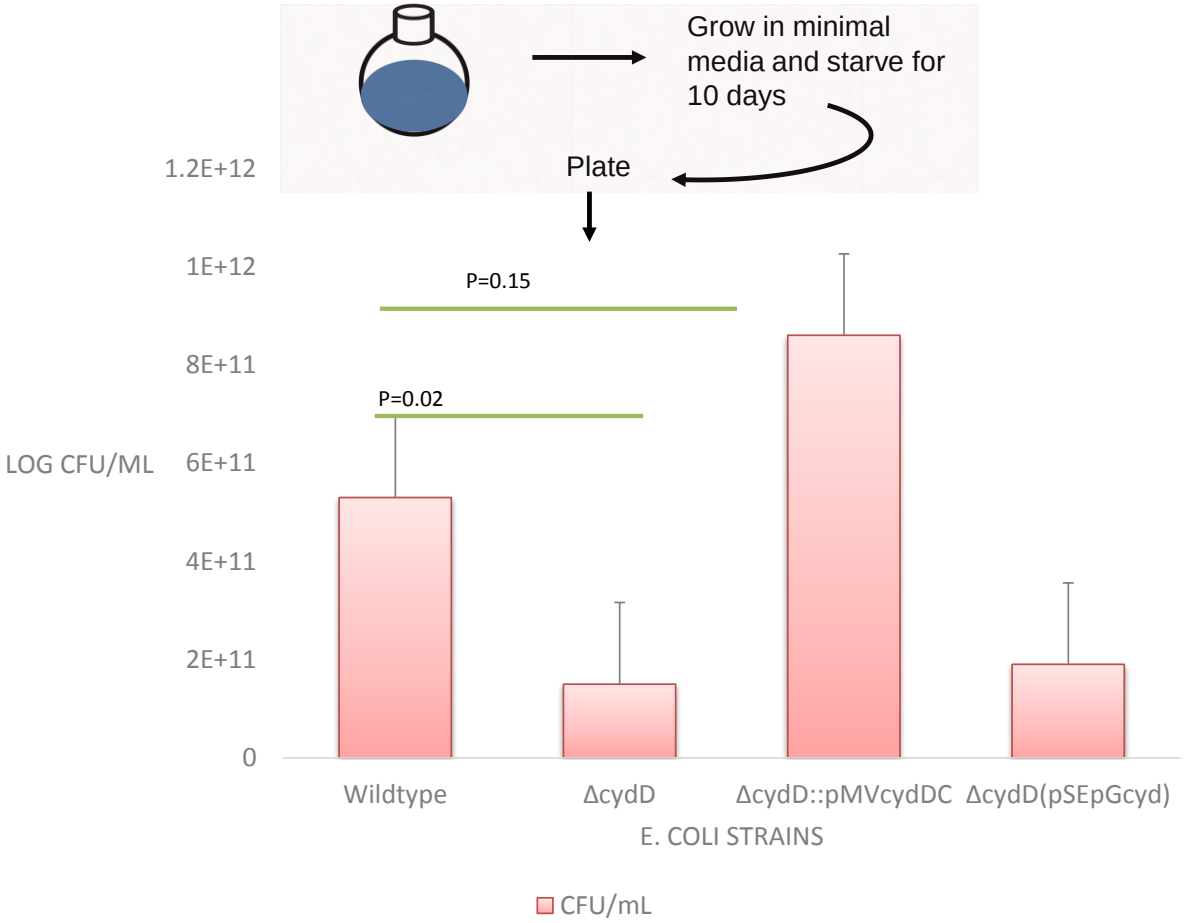


**Figure 3.8**. Nutrient starvation assay in *E. coli* and its derivative strains including wild-type (3561), Δ*cydD (3562),* Δ*cydD::*pMV_*cydDC* and Δ*cydD*(pSE:pGcyd). Following 24 hour incubation period, all plates had growth but a stationary phase defect was evident in the Δ*cydD* strain. The Δ*cydD::*pMV_*cydDC* strain was able to exit from stationary phase arrest better than the Mtb pGcyd complement. Error bars from this this data represents a standard deviation between two experimental replicates. Data analysis revealed statistical significance between wild type *E. coli* and the Δ*cydD* strain

Following the 24 hour incubation probation, all plates had growth, but a stationary arrest phenotype was clearly discernable from the plating efficiency with regards to Δ*cydD* strain relative to wild-type (Figure 3.8). Although the colony size of Δ*cydD* strain was unaffected, the number of platable CFUs were dramatically reduced relative to wild-type and the *M*. *smegmatis* heterologous complement. Complementation with the Mtb genes did not restore stationary phase recovery, which was surprising as this strain showed restoration of the heme *d* peak, associated with functional C*bd*O. The difference between wildtype and *E. coli* and Δ*cydD* was statistically significant (p value of 0.02) as determined by the student t-test.

`

### 3.8. Heterologous expression to assess the temperature sensitivity defect of the *E. coli* Δ*cydD* strain

Previous studies demonstrated that *E. coli* mutant that lacks either *cydD* or *cydC* is unable to form colonies at 42 °C. To establish if supplementation with the mycobacterial counterparts is able to reverse this defect, *E. coli* and its derivative strains were assayed for growth at high temperatures as previously described (2.19.3). Following 24 hrs of incubation at 42 °C, the plated dilutions from $10^{-7}$ across to $10^{-9}$ were examined for growth from three independent biological replicates. Across all three independent experiments, the *cydD* null mutant had distinct growth with reduced colony morphology and plating efficiency relative to wild-type (Figure 3.9).

`

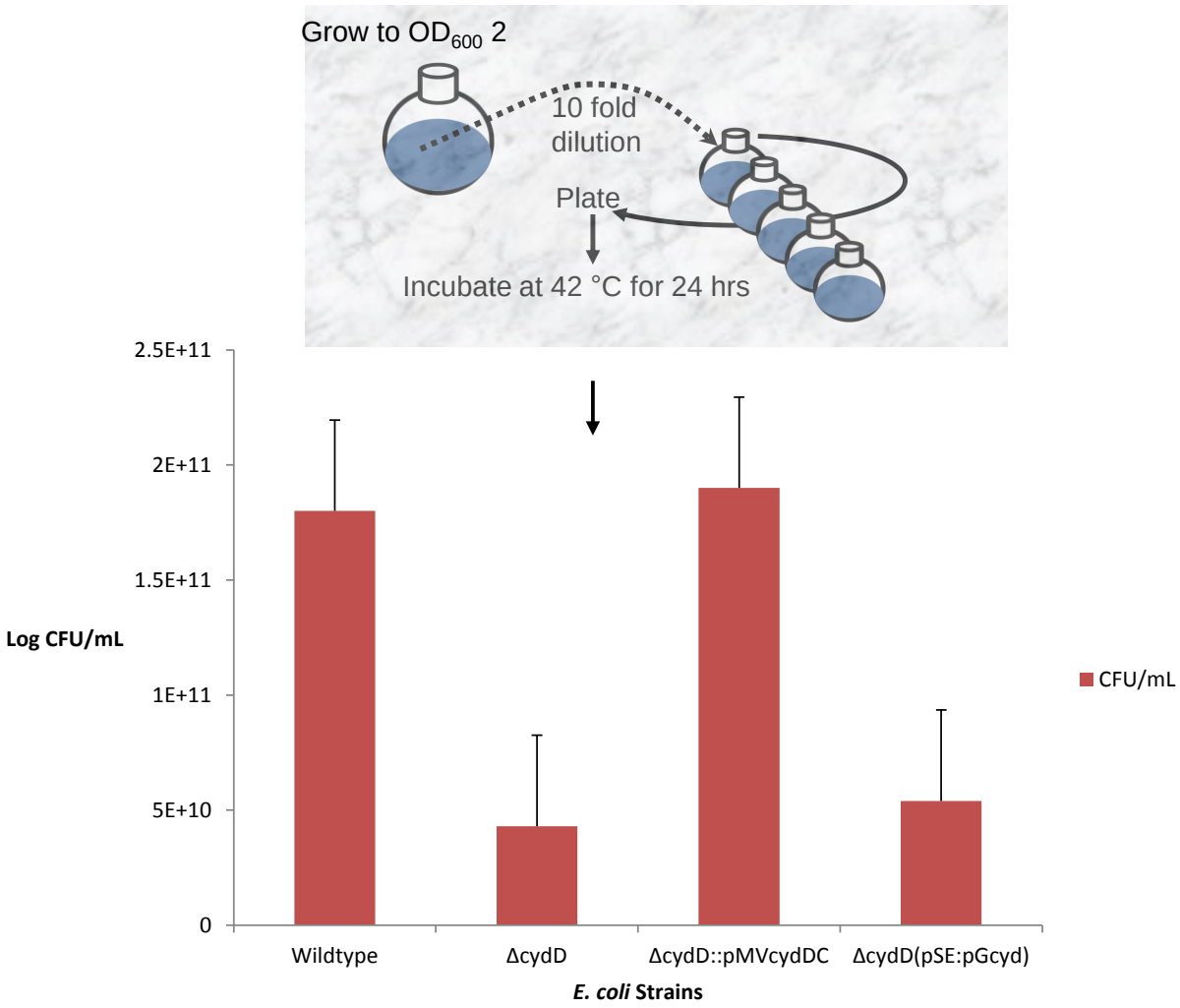


**Figure 3.9.** Assaying for the ability of *E. coli* and its derivative strains to grow at high temperatures. Serial dilutions of cultures cultivated to stationary phase were allowed to dry and subsequently incubated at 42 °C for 24 hrs. Wild-type (3561) grows better than Δ*cydD* mutant (3562) at higher temperatures. Heterologous expression with the *M. smegmatis* exporter is able to rescue sensitivity due to high temperature while the Mtb transporter fails to confer growth at higher temperatures.

This defect was reversed to wild type levels when the *E. coli* mutant was complemented with the *M. smegmatis cydDC* genes. However, as observed with the stationary phase defect, heterologous complementation with the Mtb genes did not reverse the temperature sensitivity defect.

`

### 3.9 Heterologous expression is able to restore sensitivity towards exposure to exogenous hydrogen peroxide

The respiratory burst is one mechanism that the host immune response employs to eradicate intracellular pathogens such as Mtb. It involves the release of antimicrobial agents such as reactive oxygen intermediates, which exerts oxidative stress on infecting bacteria. It is well established that the *E. coli cydD* mutant is sensitive to exogenous $H_2O_2$ treatment (Goldman et al., 1996a). Next, we assessed if heterologous expression of the *cydDC* exporter from the two mycobacterial species can desensitize the oxidative stress phenotype observed in *E. coli* due to *cydD* loss. To mimic oxidative stress, challenge with $H_2O_2$ was carried out as described in section (2.19.2). To confirm that the *E. coli* Δ*cydD* mutant is sensitive to treatment with $H_2O_2$ after 15 min and 30 min (Figure 3.10).

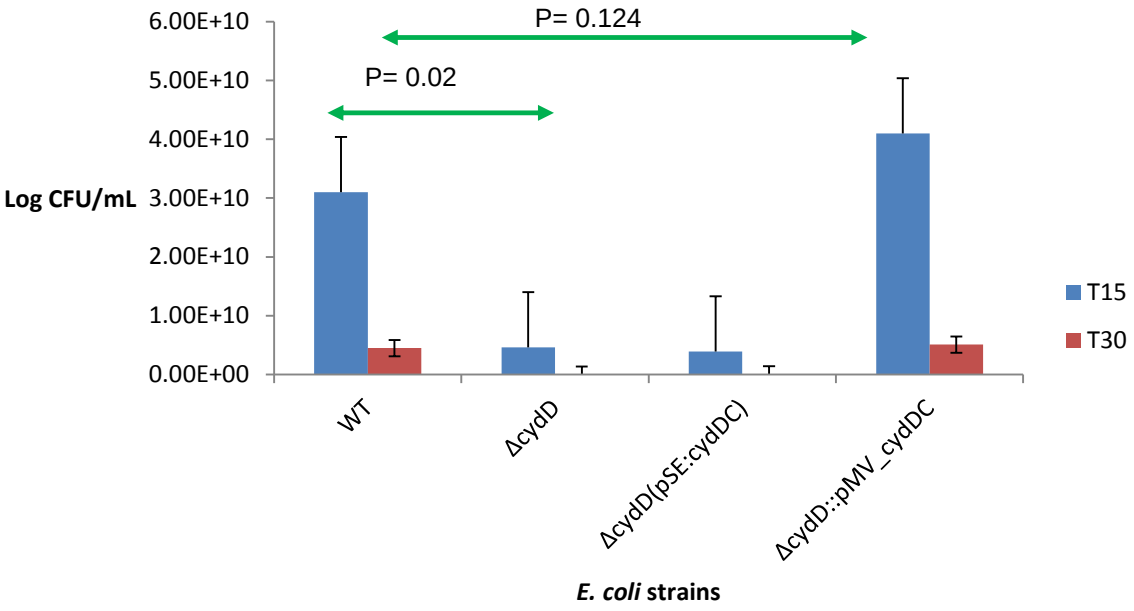


**Figure 3.10**. Survival of *E. coli* and its derivative strains in the presence of exogenous hydrogen peroxide ($H_2O_2$). *E. coli* and its derivatives were assayed for sensitivity to exogenous $H_2O_2$ (2%) at different time points (15 and 30 min). Each graph represents a mean value of three independent replicates for each strain. The error bars represent standard deviations. Notably, Δ*cydD* was sensitive to $H_2O_2$. Error bars represent a standard deviation of three experimental replicates. This data were statistically significant as shown by a p value of 0.02 between wildtype and the *cydD* mutant. Heterologous expression of the *M. smegmatis* putative exporter rescued this phenotype. Heterologous expression of the Mtb genes failed to complement this phenotype.

`

Heterologous complementation with the *M. smegmatis cydDC* genes completely rescued this phenotype, while heterologous expression of the Mtb transporter failed to complement the defect (Figure 3.10). It is unclear why the Mtb *cydDC* genes were unable to restore some of the defects in the *E. coli* Δ*cydD* mutant. The most likely explanation that is sufficient levels of expression were not achieved or that over-expression caused some toxicity effect. Due to time constraints this was not investigated further.

Collectively, protein modeling, stationary phase recovery assays, temperature sensitivity assays and oxidative stress assessment provided unequivocal evidence that the *M. smegmatis cydDC* genes encoded a functional transporter. To further investigate the biological role of the *cydDC* genes in *M. smegmatis*, these genes were targeted for site specific deletion. Two approaches were taken to construct a knockout mutant. The first was allelic exchange using a suicide plasmid (described in section 2.14 of the Materials and Methods) and recombineering (using the lamba red recombinase described in section 2.15 of the Materials and Methods).

### 3.10 Construction of an in-frame double deletion mutant of the *M. smegmatis* that lacks the *cydDC* operon.

Gene knock out primers (Table 2.4) were designed as outlined in (See 2.6.1) Upstream and downstream regions were PCR amplified as previously described (See 2.6.1) and the amplicons were verified by restriction analysis (Figure A 10). A cloning vector was also verified by restriction digest before cloning (data not shown). First, the three way cloning strategy into pBlueScript was carried out. White colonies were sub-cultured in liquid and screened with various restriction enzymes (Figure A10). The insert containing the *cydDC* deletion allele and associated homologous regions for gene editing was recovered as a 2007 bp *Hin*dIII fragment and sub-cloned into p2NIL which was previously digested with *Hin*dIII. White colonies were sub-cultured in broth and subsequently screened (Figure A10).This suicide construct was sent for sequencing to ensure that no mutations were carried on both the upstream and downstream region during PCR amplification. Sequencing data showed that the amplification procedure

`

was carried out with high fidelity and with no mutations in the amplified genomic regions (Figure A 10). Selective marker genes in the pGOAL17 plasmid were excised and cloned as a *Pac*I. The putative clones were plated on LA supplemented with Xgal. The plates were incubated at 30 °C to prevent plasmid re-arrangement. Blue colonies were picked and sub-cultured for bulk DNA extraction. The 13119 bp final construct was profiled as previously described (See 2.6.4) (Figure 3.11).

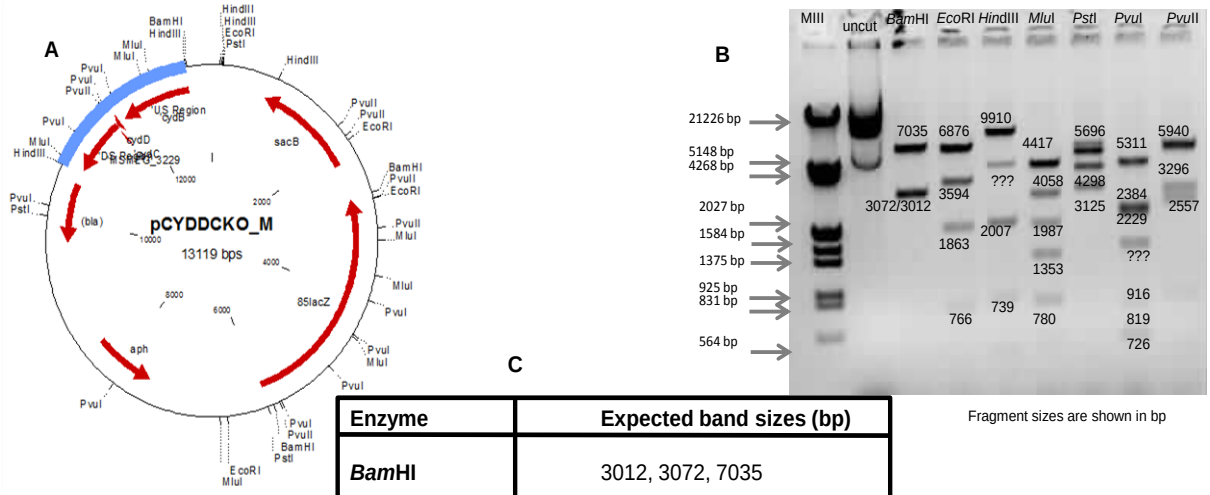


C

| Enzyme | Expected band sizes (bp) |
|---|---|
| ***Bam*HI** | 3012, 3072, 7035 |
| ***Eco*RI** | 1863, 766, 3594, 6876 |
| ***Hind*III** | 27, 739, 9910, 2007, 436 |
| ***Pvu*I** | 453, 480, 726, 2229, 2384, 916, 477, 143, 5311 |
| ***Pvu*II** | 144, 819, 363, 2557, 5940, 3296, |
| ***Mlu*I** | 425, 780, 1987, 4417, 1353, 99, 4058 |
| ***Pst*I** | 5696, 4298, 3125 |

Fragment sizes are shown in bp

**Figure 3.11**. Restriction profiling of the *cydDC* knock out construct with various restriction endonucleases. **(A)** Map of the construct showing the sites where restriction sites are located. **(B)** Restriction digest of the construct visualized on a 1% agarose gel. Labelled from left to right: Lane1 and 2, Marker III and the uncut control. Lane 3-9, digest with the following restriction enzymes: *Bam*HI, *Eco*RI, *Hind*III, *mlu*I, *Pst*I, *Pvu*I and *Pvu*II respectively. *Hind*III and *Pvu*I yielded two stray bands respectively which were not expected following digestion. **(C)** Table showing enzymes used and the expected band sizes. The question marks indicate the products of partial digests.

Plasmid digests yielded corresponding expected band sizes, Figure 3.11. Two unexpected bands in the *Hind*III and the *Pvu*I digests respectively were observed. These are the result of partial digestion. This construct was subsequently electroporated into *M. smegmatis* $mc^2$ 155.

`

### 3.10.1 Construction generation of the double deletion of the *cydDC* operon by recombineering in *M. smegmatis*

As already mentioned, due to technical difficulties, two strategies to knock out the *cydDC* operon in *M. smegmatis* were adopted. The substrate to generate an inframe double deletion allele was designed as previously described (Methods and materials section 2.15). The substrate was successfully designed and ordered through GeneScript. The streptomycin cassette was subsequently cloned into the plasmid designated pUC 57**:***cydDC*KO. The aadA marked construct was mapped with several restriction enzymes (Figure 3.11.1).

`

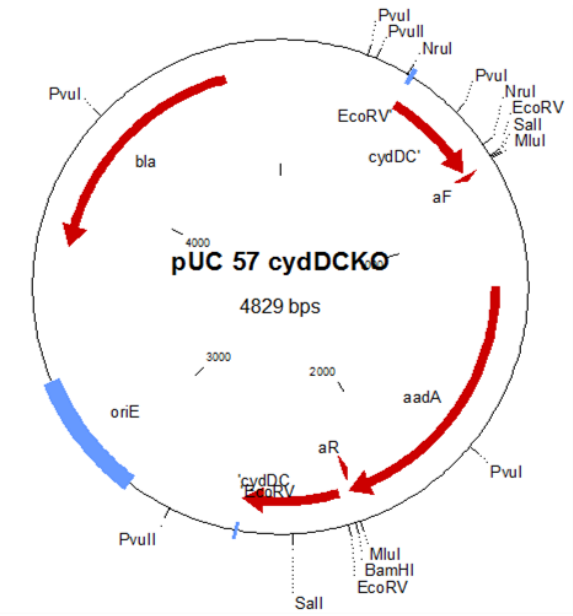


| Enzyme | Expected band sizes (bp) |
|---|---|
| *Bam*HI | 2033; 896; 328; 1143; 429 |
| *Eco*RV | 3403; 1426 |
| *Mlu*I | 1376; 3453 |
| *Nru*I | 4508; 321 |
| *Nsp*I | 2912; 1917 |
| *Pac*I | 2111; 2718 |
| *Pvu*I | 328; 1143; 2462; 896 |
| *Sal*I | 1597; 3232 |

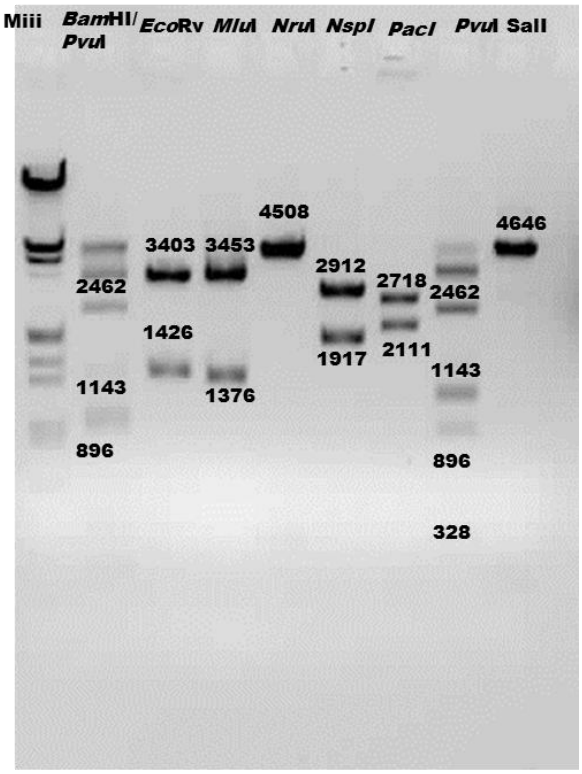


Fragments represented in bp

**Figure 3.11.1.** Extraction and restriction profiling of streptomycin marked knock out construct of Δ*cydDC* generated by lamda phage genetic recombineering. Separation of fragments was done on a 1% agarose gel by electrophoresis. All fragments except the *Bam*HI/*Pvu*I double digest and *Sal*I yielded expected band sizes. The *Bam*HI/*Pvu*I double digest shows yielded partial digests. The plasmid was sequenced to verify the *Sal*I site.

A double digest of *BamH*I and *Pvu*I and *Pvu*I respectively yielded partial digests while the *Sal*I digest did not yield expected band sizes. The plasmid was sequenced to confirm Sal*I* restriction sites. The *Pac*I fragment of the substrate was successfully PCR amplified and electroporated into wildtype *M. smegmatis*. Several colonies emerged after four days of incubation at 37 °C. Due to time constraints, these were not screened to confirm *cydDC* deletion.

`

### 3.12 Selection of Single Crossover recombinants

A 100 mL culture of *M*. *smegmatis* $mc^2$ 155 was cultivated to log phase and washed three times with 10% glycerol as previously described (See 2.7.2). At least 1 µg of purified DNA (See 2.4.2) of the final construct was mixed with 400 µL of washed cells and electroporated as previously described (See 2.7.2). The following controls were included alongside the experimental: No plasmid control and 2 µL of 560 ng of pMV306H. Additionally, 10X serially diluted unwashed culture was also plated to assess the proportion of cells lost during the washing procedure. These troubleshooting approaches were used as various technical difficulties were encountered during electroporation. Eventually, several blue, single crossover recombinants emerged from various electroporations. These isolates were subjected to counterselection as described in the Materials and Methods (2.14)

### 3.13. Genomic confirmation of the Δ*cydDC* mutant

Following sucrose counter selection, ten white colonies were screened as outlined in 2.6.1, five potential mutants (DCOs) were obtained by a preliminary PCR screen, as evidenced by the presence of  220 bp mutant amplicon (Figure 3.12).

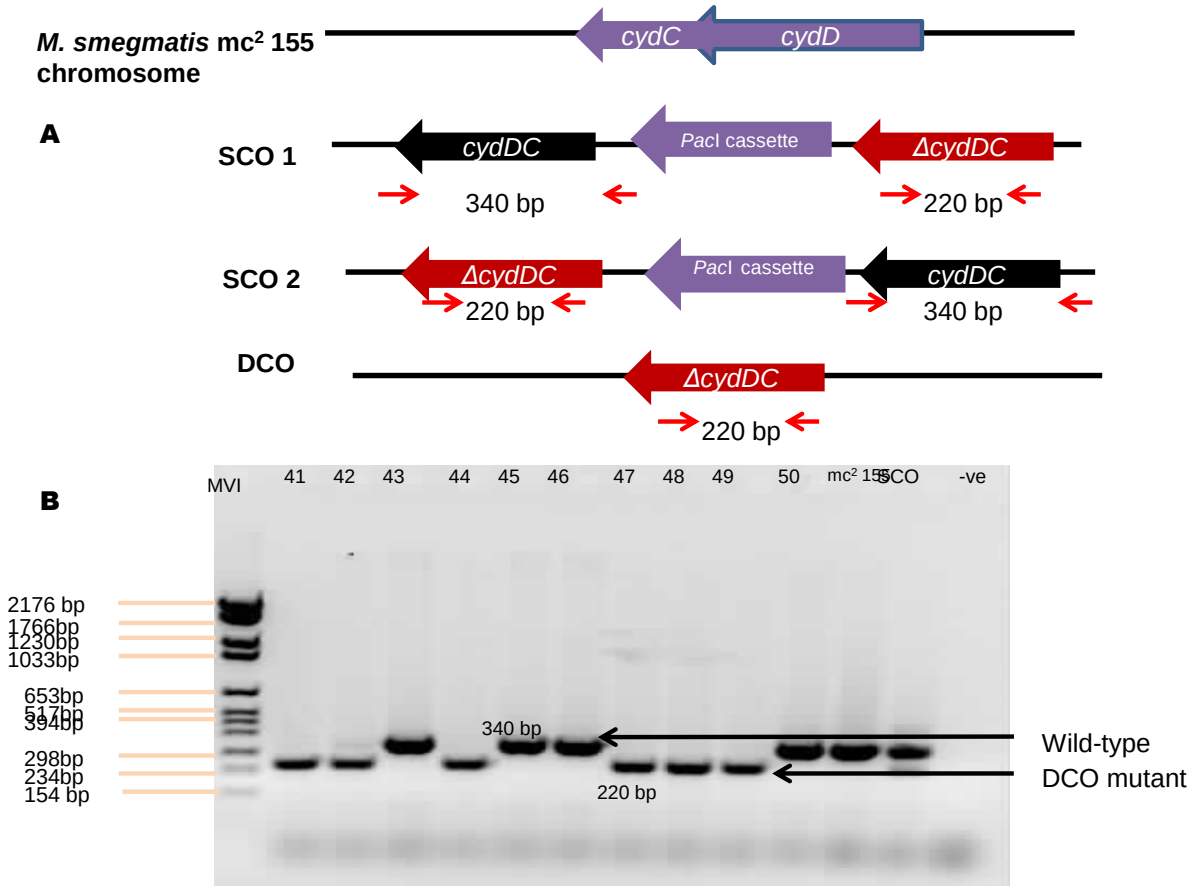


**Figure 3.12**. Preliminary screen for potential mutants [Double Cross Overs (DCOs)] by PCR. **A)** Schematic illustration of primer binding sites (red arrows) for screening of DCOs. **B)** PCR amplicons were separated on a 1% agarose gel by electrophoresis and visualized with GeneSnap software. Loaded from left to right, Marker VI in lane 1, lane 2-11, sample 41-50 respectively. Lane 12-14, *M. smegmatis* mc$^2$ 155, Single Cross Over (SCO) and No template control respectively. Five DCOs were obtained from the screen and were taken forward for confirmation by southern blot analysis.

Clones 41, 44, 47, 48, and 49, which displayed this band were then confirmed by southern blot analysis as mutants Figure 3.12.

**Figure 3.13. A**

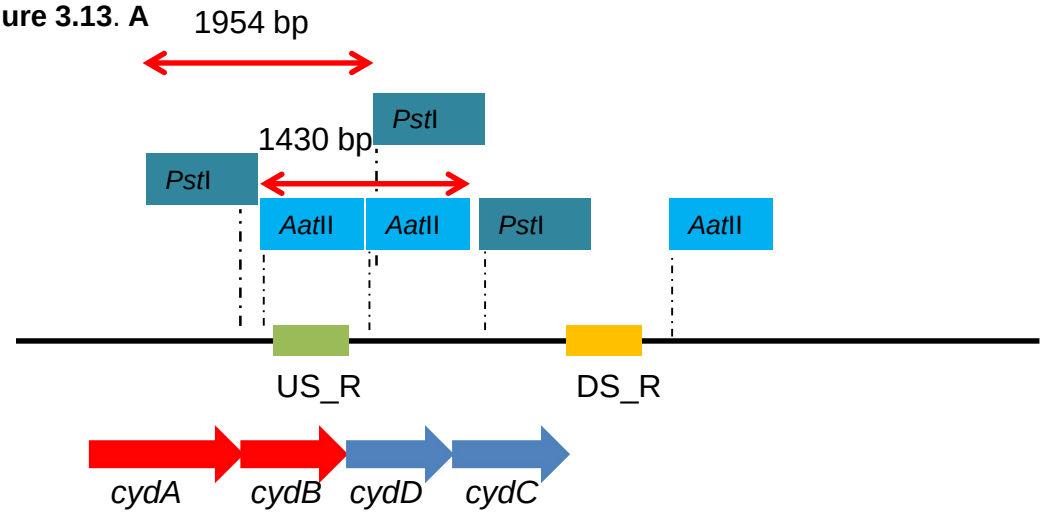


**Wild type**

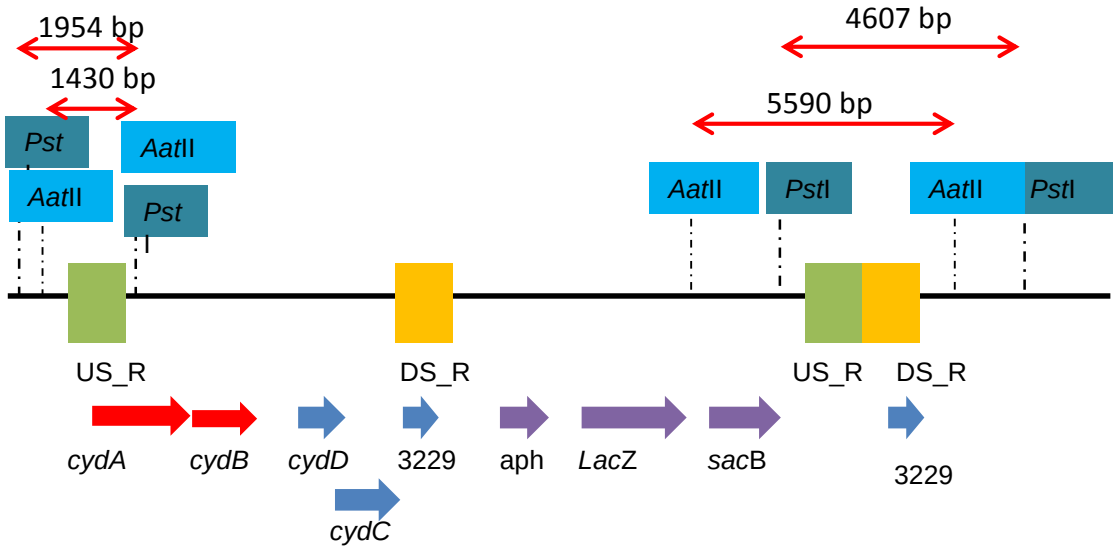


**Down Stream Single Crossover**

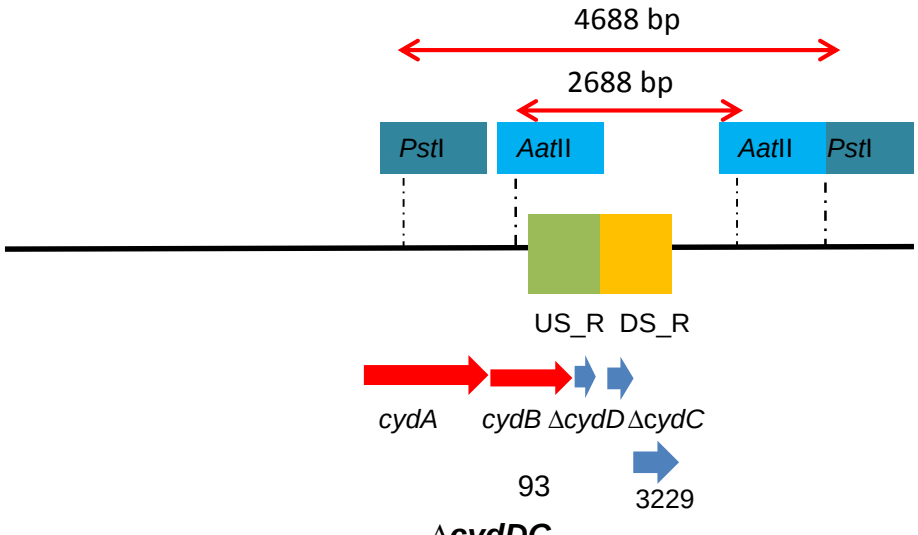


***ΔcydDC***

`

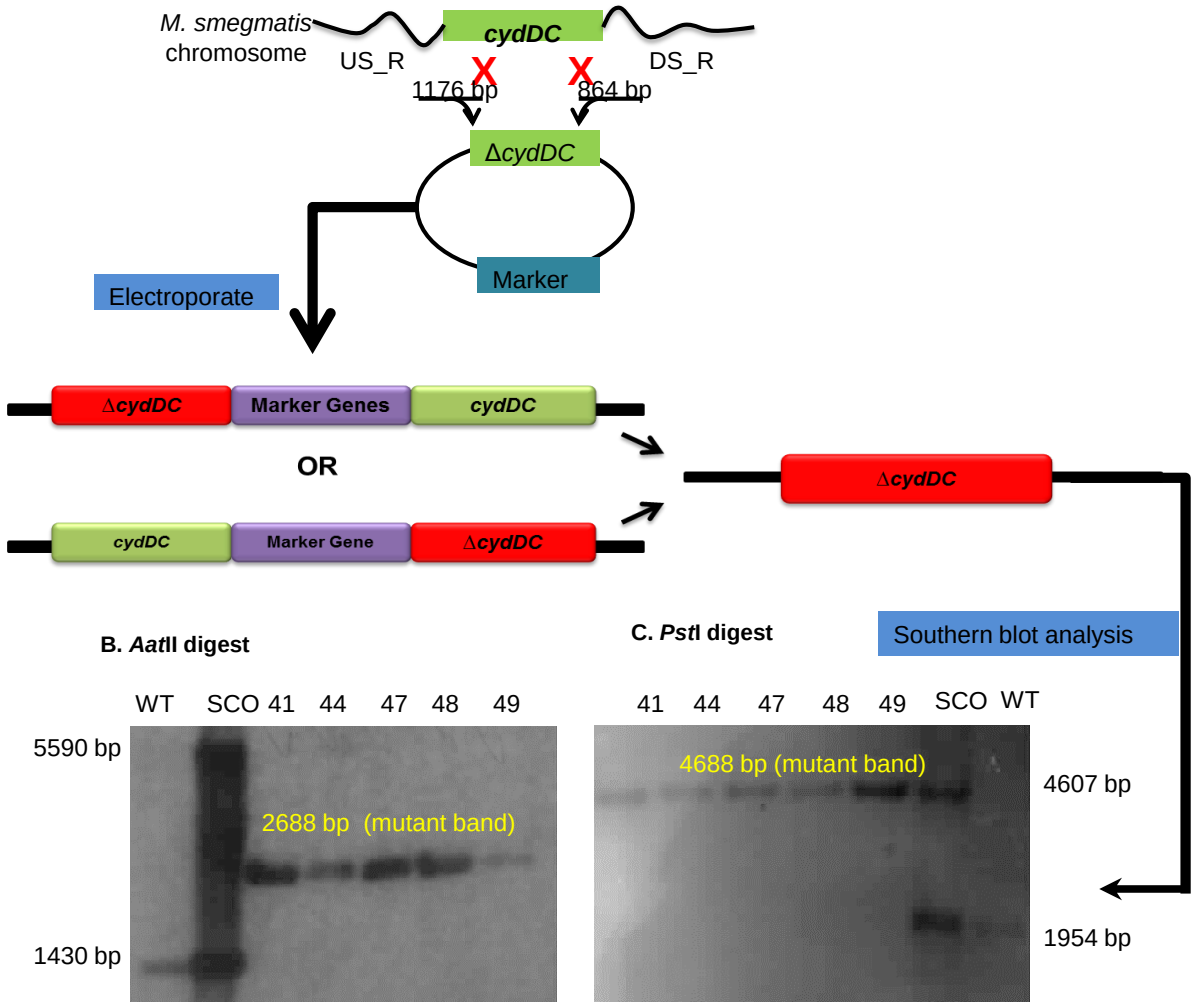


**Figure 3.13**. Southern blot analysis for mutant confirmation. A) Clone manager maps giving expected band sizes for the mutant (2688 bp for the *Aat*II digest, and 4688 bp for the *Pst*I digest), wild-type (1430 bps for the *Aat*II digest, and 1954 bps for the *Pst*I digest). Also shown is the map of the down stream integration Single Cross Over (DS_SCO) yielding 5590 bp and 1430 bp for the *Aat*II digest, 4607 and 1954 bps for the *Pst*I digest). The green upstream region was used as a probe.

## 3.13 Construction of the *M smegmatis* Δ*cydDC* genetically complemented strain.

To complement the *M. smegmatis* Δ*cydDC* strain, the plasmid used for heterologous complementation in *E. coli* (section 3.4) was used. This plasmid was electroporated into the mutant strain and the resulting genetically complemented derivative (Δ*cydDC*::pMV_*cydDC*) was used for phenotypic analysis.

`

### 3.14. Deletion of *cydDC* leads to loss of the heme *d* peak in the membrane fraction of *M. smegmatis*

The role of the *cydDC* in C*bd*O biogenesis was assessed by absorption difference spectroscopy in *M*. *smegmatis* and its derivative strains. Cultures of *M*. *smegmatis* $mc^2$ 155, *M*. *smegmatis* ∆*cydDC* strain and the Δ*cydDC*::pMV_*cydDC* complement were cultivated in a bioreactor at 21% and 1% dissolved oxygen tension as detailed in (2.3). A gradual decline in dissolved oxygen was maintained at 1% for at least one hour. Cultures were lysed with a french press as detailed in (2.17) and the cell lysate prepared for extraction of membrane fractions as previously described (See 2.18). Absorption difference spectroscopy was performed on all three strains as outlined in (Materials and Methods section 2.20). The results from these experiments are shown in (Figure 3.14).

The reduced minus oxidized spectra for wild-type *M. smegmatis* $mc^2$ 155 showed a diagnostic peak of C*bd*O at 630 nm, while the same was absent in the *cydDC* mutant strain. Complementation with *M*. *smegmatis cydDC* operon restored the loss of C*bd*O proving that the *cydDC* contributes to the biogenesis of the holoform of C*bd*O.

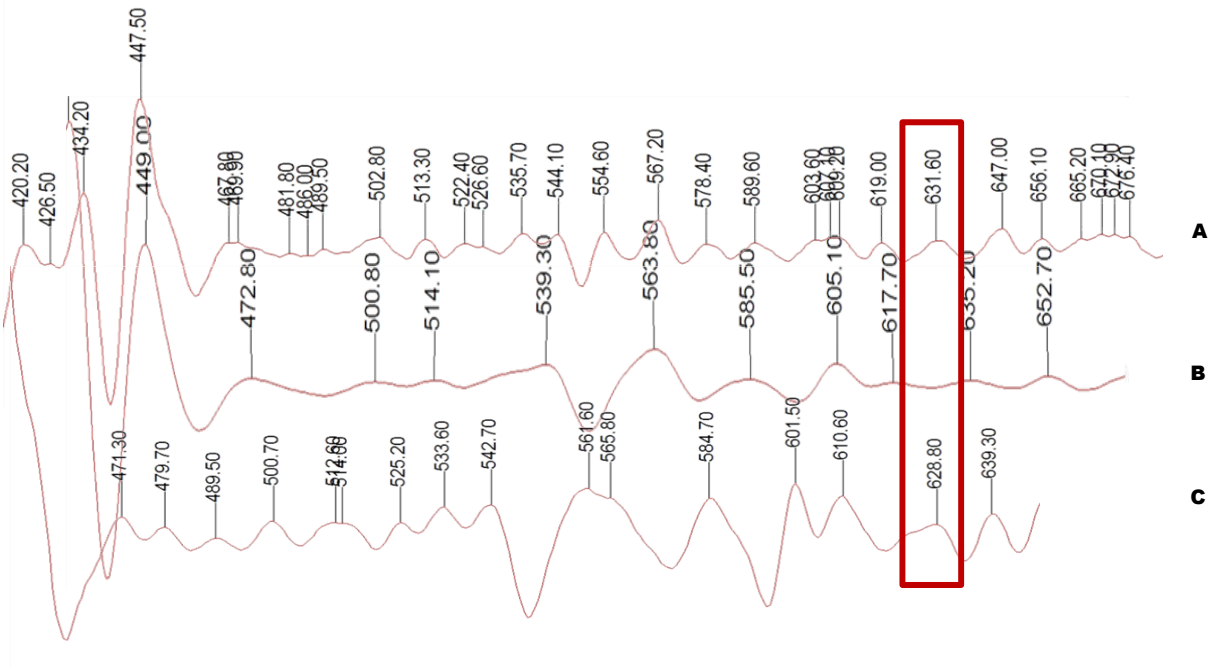


**Figure 3.14**. Absorption difference spectroscopy of *M. smegmatis* mc$^2$ 155 and its derivative strains. **A**) *M. smegmatis* mc$^2$ 155 **B)** *M. smegmatis* Δ*cydDC* and **C)** Δ*cydDC*::pMV_*cydDC.* Deletion of the *M. smegmatis cydDC* resulted in the loss of cytochrome *bd* oxidase (C*bd*O). This is exemplified by the absence of the heme *d* signature peak which is a diagnostic feature of C*bd*O. Complementation with the *M. smegmatis cydDC* restores this signature peak. This is also exemplified by the increase in expression of certain cytochromes which were dramatically reduced upon deleting the *cydDC*.

### 3.16. Growth kinetic analysis of *M. smegmatis* and its derivative strains.

It has been demonstrated that loss of C*bd*O resulted in defective growth of *M. smegmatis* at reduced oxygen tensions, consistent with the proposed role of C*bd*O for growth under hypoxic conditions in *E. coli* (Kana et al., 2001). To further assess this, *M. smegmatis* was grown in a bioreactor at 21% air saturation (reflecting normoxic conditions), followed by a reduction in the air saturation in the bioreactor to 0.7% air saturation. Under normoxic conditions, loss of C*bd*O did not affect growth (Figure 3.15). However, under hypoxic conditions, the growth rate of *M. smegmatis* was significantly lower than that of the wild type. The genetically complemented counterpart displayed growth kinetics comparable to wild-type (Figure 3.15). Due to time constraints, this experiment was done only once before submission of the MSc dissertation.

`

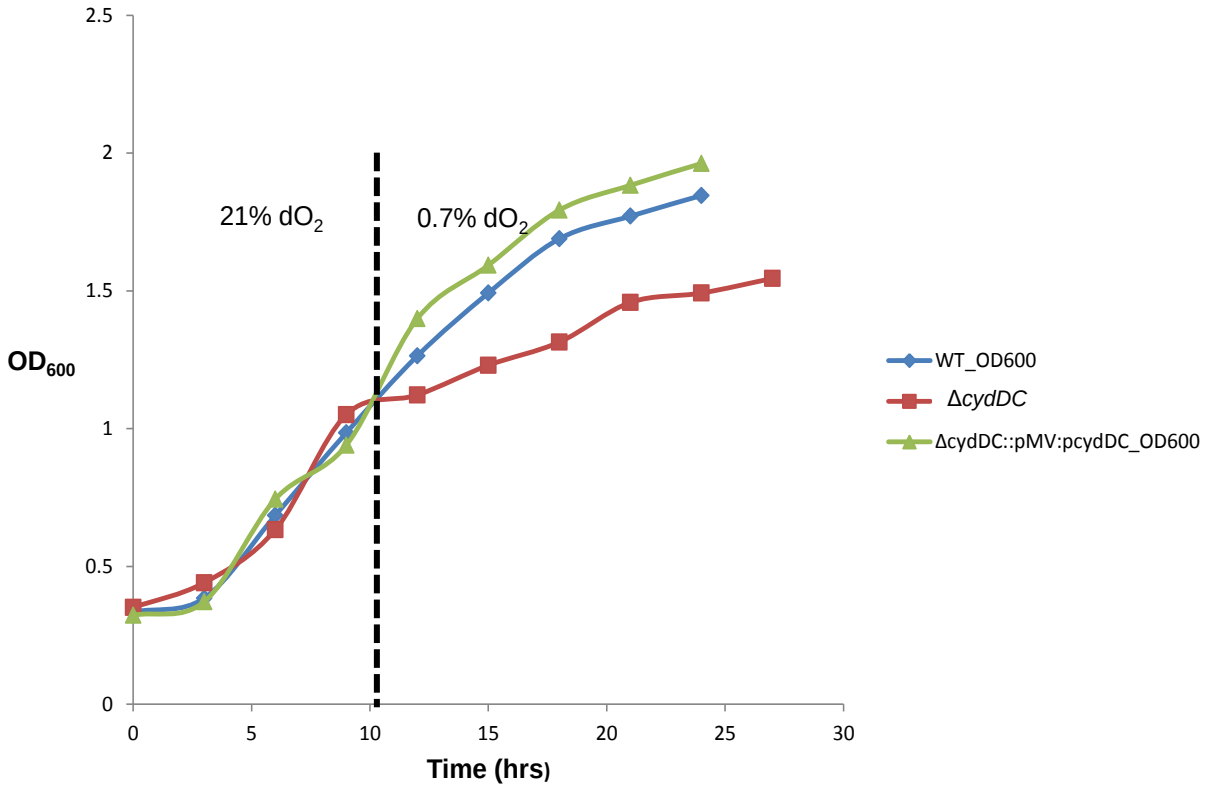


**Figure 3.15**. Growth curve analysis of *M. smegmatis* and its derivative strains in 7H9 in a Bioflow 110 fermentor at 21% and 0.7% dissolved oxygen ($dO_2$ ). **Blue squares** represent *M. smegmatis* $mc^2$ 155, **Red squares** represent *M. smegmatis* deficient of the *cydDC* encoded ABC-type transporter (Δ*cydDC*) and **green triangle**, *M. smegmatis* Δ*cydDC* complemented with *M. smegmatis cydDC* operon in its native locus. C) Δ*cydDC*::*cydDC. M. smegmatis* deficient of the *cydDC* operon struggles to grow at low oxygen tension. Bacteria were first grown at 21% air saturation and after 10 hours at 0.7% air saturation. This data set represents one experimental replicate of each strain as alreadydescribed.

### 3.17 The Δ*cydDC* mutant strain is sensitive to exogenous hydrogen peroxide

It has been previously established in *E. coli* that the presence of C*bd*O protects from oxidative stress. To prove that the same holds in mycobacteria, cultures of *M. smegmatis* and its derivative strains were washed twice in 7H9 as previously described (See 2.7.1) and treated with 2 mM ($H_2O_2$) for 15 and 30 min to induce oxidative stress as detailed in 2.19.2 (Figure 3.16).

`

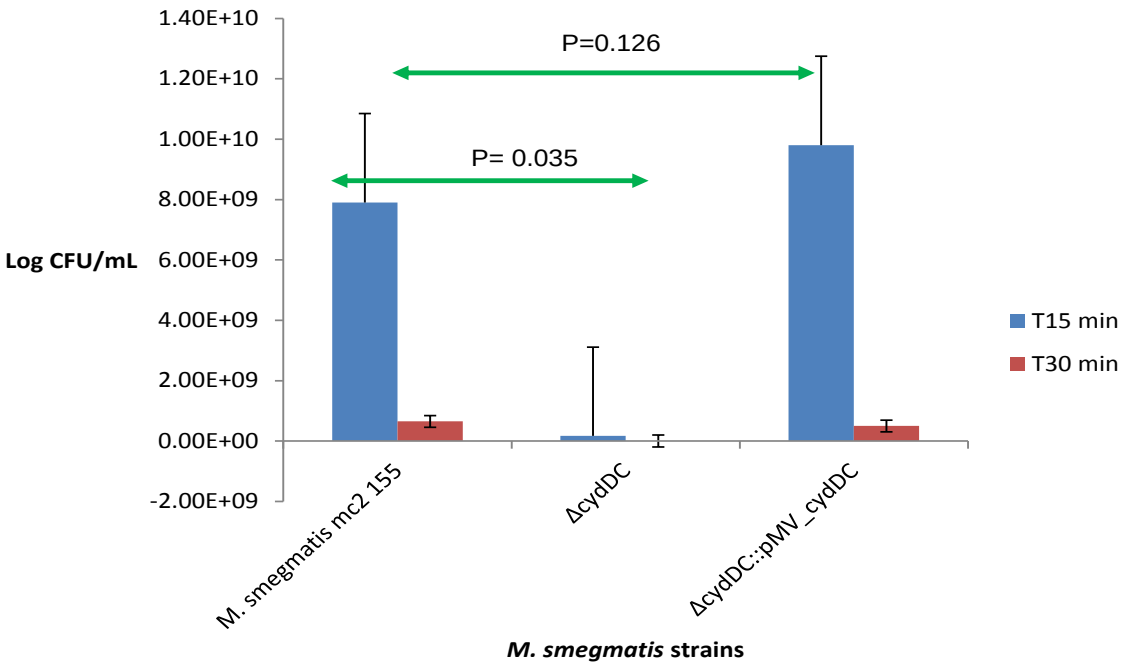


**Figure 3.16.** Survival of *M. smegmatis* and its derivative strains to exogenous hydrogen peroxide ($H_2O_2$). *M. smegmatis* and its derivatives were exposed to 2% exogenous $H_2O_2$ at different time points (15 and 30 min). Each graph represents a mean value of three independent experiments for each strain. A 10-fold dilution series of each culture was plated and the colony forming units (CFU/mL) were enumerated. Shown are the colonies that emerged on the $10^7$, $10^8$ and $10^9$ dilutions. Notably, Δ*cydDC* was sensitive to exposure to exogenous $H_2O_2$. Complementation with the *M. smegmatis cydDC* operon rescued sensitivity to $H_2O_2$. This data set represents a standard deviation of three experimental replicates. Data analysis with the student t test showed statistical difference with a p value of 0.035 between wildtype *M. smegmatis* and Δ*cydDC* mutant strain.

As expected, Δ*cydDC* mutant strain was more sensitive to $H_2O_2$ treatment relative to wild-type cells, which showed tolerance after 15 min exposure. This phenotype was rescued when the mutant gene was complemented with the wild-type gene (Figure 3.16).

### 3.18. The Δ*cydDC* mutant strain fails to exit stationary growth phase

It was previously observed that the *E. coli* strain lacking the *cydD* gene had a stationary phase growth phenotype were it could not re-establish growth when plated on solid media with minimal glucose. This assay was used during heterologous complementation. Hence, the ability of *M. smegmatis cydDC* mutant strain to exit from stationary growth phase was investigated. *M. smegmatis* and its derivative strains were

`

cultivated in Sautons minimal media for mycobacterial growth and plated on 7H10 containing 0.05% glucose. As expected the mutant was not able to exit out of stationary phase while the wild type and genetically complemented strain was able to exit stationary phase (Figure 3.17).

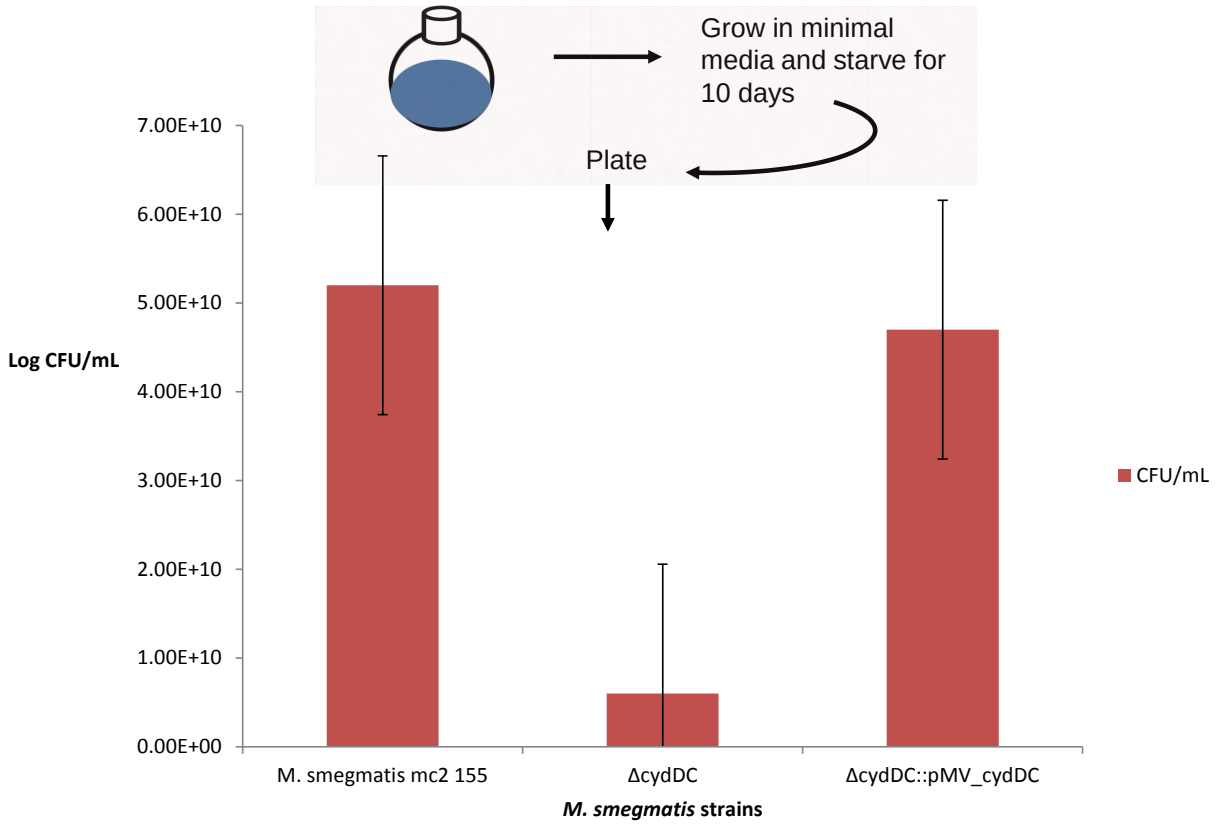


**Figure 3.17**. Nutrient starvation assay in *M. smegmatis* and its derivative strains. The cultures were cultivated in minimal media for mycobacterial growth and starved for 7 days. Serial dilutions of each strain were plated and the ability to resume growth in 7H10 with minimal glucose media at 37 °C was assessed.

`

## 4. Discussion

With a plethora of antibiotic armament and numerous other control measures to combat TB, the disease remains a public health concern, deeply embedded in low income societies. This is in part due to the inherent ability of Mtb to rapidly develop resistance to many of the anti-TB agents or assume a dormant state during immune assault and drug exposure, only to reactivate later and cause clinical disease. This bacterial scourge has necessitated a search for the identification of new drug targets which can be exploited in the design of new drugs with novelty in their action. For this, the ETC of Mtb is relatively unexplored and the validation of Bedaquiline highlights the ETC's potential to be mined for new drug targets. In this regard, C*bd*O is present in a number of pathogenic microbial species including Mtb. In this study, we endeavored to understand the role of the *cydDC* operon in the assembly of C*bd*O and their role in *M. smegmatis*. We believe this understanding will contribute to ending the TB epidemic.

### 4.1 Modeling the CydDC subunits

According to the Smegmalist database, the genome organization of the *cyd* gene cluster in *M*. *smegmatis* suggests that *cydD* and *cydC* are transcribed as a single polycistronic mRNA message (Figure 3.1 and Figure 4) (Aung et al., 2014). Also, the role of the *cydDC* operon is unknown according to the Smegmalist database (Figure 4).

`

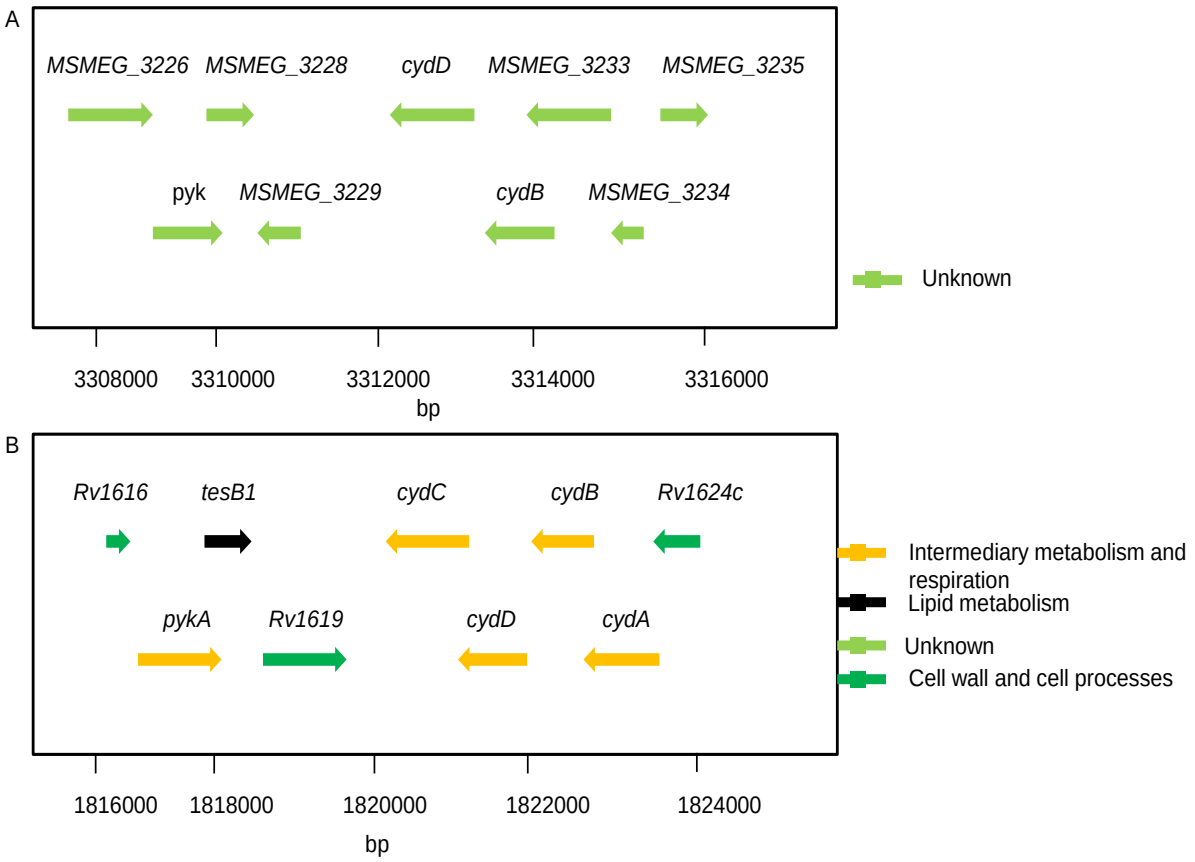


**Figure 4**. Diagrammatic illustration of the *cyd* gene cluster organization in **(A)** *M. smegmatis* and **(B)** Mtb respectively. In both organisms, the *cydDC* are operonic, The function of the *cydDC* operon is unknown in *M. smegmatis* while their counterpart in Mtb are predicted to function in metabolism and respiration.

However, the Tuberculist database annotates the *cydDC* homologs in TB as heterodimeric subunits of the ABC-type transporter superfamily with a possible role in intermediary metabolism and respiration (Figure 4). To elucidate this, structural analysis of the CydDC subunits was successfully completed (Figure 3.3). These analyses confirmed that the *M. smegmatis cydDC* genes encode heterodimeric subunits of the ABC-type transporter superfamily (Poole et al., 1993). Each subunit is characterized by the presence of two domains, a single TMD which preserve substrate binding sites and a single ABC domain which is a four membered helical domain with conserved residues (Linton and Higgins, 1998, Cruz-Ramos et al., 2004, Poole et al., 1993). In addition to these domains, the topology of each subunit shows three minor periplasmic loops and two major cytoplasmic loops (Figure 3.3). All of these features, together with the four membered helical domain are characteristic of the ABC-type superfamily of transporters. These conserved residues and domains are found in CydDC homologues

`

across the three domains of life, and have helped to define ABC-type transporters (Linton and Higgins, 1998, Higgins, 2001). The *M*. *smegmatis* CydDC subunits are no exception in this regard. Both subunit III and IV preserve a total of 5 conserved residues in the ABC domain (Figure 3.3). The following conserved residues were identified for subunit III and subunit IV respectively, the highly conserved Walker A motif at position 330 and 338 bp. This motif is characterized by the **G**xx**G**x**GKS**/**T** motif, where bold capital letters signify conserved residues and x represents any amino acid. This motif is conserved across many bacterial species (Davidson et al., 2008). The Q loop defined by a conserved glutamine (xx**Q**xx) was identified 14 and 34 amino acids downstream of the Walker A motif at position 344 and 364 bps respectively. This residue is not conserved across all microorganisms but has been identified in most proteobacterial species (Linton and Higgins, 1998, Higgins, 2001, Davidson et al., 2008). The signature motif represented by the **LSLGQ** motif was mapped to position 429 bp and is present in most microorganisms as **LSGGQ** motif, however, in several mycobacterial species, this motif was identified as the **LSLGQ** motif (Figure 3.3). The Walker B motif was mapped to position 449 bp and is characterized by xxxx**DEPT** were bold capital letters represent conserved residues whilst x is any hydrophobic residue (Davidson et al., 2008). Finally, the H-loop defined by a conserved Histidine xx**H**xx was mapped to position 496 bp, were x is any amino acid. Notably, the organization of the conserved residues in the helical ABC domain and the structural topology for the CydDC in *M. smegmatis* is consistent in *E. coli* (Cruz-Ramos et al., 2004). Although X-ray crystallographic structures of the CydDC subunits have not been determined, structural prediction algorithms such as ITTASER have enabled preliminary assessment of these subunits with high structural threading and prediction confidence. The *M*. *smegmatis* CydDC subunits have high sequence similarity and structural identity to some of the best characterized CydDC subunits (Cruz-Ramos et al., 2004). Collectively, from the above analysis, we conclude that the mycobacterial *cydDC* genes also encode heterodimeric members of the ABC-type transporters. Moreover, given the high degree of conservation between the *M. smegmatis* and the *E. coli* homologue, we predicted that the mycobacterial counterparts most likely transport that same metabolites as those transported by the *E. coli* CydDC transporter (Pittman et al., 2002, Pittman et al., 2005).

`

## 4.2 The presence of the *cydDC* genes is necessary for C*bd*O biogenesis

The high degree of conservation between the *E. coli* and mycobacterial CydDC transporters suggested that these transporters would be functionally interchangeable. To further test this, we sought to heterologously express the mycobacterial CydDC transporter in an *E. coli* mutant that lacked *cydD* (Poole et al., 1989). In *E. coli*, loss of *cydD* leads to defective C*bd*O assembly. Absorption difference spectroscopy of the *E. coli cydD* mutant and its heterologous derivative strains revealed interesting outcomes. First, reduced minus oxidized cytoplasmic fractions of wild-type *E. coli* revealed absorption peaks associated with both types of oxidases (cytochrome *bo* oxidase and C*bd*O) that are induced under various oxygen tensions (Figure 3.6). C*bd*O biosynthesis was evidenced by the 630 nm chlorin heme *d* peak, which has been reported by various studies as the diagnostic peak denoting the presence of C*bd*O (Poole et al., 1989, Georgiou et al., 1987). Other spectral features associated with C*bd*O biogenesis observed include hemoprotein $b_{558}$ and $b_{595}$ (Poole et al., 1983) (Figure 3.6). Notably, as the *E. coli* strains were grown under reduced oxygen tension, where the C*bd*O is optimally induced, a greater abundance of the above-mentioned peaks, related to C*bd*O, were observed relative to the reduced levels of the diagnostic 600 nm peak associated $aa_3$ type C*c*O. The *E. coli* derivative lacking *cydD* displayed full spectral features of C*c*O which is the main terminal electron acceptor under high oxygen tension. However, some of the spectral features associated with C*bd*O were missing, indicating the presence of defective C*bd*O (Figure 3.6). For instance, the signature diagnostic chlorin heme *d* peak was not present (Figure 3.6) consistent with observations of Poole and coworkers (Poole et al., 1989).

Heterologous expression of the putative Mtb exporter restored the loss of C*bd*O as the chlorin heme *d* signature reappeared in the Δ*cydD* (pSE**::**pGcyd) strain that ectopically expressed the Mtb *cydDC* genes, Figure 3.6. Other peaks such as hemoprotein $b_{558}$ and $b_{595}$ associated with C*bd*O biogenesis were also detected near their absorption maximum. These data provide the first evidence that heterologous expression of the putative Mtb transporter is able to restore loss of C*bd*O biogenesis due to *cydD* deletion in *E. coli* suggesting conservation of function in mycobacteria.

`

To further investigate the biological role of the *cydDC*-encoded ABC-type transporter in mycobacteria, these genes were deleted in *M. smegmatis* and resulting mutant was tested for C*bd*O biogenesis using membrane spectroscopy. . As observed in *E. coli*, the Δ*cydDC* knock out strain of *M. smegmatis* was unable to synthesize a holoform of C*bd*O characterized by the presence of the 630 nm peak in the reduced form (Figure 3.14). This is consistent with observations made by several studies in different gram negative and gram positive organisms (Poole et al., 1989, Georgiou et al., 1987, Winstedt et al., 1998, Kelly et al., 1990). Furthermore, genetic complementation with *M. smegmatis cydDC* genes restored C*bd*O assembly and certain cytochromes whose expression was decreased or completely abrogated due to *cydDC* loss (Figure 3.14). For instance all cytochromes detected near the 520 nm region were missing and these were restored by genetic reconstitution of the *cydDC* allele. As with the *E. coli* strains, membrane spectroscopy was conducted under microaerophillia and the expression of the diagnostic 600 nm peak associated with C*c*O was significantly reduced relative to C*bd*O as exemplified by difference in peak sizes. This is due to the differential expression of each oxidase as dictated by $O_2$ saturation as has been demonstrated in *M. smegmatis* (Kana et al., 2001, Matsoso et al., 2005). Collectively, these data show that the CydDC encoded ABC-type transporter is essential for C*bd*O biosynthesis in *M. smegmatis*. To further assess the functionality of the *cydDC* genes in *E. coli* and to assess the phenotypes of the *M. smegmatis* Δ*cydDC* knockout, various assays that provide insight into C*bd*O function were conducted.

### 4.3 Growth kinetics of *E. coli* derivative strains and the *M. smegmatis* Δ*cydDC* mutant

It is widely accepted that C*bd*O is induced under conditions of low oxygen tension but this enzyme has also been implicated in stationary phase growth and survival (Siegele and Kolter, 1993) . To test stationary phase survival, a protocol adapted from Cruz-Ramoz and co-workers was adopted (Siegele and Kolter, 1993). *E. coli* and its derivatives were cultivated in a final volume of 150 mL of LB media in 250 mL flasks and incubated at 37 °C with shaking at 50 rpm. Initially, all strains displayed comparable growth rates. At the onset of exponential growth phase, all strains exhibited identical

`

growth patterns (Figure 3.7). This is most likely due to the induction of the main aerobic branch (C*c*O). At $OD_{600}$ 1.4, the growth pattern of *E. coli* Δ*cydD* began to decrease as exemplified by a decrease in growth rate (Figure 3.7). The *cydD* null mutant appeared to be growing exponentially but with a decrease in biomass, a feature that was noted till the end of the growth curve, when the bacteria entered stationary phase. As the difference was marginal, the biological significant of this is unclear but it points towards a growth defect experienced by Δ*cydD* due to the absence of a functional C*bd*O at the onset of stationary phase.

A previous study reported the induction of C*bd*O at late exponential and stationary growth phase, under aerobic conditions (Anraku and Gennis, 1987). This implicates C*bd*O in facilitating growth and providing for energetic requirements beyond the exponential growth phase. This was confirmed in this study by heterologous expression. The ability of *E. coli cydD* null strain to increase in biomass at stationary phase when complemented with the Mtb *cyd* operon provided evidence that, heterologous expression of the Mtb pG*cyd* operon is able to correct the growth defect associated with Δ*cydD* at the onset of stationary phase and further shows that a functional terminal oxidase in a form of C*bd*O is necessary for optimum growth at stationary phase. Similarly, growth kinetics of *M. smegmatis* and its derivative strains was performed to investigate the effect of the loss of the *cydDC* operon. This was done in a meticulously controlled environment where oxygen supply was tightly monitored in a bioreactor (Kana et al., 2001). As with the *E. coli* growth kinetics, *M. smegmatis* and its derivative strains displayed comparable growth kinetics until OD readings of approximately 1.2. Until this point, *M. smegmatis* cells were grown at an air saturation of 21% $dO_{2.}$ This was maintained for approximately 45 min before dropping to air saturation of 0.7% to induce C*bd*O activity (Aung et al., 2014). At this point the growth trend of the graphs changed where the growth rate of Δ*cydDC* mutant was dramatically lower when compared to the wild-type and genetically complemented strain. This is consistent with the observation made by Kana and coworkers with the competitive growth of *M smegmatis* and its *cydAB* mutant derivative at 5 % and 0.5% dissolved $O_2$ (Kana et al., 2001). The wild-type and the Δ*cydDC*::pMVp*cydDC* complement continued to grow at comparable rates until stationary phase while the Δ*cydDC* knock out strain struggled to

`

grow at stationary phase under hypoxic conditions (Figure 3.15). Many factors can affect the growth rate of *M. smegmatis*. These data implicated defective C*bd*O function under hypoxic conditions due loss of the *cydDC* operon and further confirmed that in mycobacteria, the *cydDC* genes are necessary for C*bd*O function.

### 4.4 The role of C*bd*O in exit from stationary phase.

Microorganisms respond to nutritional deprivation by activating starvation or stationary growth phase programs that allow for shut down of growth in an orderly manner and survival under prolonged starvation. Also, changes in gene expression partially account for the differences in physiology and morphological traits of stationary cells. Transposon mutagenesis was used to identify genes that failed to resume growth after several days of starvation (Siegele and Kolter, 1992). The phenotype was designated a $Sur^-$ phenotype due to an incurred survival defect. The mutation was later mapped to the *cydC* locus (Siegele and Kolter, 1993, Siegele and Kolter, 1992). However, later *cydD* was also described by another study as having a stationary phase survival defect (Goldman et al., 1996a). To investigate the functionality of the mycobacterial *cydDC* in a similar biological context, the heterologously complemented *E. coli* strains were tested for exit from stationary phase. Unexpectedly, the *E. coli cydD* mutant was able to form colonies in minimal media after 7 days of starvation. Considering that the first group to describe this phenotype conducted their study by transposon mutagenesis, these discrepant results could be due to aberrant transposon insert in other parts of the genome. Nonetheless, a stationary phase exit defect phenotype was discernible. There are regulatory mechanisms in place that control coordinated re-entry of nutritionally starved cells back in cell growth cycle. For instance, bacteria are able to metabolize fresh nutrients but do not immediately reinitiate grow (Oliver et al., 1991, Roszak and Colwell, 1987). This suggests that bacteria can respond to an increase in nutrients but remain paralyzed for growth or alternatively are able to re-initiate growth at a later time point. Other dogma hold that specific proteins are synthesized during out growth from stationary phase but are not necessary for maintenance of growth (Ross et al., 1990). For instance, Ross and co-workers established that when *E*. *coli* is sub-cultured in fresh media, induction of the *fis* genes occurs, but the expression of the same is diminished

`

once growth is re-established (Ross et al., 1990). However, in this regard, lack of extensive re-growth from stationary growth phase was simply attributed directly to the loss of C*bd*O (Siegele et al., 1996). When there is defective C*bd*O, under microaerophillic conditions, there is no terminal electron acceptor, alluding to stalled aerobic respiration or the need to direct electron flux through another branch of the ETC. Heterologous expression with putative mycobacterial exporters were able to restore the stationary phase defect, possibly signaling the presence of a functional terminal oxidase. It is unclear why heterologous complementation with the Mtb *cydDC* genes did not recue the phenotype of the *E. coli cydD* mutant but we expect that this may be related to the promoter or expression system used. For the *M. smegmatis* genes, the single pMV306 vector was used, with the native *cydDC* promoter region. For the Mtb genes, the pSE100 vector was used, which contained the tetracycline operator upstream of the native *cydDC* promoter, followed by the *cydDC* genes. These differences, and other unknown reasons, could have contributed to the inability of the Mtb genes to complement the *E. coli cydD* mutant defects. In *M. smegmatis*, loss of the *cydDC* genes also led to defective exit from stationary phase confirming that in mycobacteria also, the C*bd*O is required for the successful transitions between replicative and non-replicative states.

### 4.5 Heterologous expression corrects temperature sensitivity phenotype

One of the highly conserved responses to environmental stress is the heat shock response (Yura and Nakahigashi, 1999). *E*. *coli* has approximately 20 genes which constitute an operon under the coordinate control of sigma factors which appear to be auto regulated (Yura and Nakahigashi, 1999, Goff and Goldberg, 1985). Furthermore, the expression of this operon seems to increase following an increase in growth temperature. Survival under adverse environmental conditions is a reality with which all microorganisms must cope. Fluctuations in temperatures which permit growth is one such condition (Siegele and Kolter, 1993). *E*. *coli* has an optimal growth temperature of 37 °C. However, *E*. *coli* lacking *cydD* was reported to have a temperature sensitive growth defect at both 37 and 42 °C (Siegele and Kolter, 1992, Siegele and Kolter, 1993). This defect was originally described when *cydD* was isolated by transposon

`

mutagenesis in a screen for genes that allowed growth of *E*. *coli* at high temperatures (Delaney et al., 1992). The gene was initially designated *HtrD* denoting a high temperature requirement. Further mapping and characterization of the gene showed that *HtrD* mapped to the same genomic locus as *cydD*, which had previously been described (Poole et al., 1989). The nucleotide sequence of *HtrD* was the same as *cydD* however had an extra Guanine at position 394 bp. Therefore, heterologous expression of the putative mycobacterial exporters yielded interesting findings. We tested the ability of *E*. *coli* Δ*cydD* for growth at high temperatures. Across all three experimental replicates, a few colonies were observed for *E. coli cydD (*Figure 3.8). Heterologous expression of the *M*. *smegmatis cydDC* genes corrected the temperature sensitive phenotype. The *E. coli cydD* mutant displayed far less platable CFUs with reduced colony morphology following 24 hrs incubation period, this phenotype was completely corrected when the *M*. *smegmatis cydDC* was used for heterologous complementation. However, it must be noted that the original study reported late emerging colonies and these were attributed to a high reversion rate (Delaney et al., 1992). These, pin point colonies were observed in this study also (data not shown). It was interesting to observe that the Mtb pG*cyd* operon restored the loss of C*bd*O spectroscopically, but only partially restored the temperature sensitivity phenotype. A possible explanation for this has been detailed above.

### 4.6 Loss of C*bd*O leads to sensitivity to oxidative stress induced by hydrogen peroxide

One of the earlier findings in bacterial respiration was that *E*. *coli* mutants defective in the C*bd*O due to *cydD* or *cydC* loss were sensitive to exogenous $H_2O_2$ (Poole et al., 1989). Sensitivity to $H_2O_2$ is historically been attributed to DNA damage (Imlay and Linn 1986). In *E. coli*, the damage that occurs as a result $H_2O_2$ activity yields modes of killing that are distinguishable based on metabolic, genetic and kinetic criteria. Metabolically inactive cells exhibit a single mode of killing whereas metabolically active cells exhibit a mode of killing characterized by rapid killing kinetics when low amounts of peroxide are employed momentarily (1-3 mM) (Imlay and Linn 1986). In this study, the *E.coli cydD* mutant was clearly susceptible to treatment with 2 mM exposure to $H_2O_2$. $H_2O_2$

`

displayed rapid killing kinetics at 15 min and this effect was abrogated by heterologous expression of putative mycobacterial exporters. The killing effect retained potency at extended exposure time points. No CFUs were recorded for the *E. coli cydD* mutant at 30 min of exposure to $H_2O_2$ (Figure 3.9). Heterologous expression was able to correct sensitivity to $H_2O_2$ (Figure.3.9).

Similarly, *M. smegmatis* and its derivative strains were assayed for ability to survive exogenous exposure to $H_2O_2$. As expected, the Δ*cydDC* mutant strain displayed hypersensitivity to 2 mM of $H_2O_2$, (Figure 3.16). This phenotype was more severe for the *M. smegmatis* Δ*cydDC* knock out strain at extended incubation periods). C*bd*O has been reported to possess both superoxide activity in *A. vinelandii* and peroxide activity in *M. smegmatis* (Kelly et al., 1990, Lu et al., 2015). The absence of C*bd*O renders these bacteria hyper-susceptible to both oxygen radicals and nitrogen reactive intermediates. From this, we conclude that the presence of the *cydDC* operon in *M. smegmatis* contributes to a functional terminal C*bd*O, which under oxidative stress detoxifies reactive oxygen intermediates that can cause cell death.

`

## 5. Conclusion

The mycobacterial ETC has become a prominent area for the discovery and validation of new drug targets for TB. In this regard, the C*bd*O has been of particular interest and whilst the role of the structural subunits of this enzyme have been extensively studied, the assembly of this respiratory complex in mycobacteria has remained a mystery. In this study, we advance the scientific knowledge on the mycobacterial CydDC by demonstrating that this transporter is functionally interchangeable with its counterpart from *E. coli*. Consequently, we expect that the mycobacterial *cydDC*-encoded ABC-type transporter retains similar biological roles as that in *E. coli*, the principal one being the assembly of a functional C*bd*O. We confirmed this hypothesis by generating a mutant of *M. smegmatis* that lacked the *cydDC* genes and demonstrated that it cannot assemble C*bd*O and thus displayed reduced growth under hypoxic conditions and increased sensitivity to oxidative stress. This work provides novel insight into the mycobacterial ETC and creates various new avenues for future studies to validate the C*bd*O as a novel TB drug target.

## 6. Limitations and future studies

This study presented herein has various limitations. Some technical limitations include the inability of the Mtb *cydDC* genes to complement some of the *E. coli cydD* mutant defects. This could be addressed by using a different vector system and monitoring the expression of heterologous genes. Also, the growth kinetics experiments for *M. smegmatis* under hypoxic conditions could require biological repeats, which could not be completed due to time limitations. This is currently being addressed as these are time consuming experiments because only one strain can be cultured in the bioreactor at any single time. Future experiments include the measurement of glutathione and homocysteine transport in the *M. smegmatis* Δ*cydDC* mutuant. In *E. coli*, these two metabolites have been proposed to be the substrates of the *cydDC*-encoded ABC-type transporter and hence, this requires validation in mycobacteria. Future experiments will

`

also include a study of the regulation of the *cydDC* operon under aerobic and hypoxic conditions.

`

## 7. Appendices

Table A1: Bacterial culture Media ingredients recipes

| Medium | Components |
|---|---|
| 7H9 | 4.9 g powder, Middlebrook, 0.085 % NaCl, 0.2% glucose, 0.2% glycerol, 0.05% Tween 80 (Autoclaved) |
| 7H10 | 19 g powder, 0.085 % NaCl, 0.2% glucose, 0.2% glycerol made up to 1 L in dH2O (autoclaved) |
| 2xTY | 2% tryptone, 0.5% NaCl, 1% yeast extract dissolved in $dH_2O$ (autoclaved) |
| LA | 1% tryptone, 0.5% NaCl, 0.5% yeast extract dissolved in $dH_2O$ (autoclaved) |
| LB | 1% tryptone, 0.5% NaCl, 0.5% yeast extract, 1.5% agar dissolved in $dH_2O$ (autoclaved) |
| M63 | [10 g $(NH_4)_2SO_4$, 68g $KH_2PO_4$, pH 7 with KOH = 5X stock] Working solution: 200 mL 5X stock, |

Table A2 Stock recipes for media supplementation

| Supplement | Components |
|---|---|
| Glucose salts (100X) | 20 g glucose, 8.5 g NaCl dissolved in 100 ml $dH_2O$ (autoclaved) |
| Tween80 (25 %) | 12.5 ml Tween80 dissolved in 40 ml$dH_2O$ (filter sterilized) |
| X-gal (2%) | 1 g X-gal in 50 ml deionised DMF |

`

Table A3 Solutions used in extraction of *M*. *smegmatis* genomic DNA

| Solution | Ingredients |
|---|---|
| CTAB/NaCl | 4.1 % NaCl, 10% N-cetyl-N,N, N-trimethyl ammonium bromidedissolved in $dH_2O$ (filter sterilized) |
| TE buffer | 10 mM Tris-HCl (pH 8), 10 mM EDTA dissolved in $dH_2O$ (autoclaved) |

Table A4 Solutions used for DNA precipitation

| Solution | Ingredients |
|---|---|
| Chloroform: Isoamyl alcohol | 24 ml chloroform, 1 ml isoamyl alcohol |
| Sodium acetate | 3M sodium acetate dissolved in $dH_2O$, pH 5.2 (autoclaved) |

Table A5 Solutions for extracting plasmids from E. coli

| Solution | Ingredients |
|---|---|
| Solution I | 50mM Glucose, 25mM Tris-HCl (pH 8), 10 mM EDTA dissolved in $dH_2O$ (autoclaved) |
| Solution II | 1% SDS, 0.2 M NaOH dissolved in $sdH_2O$ |
| Solution III | 3 M Potassium acetate, 11.5% Acetic acid dissolved in $sdH_2O$ |

`

Table A6. Solutions for preparing competent *E*. *coli* cells

| Solution | Ingredients |
|---|---|
| TfbI | 30 mM Potassium acetate, 100 mM Rubidium chloride, 10 mM Calcium chloride, 50 mM Manganese chloride, 15% v/v Glycerol made up in $dH_2O$ and pH 5.8 with dilute acetic acid |
| TfbII | 10 mM MOPS, 75 mM calcium chloride, 10 mM rubidium chloride, 15 % v/v glycerol made up in $dH_2O$ and pH 6.5 with dilute NaOH |

Table A7. Electrophoresis solutions

| Solution | Ingredients |
|---|---|
| TAE | (50x stock solution): 242 g Tris base, 57.1 ml glacial acetic acid, 100 ml 0.5 M EDTA (pH 8) make up to 1L in $dH_2O$ (1x working solution contains 40 mM Tris-acetate and 1 mM EDTA) |
| Ethidium bromide | 10 mg/ml in sdH2O |

TableA8. Agarose gel recipe

| Gel percentage | Amount of Agarose in 50 mL TAE (g) |
|---|---|
| 0.8 | 0.4 |
| 1 | 0.5 |

`

2 1

Table A9. Southern blot solutions

| Solution | Ingredients |
|---|---|
| Denaturation solution | 0.5 M NaOH, 1.5 M NaCl in $dH_2O$ |
| Depurination solution | 0.25M HCl in $dH_2O$ |
| TBE (5X) | Tris-Borate-EDTA powder (Sigma) dissolved in 2 L $dH_2O$ |
| SSC (20X) | 3M NaCl, 0.3M sodium citrate in $dH_2O$ |
| Solution I | 2X SSC, 0.1% SDS in $dH_2O$ |
| Solution II | 0.5X SSC, 0.1% SDS in $dH_2O$ |
| Maleic acid buffer | 1M Maleic acid, 1.5M NaCl in $dH_2O$ (adjust to pH 7.5 with NaOH pellets) |
| Wash buffer | 0.1M Maleic acid buffer, 0.3 % Tween20 |
| Blocking solution (Roche) | 1X blocking solution in maleic acid buffer |
| Detection buffer | 0.1M Tris-HCl, 0.1M NaCl in dH2O (pH 9.5) |
| Antibody solution(Roche) | Dilute 1 in 10 000 in blocking solution |

`

| | |
|---|---|
| CSPD (Roche) | Disodium 2-chloro-5-(4-methoxyspiro (2-dioxetane-3,2 (2-dioxetane3,2‟ -(5‟ -chloro)-tricyclo[3.3.1.1. 3, 7. ]decan(-. 4-yl)-1-phenyl phosphate |

## Appendix A10

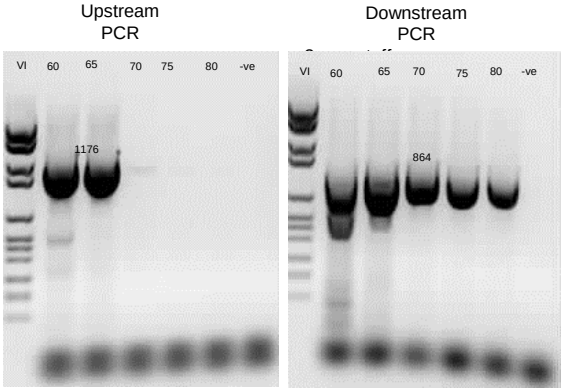


Figure A10.1. Gradient PCR of the Upstream and and downstream Region of *cydD* (1176 bp*) and cydC* (864 bp*)* respectively.

**Cycling conditions**

- 95 $^0$C-3 min
- 95 $^0$C-30 sec
- Primer annealing-Gradient
- Primer extention-72 $^0$C 1 min
- Final extention-72 $^0$C 10min
- Hold-12 $^0$C ∞

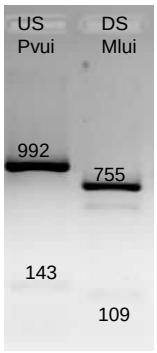


Figure A10.1. Confirmation of specific amplification of genomic fragments

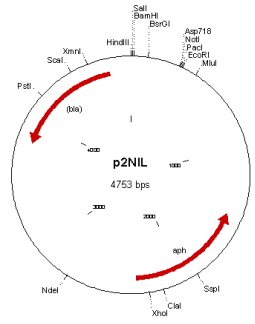


| | |
|---|---|
| ***Bsp*HI** | 3388; 1365 |
| ***Bam*HI** | 4753 |
| ***Pvu*I** | 3853; 896 |
| ***Bam*HI/ *Pst*I** | 4102; 651 |

Figure A10.2. Extraction and mapping of p2NIL.

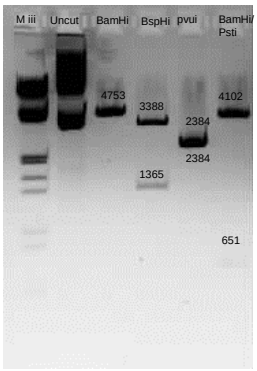


3 way fragment gel extraction

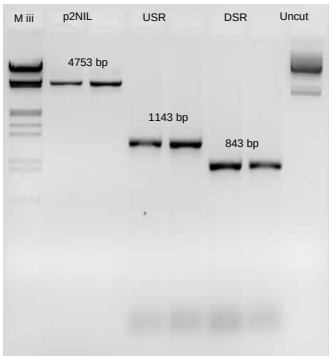


Figure A10.3 Gel purification of three way fragments.

Figure A10. Intermediary steps in cloning showing Amplification of fragments, verification of amplicons and cloning vector by restriction digest and gel purification of fragments

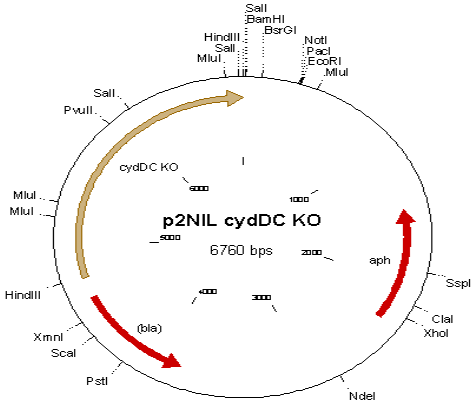


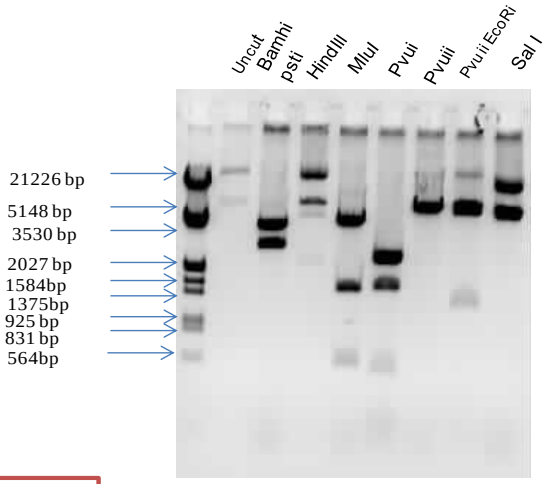


| Enzyme | Expected size |
|---|---|
| *Hind III* | 2007, 4753 |
| *BamH I/Pst I* | 4102, 2658 |
| *Pvu II/EcoR I* | 5577, 1183 |
| *Mlu I* | 4776, 1353, 99, 532 |
| *Pvu I* | 2263, 2384, 1493, 477, 143 |
| *Pvu II* | 6760 |
| Sal I | 6056, 670, 34 |

**Figure A10.1**. Restriction profile of suicide construct with various restriction enzymes.

`

Appendix B Molecular weight markers

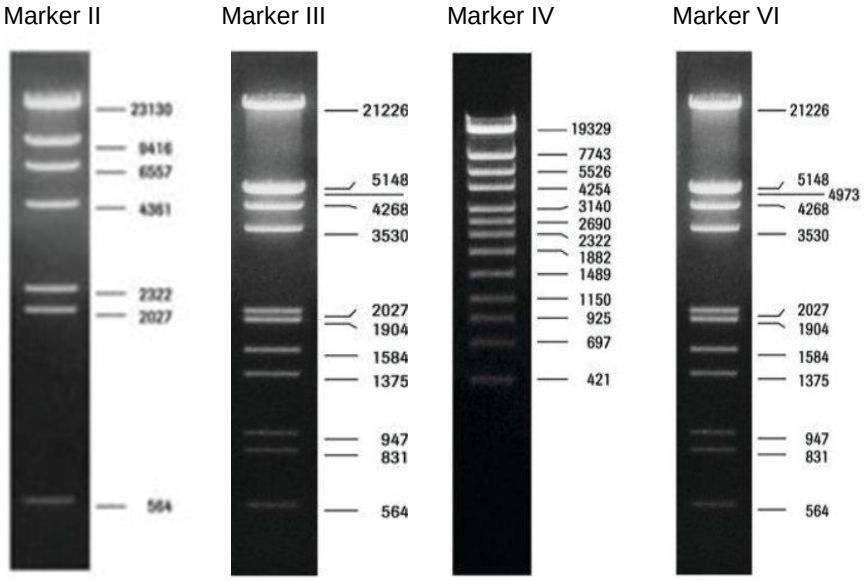


**Appendix B**. DNA molecular weight markers used in this study.
From left to right, Marker II, III, IV and Marker VI.

## 8. References

ADANE, A. A., ALENE, K. A., KOYE, D. N. & ZELEKE, B. M. 2013. Non-adherence to anti-tuberculosis treatment and determinant factors among patients with tuberculosis in northwest Ethiopia. *PloS one,* 8**,** e78791.

`

AMARAL, L., KRISTIANSEN, J., ABEBE, L. & MILLETT, W. 1996. Inhibition of the respiration of multi-drug resistant clinical isolates of *Mycobacterium tuberculosis* by thioridazine: potential use for initial therapy of freshly diagnosed tuberculosis. *Journal of Antimicrobial Chemotherapy,* 38**,** 1049-1053.

ANRAKU, Y. & GENNIS, R. B. 1987. The aerobic respiratory chain of *Escherichia coli*. *Trends in Biochemical Sciences,* 12**,** 262-266.

AUNG, H. L., BERNEY, M. & COOK, G. M. 2014. Hypoxia-activated cytochrome *bd* expression in *Mycobacterium smegmatis* is cyclic AMP receptor protein dependent. *Journal of bacteriology,* 196**,** 3091-3097.

BAFICA, A., SCANGA, C. A., FENG, C. G., LEIFER, C., CHEEVER, A. & SHER, A. 2005. TLR9 regulates Th1 responses and cooperates with TLR2 in mediating optimal resistance to *Mycobacterium tuberculosis*. *The Journal of experimental medicine,* 202**,** 1715-1724.

BALASUBRAMANIAN, V., WIEGESHAUS, E., TAYLOR, B. & SMITH, D. 1994. Pathogenesis of tuberculosis: pathway to apical localization. *Tubercle and Lung Disease,* 75**,** 168-178.

BAUGHN, A. D. & MALAMY, M. H. 2004. The strict anaerobe Bacteroides fragilis grows in and benefits from nanomolar concentrations of oxygen. *Nature,* 427**,** 441-444.

BEBBINGTON, K. J. & WILLIAMS, H. D. 1993. Investigation of the role of the *cydD* gene product in production of a functional cytochrome *d* oxidase in *Escherichia coli*. *FEMS microbiology letters,* 112**,** 19-24.

BECHER, B. & MÜLLER, V. 1994. Delta mu $Na^+$ drives the synthesis of ATP via an delta mu Na (+)-translocating $F_1F_0$-ATP synthase in membrane vesicles of the archaeon *Methanosarcina mazei* Gö1. *Journal of bacteriology,* 176**,** 2543-2550.

BERNEY, M. & COOK, G. M. 2010. Unique flexibility in energy metabolism allows mycobacteria to combat starvation and hypoxia. *PloS one,* 5**,** e8614.

BLACK, P. A., WARREN, R. M., LOUW, G. E., VAN HELDEN, P. D., VICTOR, T. C. & KANA, B. D. 2014. Energy metabolism and drug efflux in *Mycobacterium tuberculosis*. *Antimicrobial agents and chemotherapy,* 58**,** 2491-2503.

BORISOV, V. B., BELEVICH, I., BLOCH, D. A., MOGI, T. & VERKHOVSKY, M. I. 2008. Glutamate 107 in subunit I of cytochrome *bd* from *Escherichia coli* is part of a

transmembrane intraprotein pathway conducting protons from the cytoplasm to the heme *b* $_{595}$/heme *d* active site. *Biochemistry,* 47**,** 7907-7914.

BORISOV, V. B., GENNIS, R. B., HEMP, J. & VERKHOVSKY, M. I. 2011. The cytochrome *bd* respiratory oxygen reductases. *Biochimica et Biophysica Acta (BBA)-Bioenergetics,* 1807**,** 1398-1413.

BRAGG, P. & HOU, C. 1967. Reduced nicotinamide adenine dinucleotide oxidation in *Escherichia coli* particles: I. Properties and cleavage of the electron transport chain. *Archives of biochemistry and biophysics,* 119**,** 194-201.

BROCHIER-ARMANET, C., TALLA, E. & GRIBALDO, S. 2009. The multiple evolutionary histories of dioxygen reductases: implications for the origin and evolution of aerobic respiration. *Molecular biology and evolution,* 26**,** 285-297.

CALGIN, M. K., SAHIN, F., TUREGUN, B., GERCEKER, D., ATASEVER, M., KOKSAL, D., KARASARTOVA, D. & KIYAN, M. 2013. Expression analysis of efflux pump genes among drug-susceptible and multidrug-resistant *Mycobacterium tuberculosis* clinical isolates and reference strains. *Diagnostic microbiology and infectious disease,* 76**,** 291-297.

CALHOUN, M. W., THOMAS, J. W. & GENNIS, R. B. 1994. The cytochrome oxidase superfamily of redox-driven proton pumps. *Trends in biochemical sciences,* 19**,** 325-330.

CECCHINI, G., MAKLASHINA, E., YANKOVSKAYA, V., IVERSON, T. M. & IWATA, S. 2003. Variation in proton donor/acceptor pathways in succinate: quinone oxidoreductases. *FEBS letters,* 545**,** 31-38.

CHANCE, B. & WILLIAMS, G. 1956. The respiratory chain and oxidative phosphorylation. *Adv Enzymol Relat Areas Mol Biol,* 17**,** 65-134.

CHEN, M., GAN, H. & REMOLD, H. G. 2006. A mechanism of virulence: virulent *Mycobacterium tuberculosis* strain H37Rv, but not attenuated H37Ra, causes significant mitochondrial inner membrane disruption in macrophages leading to necrosis. *The Journal of Immunology,* 176**,** 3707-3716.

COHEN, J. 2013. Approval of novel TB drug celebrated—with restraint. *Science,* 339**,** 130-130.

`

COHEN, T., LIPSITCH, M., WALENSKY, R. P. & MURRAY, M. 2006. Beneficial and perverse effects of isoniazid preventive therapy for latent tuberculosis infection in HIV–tuberculosis coinfected populations. *Proceedings of the National Academy of Sciences,* 103**,** 7042-7047.

COLE, S., EIGLMEIER, K., PARKHILL, J., JAMES, K., THOMSON, N., WHEELER, P., HONORE, N., GARNIER, T., CHURCHER, C. & HARRIS, D. 2001. Massive gene decay in the leprosy bacillus. *Nature,* 409**,** 1007-1011.

COLLINS, M. & JONES, D. 1981. Distribution of isoprenoid quinone structural types in bacteria and their taxonomic implication. *Microbiological Reviews,* 45**,** 316.

COLLINS, M., PIROUZ, T., GOODFELLOW, M. & MINNIKIN, D. 1977. Distribution of menaquinones in actinomycetes and corynebacteria. *Microbiology,* 100**,** 221-230.

COMSTOCK, G. W. 1982. Epidemiology of Tuberculosis 1–3. *American Review of Respiratory Disease,* 125**,** 8-15.

COOK, G. M., CRUZ-RAMOS, H., MOIR, A. J. & POOLE, R. K. 2002. A novel haem compound accumulated in *Escherichia coli* overexpressing the *cydDC* operon, encoding an ABC-type transporter required for cytochrome assembly. *Archives of microbiology,* 178**,** 358-369.

COOK, G. M., LODER, C., SØBALLE, B., STAFFORD, G. P., MEMBRILLO-HERNÁNDEZ, J. & POOLE, R. K. 1998. A factor produced by *Escherichia coli* K-12 inhibits the growth of *E. coli* mutants defective in the cytochrome *bd* quinol oxidase complex: enterochelin rediscovered. *Microbiology,* 144**,** 3297-3308.

COOK, G. M. & POOLE, R. K. 2000. Oxidase and periplasmic cytochrome assembly in *Escherichia coli* K-12: CydDC and CcmAB are not required for haem–membrane association. *Microbiology,* 146**,** 527-536.

COOKE, J. V. 1915. Immunity tests in coccidioidal granuloma. *Archives of Internal Medicine,* 15**,** 479-486.

CORBETT, E. L., WATT, C. J., WALKER, N., MAHER, D., WILLIAMS, B. G., RAVIGLIONE, M. C. & DYE, C. 2003. The growing burden of tuberculosis: global trends and interactions with the HIV epidemic. *Archives of internal medicine,* 163**,** 1009-1021.

`

COTTER, P. A., CHEPURI, V., GENNIS, R. & GUNSALUS, R. 1990. Cytochrome *o* (*cyoABCDE*) and *d* (*cydAB*) oxidase gene expression in *Escherichia coli* is regulated by oxygen, pH, and the fnr gene product. *Journal of bacteriology,* 172**,** 6333-6338.

CRELLIN, P. K., BRAMMANANTH, R. & COPPEL, R. L. 2011. Decaprenylphosphoryl-β-D-ribose 2′-epimerase, the target of benzothiazinones and dinitrobenzamides, is an essential enzyme in *Mycobacterium smegmatis*. *PloS one,* 6**,** e16869.

CRUZ-RAMOS, H., COOK, G. M., WU, G., CLEETER, M. W. & POOLE, R. K. 2004. Membrane topology and mutational analysis of *Escherichia coli* CydDC, an ABC-type cysteine exporter required for cytochrome assembly. *Microbiology,* 150**,** 3415-3427.

D'MELLO, R., HILL, S. & POOLE, R. K. 1996. The cytochrome *bd* quinol oxidase in *Escherichia coli* has an extremely high oxygen affinity and two oxygen-binding haems: implications for regulation of activity *in vivo* by oxygen inhibition. *Microbiology,* 142**,** 755-763.

DANIEL, O., OSMAN, E., OLADIMEJI, O. & DAIRO, O. G. 2013. Preextensive drug resistant tuberculosis (Pre-XDR-TB) among MDR-TB patients in Nigeria. *Global Advanced Research Journal of Microbiology,* 2**,** 22-25.

DAVIDSON, A. L., DASSA, E., ORELLE, C. & CHEN, J. 2008. Structure, function, and evolution of bacterial ATP-binding cassette systems. *Microbiology and Molecular Biology Reviews,* 72**,** 317-364.

DAWSON, R. J. & LOCHER, K. P. 2006. Structure of a bacterial multidrug ABC transporter. *Nature,* 443**,** 180-185.

DE BACKER, A., MORTELE, K., DE KEULENAER, B. & PARIZEL, P. 2006. Tuberculosis: epidemiology, manifestations, and the value of medical imaging in diagnosis. *JBR BTR,* 89**,** 243.

DELANEY, J. M., ANG, D. & GEORGOPOULOS, C. 1992. Isolation and characterization of the *Escherichia coli htrD* gene, whose product is required for growth at high temperatures. *Journal of bacteriology,* 174**,** 1240-1247.

`

DELANEY, J. M., WALL, D. & GEORGOPOULOS, C. 1993. Molecular characterization of the *Escherichia coli htrD* gene: cloning, sequence, regulation, and involvement with cytochrome *d* oxidase. *Journal of bacteriology,* 175**,** 166-175.

DHAR, N. & MCKINNEY, J. D. 2010. *Mycobacterium tuberculosis* persistence mutants identified by screening in isoniazid-treated mice. *Proceedings of the National Academy of Sciences,* 107**,** 12275-12280.

DOH 2014. Department of Health-National Tuberculosis Management Guidelines. http://www.nicd.ac.za/assets/files/National%20TB%20management%20guidelines%202014.pdf.

DOH 2015. Department Of Health Annual Performance Plan, http://www.health.gov.au/internet/main/publishing.nsf/content/annual-report2014-15.

DOOLITTLE, R., JOHNSON, M., HUSAIN, I., VAN HOUTEN, B., THOMAS, D. & SANCAR, A. 1986. Domainal evolution of a prokaryotic DNA repair protein and its relationship to active-transport proteins. *Nature,* 323**,** 451-453.

DUNPHY, P. J. & BRODIE, A. F. 1971. [233] The structure and function of quinones in respiratory metabolism. *Methods in enzymology,* 18**,** 407-461.

EDWARDS, S. E., LODER, C. S., WU, G., CORKER, H., BAINBRIDGE, B. W., HILL, S. & POOLE, R. K. 2000. Mutation of cytochrome *bd* quinol oxidase results in reduced stationary phase survival, iron deprivation, metal toxicity and oxidative stress in *Azotobacter vinelandii*. *FEMS microbiology letters,* 185**,** 71-77.

ELSTON, T., WANG, H. & OSTER, G. 1998. Energy transduction in ATP synthase. *Nature,* 391**,** 510-513.

ENDLEY, S., MCMURRAY, D. & FICHT, T. A. 2001. Interruption of the *cydB* Locus in *Brucella abortus* attenuates intracellular survival and virulence in the mouse model of infection. *Journal of bacteriology,* 183**,** 2454-2462.

EOH, H. & RHEE, K. Y. 2013. Multifunctional essentiality of succinate metabolism in adaptation to hypoxia in *Mycobacterium tuberculosis*. *Proceedings of the National Academy of Sciences,* 110**,** 6554-6559.

`

FERRARI, G., LANGEN, H., NAITO, M. & PIETERS, J. 1999. A coat protein on phagosomes involved in the intracellular survival of mycobacteria. *Cell,* 97**,** 435-447.

FILLIOL, I., DRISCOLL, J. R., VAN SOOLINGEN, D., KREISWIRTH, B. N., KREMER, K., VALÉTUDIE, G., ANH, D. D., BARLOW, R., BANERJEE, D. & BIFANI, P. J. 2002. Global distribution of *Mycobacterium tuberculosis* spoligotypes.(Dispatches). *Emerging infectious diseases,* 8**,** 1347-1350.

FREMOND, C. M., YEREMEEV, V., NICOLLE, D. M., JACOBS, M., QUESNIAUX, V. F. & RYFFEL, B. 2004. Fatal *Mycobacterium tuberculosis* infection despite adaptive immune response in the absence of MyD88. *The Journal of clinical investigation,* 114**,** 1790-1799.

FU, H.-A., IUCHI, S. & LIN, E. 1991. The requirement of *ArcA* and *Fnr* for peak expression of the *cyd* operon in *Escherichia coli* under microaerobic conditions. *Molecular and General Genetics MGG,* 226**,** 209-213.

GARAY, S. M. 1996. Pulmonary tuberculosis. *Tuberculosis,* 2**,** 353.

GARCÍA-HORSMAN, J. A., BARQUERA, B., RUMBLEY, J., MA, J. & GENNIS, R. B. 1994. The superfamily of heme-copper respiratory oxidases. *Journal of Bacteriology,* 176**,** 5587.

GEORGIOU, C. D., FANG, H. & GENNIS, R. 1987. Identification of the *cydC* locus required for expression of the functional form of the cytochrome *d* terminal oxidase complex in *Escherichia coli*. *Journal of bacteriology,* 169**,** 2107-2112.

GEOURJON, C., ORELLE, C., STEINFELS, E., BLANCHET, C., DELÉAGE, G., DI PIETRO, A. & JAULT, J.-M. 2001. A common mechanism for ATP hydrolysis in ABC transporter and helicase superfamilies. *Trends in biochemical sciences,* 26**,** 539-544.

GERCKEN, J., PRYJMA, J., ERNST, M. & FLAD, H.-D. 1994. Defective antigen presentation by *Mycobacterium tuberculosis*-infected monocytes. *Infection and immunity,* 62**,** 3472-3478.

GERLACH, J. H., ENDICOTT, J. A., JURANKA, P. F., HENDERSON, G., SARANGI, F., DEUCHARS, K. L. & LING, V. 1986. Homology between P-glycoprotein and a bacterial haemolysin transport protein suggests a model for multidrug resistance.

`

GOFF, S. A. & GOLDBERG, A. L. 1985. Production of abnormal proteins in *E. coli* stimulates transcription of Ion and other heat shock genes. *Cell,* 41**,** 587-595.

GOLDMAN, B. S., GABBERT, K. K. & KRANZ, R. G. 1996a. The temperature-sensitive growth and survival phenotypes of *Escherichia coli cydDC* and *cydAB* strains are due to deficiencies in cytochrome *bd* and are corrected by exogenous catalase and reducing agents. *Journal of bacteriology,* 178**,** 6348-6351.

GOLDMAN, B. S., GABBERT, K. K. & KRANZ, R. G. 1996b. Use of heme reporters for studies of cytochrome biosynthesis and heme transport. *Journal of bacteriology,* 178**,** 6338-6347.

GONZALEZ-JUARRERO, M., TURNER, O. C., TURNER, J., MARIETTA, P., BROOKS, J. V. & ORME, I. M. 2001. Temporal and Spatial Arrangement of Lymphocytes within Lung Granulomas Induced by Aerosol Infection with *Mycobacterium tuberculosis*. *Infection and immunity,* 69**,** 1722-1728.

GORDHAN, B. G. & PARISH, T. 2001. Gene Replacement using Pretreated DNA. *Methods Mol Med,* 54**,** 77-92.

GRAF, S., FEDOTOVSKAYA, O., KAO, W.-C., HUNTE, C., ÄDELROTH, P., BOTT, M., VON BALLMOOS, C. & BRZEZINSKI, P. 2016. Rapid Electron Transfer within the III-IV Supercomplex in *Corynebacterium glutamicum*. *Scientific Reports,* 6.

GRIFFIN, J. E., GAWRONSKI, J. D., DEJESUS, M. A., IOERGER, T. R., AKERLEY, B. J. & SASSETTI, C. M. 2011. High-resolution phenotypic profiling defines genes essential for mycobacterial growth and cholesterol catabolism. *PLoS Pathog,* 7**,** e1002251.

GROS, P., CROOP, J. & HOUSMAN, D. 1986. Mammalian multidrug resistance gene: complete cDNA sequence indicates strong homology to bacterial transport proteins. *Cell,* 47**,** 371-380.

HANAHAN, D. 1983. Studies on transformation of Escherichia coli with plasmids. *Journal of molecular biology,* 166**,** 557-580.

HEDRICK, D. B. & WHITE, D. C. 1986. Microbial respiratory quinones in the environment: I. A sensitive liquid chromatographic method. *Journal of microbiological methods,* 5**,** 243-254.

`

HIGGINS, C. F. 2001. ABC transporters: physiology, structure and mechanism–an overview. *Research in microbiology,* 152**,** 205-210.

HILES, I. D., GALLAGHER, M. P., JAMIESON, D. J. & HIGGINS, C. F. 1987. Molecular characterization of the oligopeptide permease of *Salmonella typhimurium*. *Journal of molecular biology,* 195**,** 125-142.

HOLLENSTEIN, K., FREI, D. C. & LOCHER, K. P. 2007. Structure of an ABC transporter in complex with its binding protein. *Nature,* 446**,** 213-216.

IUCHI, S., CHEPURI, V., FU, H., GENNIS, R. & LIN, E. 1990. Requirement for terminal cytochromes in generation of the aerobic signal for the *arc* regulatory system in *Escherichia coli:* study utilizing deletions and *lac* fusions of *cyo* and *cyd*. *Journal of Bacteriology,* 172**,** 6020-6025.

IUCHI, S. & LIN, E. 1991. Adaptation of *Escherichia coli* to respiratory conditions: regulation of gene expression. *Cell,* 66**,** 5-7.

JUTY, N. S., MOSHIRI, F., MERRICK, M., ANTHONY, C. & HILL, S. 1997. The *Klebsiella pneumoniae* cytochrome *bd*'terminal oxidase complex and its role in microaerobic nitrogen fixation. *Microbiology,* 143**,** 2673-2683.

KANA, B. D., MACHOWSKI. E, GORDHAN. B, NARRANDES. N AND BLACK. P 2009. Rsepiratory energetics in mycobacteria 10**,** 1-14.

KANA, B. D., WEINSTEIN, E. A., AVARBOCK, D., DAWES, S. S., RUBIN, H. & MIZRAHI, V. 2001. Characterization of the *cydAB*-Encoded Cytochrome *bd* Oxidase from *Mycobacterium smegmatis*. *Journal of bacteriology,* 183**,** 7076-7086.

KANG, S., KIM, R. Y., SEO, M. J., LEE, S., KIM, Y. M., SEO, M., SEO, J. J., KO, Y., CHOI, I. & JANG, J. 2014. Lead optimization of a novel series of imidazo [1, 2-a] pyridine amides leading to a clinical candidate (Q203) as a multi-and extensively-drug-resistant anti-tuberculosis agent. *Journal of medicinal chemistry,* 57**,** 5293-5305.

KATOCH, V., SAXENA, N., SHIVANNAVAR, C., SHARMA, V., KATOCH, K., SHARMA, R. & MURTHY, P. S. 1998. Effect of trifluoperazine on *in vitro* ATP synthesis by *Mycobacterium leprae*. *FEMS Immunology & Medical Microbiology,* 20**,** 99-102.

`

KELLY, M., POOLE, R., YATES, M. & KENNEDY, C. 1990. Cloning and mutagenesis of genes encoding the cytochrome *bd* terminal oxidase complex in *Azotobacter vinelandii*: mutants deficient in the cytochrome *d* complex are unable to fix nitrogen in air. *Journal of bacteriology,* 172**,** 6010-6019.

KERSCHER, S., DRÖSE, S., ZICKERMANN, V. & BRANDT, U. 2007. The three families of respiratory NADH dehydrogenases. *Bioenergetics.* Springer.

KESHAVJEE, S. & FARMER, P. E. 2012. Tuberculosis, drug resistance, and the history of modern medicine. *New England Journal of Medicine,* 367**,** 931-936.

KIM, J., PARK, Y., KIM, Y., KANG, S., SHIN, J., PARK, I. & CHOI, B. 2003. Miliary tuberculosis and acute respiratory distress syndrome. *The International Journal of Tuberculosis and Lung Disease,* 7**,** 359-364.

KITA, K., KONISHI, K. & ANRAKU, Y. 1984. Terminal oxidases of *Escherichia coli* aerobic respiratory chain. II. Purification and properties of cytochrome $b_{558}$-*d* complex from cells grown with limited oxygen and evidence of branched electron-carrying systems. *Journal of Biological Chemistry,* 259**,** 3375-3381.

KITAGAWA, T. & OGURA, T. 2007. Oxygen Activation Mechanism at the Binuclear Site of Heme–Copper Oxidase Superfamily as Revealed by Time-Resolved Resonance Raman Spectroscopy. *Progress in Inorganic Chemistry, Volume 45***,** 431-479.

KRAUSE, A. K. 1927. *Tuberculosis and public health*, New York Tuberculosis and Health Association.

LANCASTER, C. R. D. 2002. Succinate: quinone oxidoreductases: an overview. *Biochimica et Biophysica Acta (BBA)-Bioenergetics,* 1553**,** 1-6.

LESTER, R. & CRANE, F. 1959. The natural occurrence of coenzyme *Q* and related compounds. *J Biol Chem,* 234**,** 2169-2175.

LIENHARDT, C., RAVIGLIONE, M., SPIGELMAN, M., HAFNER, R., JARAMILLO, E., HOELSCHER, M., ZUMLA, A. & GHEUENS, J. 2012. New drugs for the treatment of tuberculosis: needs, challenges, promise, and prospects for the future. *Journal of infectious diseases,* 205**,** S241-S249.

`

LIN, S. S., GROSS, U. & BOHNE, W. 2011. Two internal type II NADH dehydrogenases of *Toxoplasma gondii* are both required for optimal tachyzoite growth. *Molecular microbiology,* 82**,** 209-221.

LINTON, K. J. & HIGGINS, C. F. 1998. The *Escherichia coli* ATP-binding cassette (ABC) proteins. *Molecular microbiology,* 28**,** 5-13.

LU, P., HEINEKE, M. H., KOUL, A., ANDRIES, K., COOK, G. M., LILL, H., VAN SPANNING, R. & BALD, D. 2015. The cytochrome *bd*-type quinol oxidase is important for survival of *Mycobacterium smegmatis* under peroxide and antibiotic-induced stress. *Scientific reports,* 5.

LYNCH, A. S. 1996. Responses to molecular oxygen. *Escherichia coli and Salmonella***,** 1526-1538.

MAHAJAN, R. 2013. Bedaquiline: First FDA-approved tuberculosis drug in 40 years. *International Journal of Applied and Basic Medical Research,* 3**,** 1.

MAHER, D., UPLEKAR, M., BLANC, L. & RAVIGLIONE, M. 2003. Treatment of tuberculosis. *Bmj,* 327**,** 822-823.

MAKAROV, V., MANINA, G., MIKUSOVA, K., MÖLLMANN, U., RYABOVA, O., SAINT-JOANIS, B., DHAR, N., PASCA, M. R., BURONI, S. & LUCARELLI, A. P. 2009. Benzothiazinones kills *Mycobacterium tuberculosis* by blocking arabinan synthesis. *Science,* 324**,** 801-804.

MATSOSO, L. G., KANA, B. D., CRELLIN, P. K., LEA-SMITH, D. J., PELOSI, A., POWELL, D., DAWES, S. S., RUBIN, H., COPPEL, R. L. & MIZRAHI, V. 2005. Function of the cytochrome $bc_1aa_3$ branch of the respiratory network in mycobacteria and network adaptation occurring in response to its disruption. *Journal of bacteriology,* 187**,** 6300-6308.

MCADAM, R. A., QUAN, S., SMITH, D. A., BARDAROV, S., BETTS, J. C., COOK, F. C., HOOKER, E. U., LEWIS, A. P., WOOLLARD, P. & EVERETT, M. J. 2002. Characterization of a *Mycobacterium tuberculosis* H37Rv transposon library reveals insertions in 351 ORFs and mutants with altered virulence. *Microbiology,* 148**,** 2975-2986.

MEGEHEE, J. A., HOSLER, J. P. & LUNDRIGAN, M. D. 2006. Evidence for a cytochrome *bcc/aa*$_3$ interaction in the respiratory chain of *Mycobacterium smegmatis*. *Microbiology,* 152**,** 823-829.

MEGEHEE, J. A. & LUNDRIGAN, M. D. 2007. Temporal expression of *Mycobacterium smegmatis* respiratory terminal oxidases. *Canadian journal of microbiology,* 53**,** 459-463.

MELO, A. M., BANDEIRAS, T. M. & TEIXEIRA, M. 2004. New insights into type II NAD (P) H: quinone oxidoreductases. *Microbiology and Molecular Biology Reviews,* 68**,** 603-616.

MIESEL, L., WEISBROD, T. R., MARCINKEVICIENE, J. A., BITTMAN, R. & JACOBS, W. R. 1998. NADH dehydrogenase defects confer isoniazid resistance and conditional lethality in *Mycobacterium smegmatis*. *Journal of bacteriology,* 180**,** 2459-2467.

MIKUŠOVÁ, K., HUANG, H., YAGI, T., HOLSTERS, M., VEREECKE, D., D'HAEZE, W., SCHERMAN, M. S., BRENNAN, P. J., MCNEIL, M. R. & CRICK, D. C. 2005. Decaprenylphosphoryl arabinofuranose, the donor of the D-arabinofuranosyl residues of mycobacterial arabinan, is formed via a two-step epimerization of decaprenylphosphoryl ribose. *Journal of bacteriology,* 187**,** 8020-8025.

MILLET, J.-P., MORENO, A., FINA, L., DEL BAÑO, L., ORCAU, A., DE OLALLA, P. G. & CAYLA, J. A. 2013. Factors that influence current tuberculosis epidemiology. *European Spine Journal,* 22**,** 539-548.

MURPHY, K. C., PAPAVINASASUNDARAM, K. & SASSETTI, C. M. 2015. Mycobacterial recombineering. *Mycobacteria Protocols***,** 177-199.

NERES, J., POJER, F., MOLTENI, E., CHIARELLI, L. R., DHAR, N., BOY-RÖTTGER, S., BURONI, S., FULLAM, E., DEGIACOMI, G. & LUCARELLI, A. P. 2012. Structural basis for benzothiazinone-mediated killing of *Mycobacterium tuberculosis*. *Science translational medicine,* 4**,** 150ra121-150ra121.

NGAIMISI, E., MUGUSI, S., MINZI, O., SASI, P., RIEDEL, K. D., SUDA, A., UEDA, N., JANABI, M., MUGUSI, F. & HAEFELI, W. 2011. Effect of Rifampicin and CYP2B6 Genotype on Long-Term Efavirenz Autoinduction and Plasma Exposure

in HIV Patients With or Without Tuberculosis. *Clinical Pharmacology & Therapeutics,* 90**,** 406-413.

NIEBISCH, A. & BOTT, M. 2001. Molecular analysis of the cytochrome $bc_1/aa_3$ branch of the *Corynebacterium glutamicum* respiratory chain containing an unusual diheme cytochrome $c_1$. *Archives of Microbiology,* 175**,** 282-294.

NORMAN, R., SMITH, J. L., KING, T., MASON, H. & MORRISON, M. 1965. Oxidases and related redox systems. *Oxidases and related redox systems,* 1.

OLIVER, J. D., NILSSON, L. & KJELLEBERG, S. 1991. Formation of nonculturable *Vibrio vulnificus* cells and its relationship to the starvation state. *Applied and Environmental Microbiology,* 57**,** 2640-2644.

ORGANIZATION, W. H. & ORGANIZATION, W. H. 2007. Improving the diagnosis and treatment of smear-negative pulmonary and extrapulmonary tuberculosis among adults and adolescents: recommendations for HIV-prevalent and resource-constrained settings.

OSBORNE, J. & GENNIS, R. 1999. Sequence analysis of cytochrome *bd* oxidase suggests a revised topology for subunit I. *Biochimica et Biophysica Acta (BBA)-Bioenergetics,* 1410**,** 32-50.

PEREIRA, M. M., BANDEIRAS, T. M., FERNANDES, A. S., LEMOS, R. S., MELO, A. M. & TEIXEIRA, M. 2004. Respiratory chains from aerobic thermophilic prokaryotes. *Journal of bioenergetics and biomembranes,* 36**,** 93-105.

PETHE, K., BIFANI, P., JANG, J., KANG, S., PARK, S., AHN, S., JIRICEK, J., JUNG, J., JEON, H. K. & CECHETTO, J. 2013. Discovery of Q203, a potent clinical candidate for the treatment of tuberculosis. *Nature medicine,* 19**,** 1157-1160.

PHAM, T. T., JACOBS-SERA, D., PEDULLA, M. L., HENDRIX, R. W. & HATFULL, G. F. 2007. Comparative genomic analysis of mycobacteriophage Tweety: evolutionary insights and construction of compatible site-specific integration vectors for mycobacteria. *Microbiology,* 153**,** 2711-23.

PITTMAN, M. S., CORKER, H., WU, G., BINET, M. B., MOIR, A. J. & POOLE, R. K. 2002. Cysteine Is Exported from the *Escherichia coli* cytoplasm by CydDC, an ATP-binding Cassette-type Transporter Required for Cytochrome Assembly. *Journal of Biological Chemistry,* 277**,** 49841-49849.

PITTMAN, M. S., ROBINSON, H. C. & POOLE, R. K. 2005. A bacterial glutathione transporter (*Escherichia coli* CydDC) exports reductant to the periplasm. *Journal of Biological Chemistry,* 280**,** 32254-32261.

POOLE, R. K. & COOK, G. M. 2000. Redundancy of aerobic respiratory chains in bacteria? Routes, reasons and regulation. *Advances in microbial physiology,* 43**,** 165-224.

POOLE, R. K., GIBSON, F. & WU, G. 1994. The *cydD* gene product, component of a heterodimeric ABC transporter, is required for assembly of periplasmic cytochrome *c* and of cytochrome *bd* in *Escherichia coli*. *FEMS microbiology letters,* 117**,** 217-223.

POOLE, R. K., HATCH, L., CLEETER, M. W., GIBSON, F., COX, G. B. & WU, G. 1993. Cytochrome *bd* biosynthesis in *Escherichia coli*: the sequences of the *cydC* and *cydD* genes suggest that they encode the components of an ABC membrane transporter. *Molecular microbiology,* 10**,** 421-430.

POOLE, R. K., KUMAR, C., SALMON, I. & CHANCE, B. 1983. The 650 nm chromophore in *Escherichia coli* is an 'oxy-'or oxygenated compound, not the oxidized form of cytochrome oxidase *d*: a hypothesis. *Microbiology,* 129**,** 1335-1344.

POOLE, R. K., WILLIAMS, H. D., DOWNIE, J. A. & GIBSON, F. 1989. Mutations affecting the cytochrome *d*-containing oxidase complex of *Escherichia coli* K12: identification and mapping of a fourth locus, *cydD*. *Microbiology,* 135**,** 1865-1874.

RABAHI, M. F., RODRIGUES, A. B., MELLO, F. Q. D., ALMEIDA NETTO, J. C. D. & KRITSKI, A. L. 2002. Noncompliance with tuberculosis treatment by patients at a tuberculosis and AIDS reference hospital in midwestern Brazil. *Brazilian Journal of Infectious Diseases,* 6**,** 63-73.

RAO, S. P., ALONSO, S., RAND, L., DICK, T. & PETHE, K. 2008. The protonmotive force is required for maintaining ATP homeostasis and viability of hypoxic, nonreplicating *Mycobacterium tuberculosis*. *Proceedings of the National Academy of Sciences,* 105**,** 11945-11950.

`

REDDY, M., NADADHUR, G. & GANGADHARAM, P. R. 1996. *In-vitro* and intracellular antimycobacterial activity of trifluoperazine. *Journal of Antimicrobial Chemotherapy,* 37**,** 196-197.

REDFEARN, E. R. 1967. Mode of action of ubiquinones (coenzymes *Q*) in electron transport systems. *Vitamins & Hormones,* 24**,** 465-488.

ROSS, W., THOMPSON, J. F., NEWLANDS, J. T. & GOURSE, R. L. 1990. *E. coli Fis* protein activates ribosomal RNA transcription *in vitro* and *in vivo*. *The EMBO Journal,* 9**,** 3733.

ROSZAK, D. & COLWELL, R. 1987. Survival strategies of bacteria in the natural environment. *Microbiological reviews,* 51**,** 365.

RUSSELL, J. B. & COOK, G. M. 1995. Energetics of bacterial growth: balance of anabolic and catabolic reactions. *Microbiological reviews,* 59**,** 48-62.

RYFFEL, B., FREMOND, C., JACOBS, M., PARIDA, S., BOTHA, T., SCHNYDER, B. & QUESNIAUX, V. 2005. Innate immunity to mycobacterial infection in mice: critical role for toll-like receptors. *Tuberculosis,* 85**,** 395-405.

SACKSTEDER, K. A., PROTOPOPOVA, M., BARRY, C. E., ANDRIES, K. & NACY, C. A. 2012. Discovery and development of SQ109: a new antitubercular drug with a novel mechanism of action. *Future microbiology,* 7**,** 823-837.

SAGBAKKEN, M., FRICH, J. C. & BJUNE, G. A. 2008. Perception and management of tuberculosis symptoms in Addis Ababa, Ethiopia. *Qualitative health research*.

SAKAMOTO, K. 2012. The pathology of *Mycobacterium tuberculosis* infection. *Veterinary Pathology Online,* 49**,** 423-439.

SAMBROOK, J., FRITSCH, E. F. & MANIATIS, T. 1989. *Molecular cloning: a laboratory manual*, Cold spring harbor laboratory press.

SASSETTI, C. M., BOYD, D. H. & RUBIN, E. J. 2003. Genes required for mycobacterial growth defined by high density mutagenesis. *Molecular microbiology,* 48**,** 77-84.

SASSETTI, C. M. & RUBIN, E. J. 2003. Genetic requirements for mycobacterial survival during infection. *Proceedings of the National Academy of Sciences,* 100**,** 12989-12994.

SAZANOV, L. A. & HINCHLIFFE, P. 2006. Structure of the hydrophilic domain of respiratory complex I from *Thermus thermophilus*. *science,* 311**,** 1430-1436.

SCHIRAWSKI, J. & UNDEN, G. 1998. Menaquinone-dependent succinate dehydrogenase of bacteria catalyzes reversed electron transport driven by the proton potential. *European Journal of Biochemistry,* 257**,** 210-215.

SENIOR, A. E., AL-SHAWI, M. K. & URBATSCH, I. L. 1995. The catalytic cycle of P-glycoprotein. *FEBS letters,* 377**,** 285-289.

SENSI, P. 1983. History of the development of rifampin. *Review of Infectious Diseases,* 5**,** S402-S406.

SHI, C. & PAMER, E. G. 2011. Monocyte recruitment during infection and inflammation. *Nature Reviews Immunology,* 11**,** 762-774.

SHI, L., SOHASKEY, C. D., KANA, B. D., DAWES, S., NORTH, R. J., MIZRAHI, V. & GENNARO, M. L. 2005. Changes in energy metabolism of *Mycobacterium tuberculosis* in mouse lung and under in vitro conditions affecting aerobic respiration. *Proceedings of the National Academy of Sciences,* 102**,** 15629-15634.

SIEGELE, D. A., IMLAY, K. & IMLAY, J. A. 1996. The stationary-phase-exit defect of *cydC* (surB) mutants is due to the lack of a functional terminal cytochrome oxidase. *Journal of bacteriology,* 178**,** 6091-6096.

SIEGELE, D. A. & KOLTER, R. 1992. Life after log. *Journal of bacteriology,* 174**,** 345.

SIEGELE, D. A. & KOLTER, R. 1993. Isolation and characterization of an *Escherichia coli* mutant defective in resuming growth after starvation. *Genes & development,* 7**,** 2629-2640.

SNAPPER, S., MELTON, R., MUSTAFA, S., KIESER, T. & WR JR, J. 1990. Isolation and characterization of efficient plasmid transformation mutants of *Mycobacterium smegmatis*. *Molecular Microbiology,* 4**,** 1911-1919.

SOMERVILLE, W., THIBERT, L., SCHWARTZMAN, K. & BEHR, M. A. 2005. Extraction of *Mycobacterium tuberculosis* DNA: a question of containment. *J Clin Microbiol,* 43**,** 2996-7.

SOUSA, F. L., ALVES, R. J., RIBEIRO, M. A., PEREIRA-LEAL, J. B., TEIXEIRA, M. & PEREIRA, M. M. 2012. The superfamily of heme–copper oxygen reductases: types and evolutionary considerations. *Biochimica et Biophysica Acta (BBA)-Bioenergetics,* 1817**,** 629-637.

SSA 2013. National TB Statistics For South Africa. http://www.tbfacts.org/tb-statistics-south-africa/.

STAVRI, H., BUCURENCI, N., ULEA, I., COSTACHE, A., POPA, L. & POPA, M. I. 2012. Use of recombinant purified protein derivative (PPD) antigens as specific skin test for tuberculosis. *The Indian journal of medical research,* 136**,** 799.

STOLPE, S. & FRIEDRICH, T. 2004. The *Escherichia coli* NADH: ubiquinone oxidoreductase (complex I) is a primary proton pump but may be capable of secondary sodium antiport. *Journal of Biological Chemistry,* 279**,** 18377-18383.

SZMELCMAN, S., SCHWARTZ, M., SILHAVY, T. J. & BOOS, W. 1976. Maltose transport in *Escherichia coli* K12. *European Journal of Biochemistry,* 65**,** 13-19.

TABER, H. 1980. Functions of vitamin K2 in microorganisms. *Vitamin K metabolism and vitamin K-dependent proteins. University Park Press, Baltimore***,** 177-187.

TENOVER, F. C., CRAWFORD, J. T., HUEBNER, R. E., GEITER, L. J., HORSBURGH JR, C. & GOOD, R. 1993. The resurgence of tuberculosis: is your laboratory ready? *Journal of Clinical Microbiology,* 31**,** 767.

TRUDEAU, E. L. 1892. *The Treatment of Experimental Tuberculosis by Koch's Tuberculin, Hunter's Modification, and Other Products of the Tubercle Bacillus*, publisher not identified.

TUFARIELLO, J. M., CHAN, J. & FLYNN, J. L. 2003. Latent tuberculosis: mechanisms of host and bacillus that contribute to persistent infection. *The Lancet infectious diseases,* 3**,** 578-590.

UNDEN, G. & BONGAERTS, J. 1997. Alternative respiratory pathways of *Escherichia coli*: energetics and transcriptional regulation in response to electron acceptors. *Biochimica et Biophysica Acta (BBA)-Bioenergetics,* 1320**,** 217-234.

VELMURUGAN, K., CHEN, B., MILLER, J. L., AZOGUE, S., GURSES, S., HSU, T., GLICKMAN, M., JACOBS JR, W. R., PORCELLI, S. A. & BRIKEN, V. 2007. *Mycobacterium tuberculosis nuoG* is a virulence gene that inhibits apoptosis of infected host cells. *PLoS Pathog,* 3**,** e110.

VERGNE, I., CHUA, J., LEE, H.-H., LUCAS, M., BELISLE, J. & DERETIC, V. 2005. Mechanism of phagolysosome biogenesis block by viable *Mycobacterium*

*tuberculosis*. *Proceedings of the National Academy of Sciences of the United States of America,* 102**,** 4033-4038.

VILCHEZE, C., WEISBROD, T. R., CHEN, B., KREMER, L., HAZBÓN, M. H., WANG, F., ALLAND, D., SACCHETTINI, J. C. & JACOBS, W. R. 2005. Altered NADH/NAD+ ratio mediates coresistance to isoniazid and ethionamide in mycobacteria. *Antimicrobial Agents and Chemotherapy,* 49**,** 708-720.

WAY, S. S., SALLUSTIO, S., MAGLIOZZO, R. S. & GOLDBERG, M. B. 1999. Impact of either elevated or decreased levels of cytochrome *bd* expression on *Shigella flexneri* virulence. *Journal of bacteriology,* 181**,** 1229-1237.

WEBER, J. & SENIOR, A. E. 2003. ATP synthesis driven by proton transport in $F_1F_0$-ATP synthase. *Febs Letters,* 545**,** 61-70.

WEINSTEIN, E. A., YANO, T., LI, L.-S., AVARBOCK, D., AVARBOCK, A., HELM, D., MCCOLM, A. A., DUNCAN, K., LONSDALE, J. T. & RUBIN, H. 2005. Inhibitors of type II NADH: menaquinone oxidoreductase represent a class of antitubercular drugs. *Proceedings of the National Academy of Sciences of the United States of America,* 102**,** 4548-4553.

WHO 1993. TB: A Global Emergency.

WHO 1995. Bridging The Gaps.

WHO 2013. Tuberculosis. *Saudi Medical Journal,* 34**,** 1205-1207.

WHO 2015. Global Tuberculosis report.

WHO 2016. TB: A global Tuberculosis report 2016. 1-32.

WINSTEDT, L., YOSHIDA, K.-I., FUJITA, Y. & VON WACHENFELDT, C. 1998. Cytochrome *bd* Biosynthesis in *Bacillus subtilis:* Characterization of the *cydABCD* Operon. *Journal of bacteriology,* 180**,** 6571-6580.

WOLUCKA, B. A. 2008. Biosynthesis of D-arabinose in mycobacteria–a novel bacterial pathway with implications for antimycobacterial therapy. *Febs Journal,* 275**,** 2691-2711.

YAGUI, M., PERALES, M., ASENCIOS, L., VERGARA, L., SUAREZ, C., YALE, G., SALAZAR, C., SAAVEDRA, M., SHIN, S. & FERROUSIER, O. 2006. Timely diagnosis of MDR-TB under program conditions: is rapid drug susceptibility

testing sufficient? *The International Journal of Tuberculosis and Lung Disease,* 10**,** 838-843.

YANG, K., ZHANG, J., VAKKASOGLU, A. S., HIELSCHER, R., OSBORNE, J. P., HEMP, J., MIYOSHI, H., HELLWIG, P. & GENNIS, R. B. 2007. Glutamate 107 in subunit I of the cytochrome *bd* quinol oxidase from *Escherichia coli* is protonated and near the heme *d*/heme $b_{595}$ binuclear center. *Biochemistry,* 46**,** 3270-3278.

YANO, T., LI, L.-S., WEINSTEIN, E., TEH, J.-S. & RUBIN, H. 2006. Steady-state kinetics and inhibitory action of antitubercular phenothiazines on *Mycobacterium tuberculosis* type-II NADH-menaquinone oxidoreductase (NDH-2). *Journal of Biological Chemistry,* 281**,** 11456-11463.

YASSIN, A., BRZEZINKA, H., SCHAAL, K., TRÜPER, H. & PULVERER, G. 1988. Menaquinone composition in the classification and identification of aerobic actinomycetes. *Zentralblatt für Bakteriologie, Mikrobiologie und Hygiene. Series A: Medical Microbiology, Infectious Diseases, Virology, Parasitology,* 267**,** 339-356.

YURA, T. & NAKAHIGASHI, K. 1999. Regulation of the heat-shock response. *Current opinion in microbiology,* 2**,** 153-158.